8-2013

System Design And Motion Artifact Removal Algorithm Implementation For Ambulatory Women Ecg Measurement System:e-Bra System

Hyeokjun Kwon
University of Arkansas, Fayetteville

SYSTEM DESIGN AND MOTION ARTIFACT REMOVAL ALGORITHM IMPLEMENTATION FOR AMBULATORY WOMEN ECG MEASUREMENT SYSTEM : E-BRA SYSTEM

SYSTEM DESIGN AND MOTION ARTIFACT REMOVAL ALGORITHM IMPLEMENTATION FOR AMBULATORY WOMEN ECG MEASUREMENT SYSTEM : E-BRA SYSTEM

A dissertation submitted in partial fulfillment
of the requirements for the degree of
Doctor of Philosophy in Electrical Engineering

By

Hyeokjun Kwon
Hallym University
Bachelor of Engineering in Electronics Engineering, 1997
Hallym University
Master of Engineering in Electronics Engineering, 1999

August 2013
University of Arkansas

This dissertation is approved for recommendation to the Graduate Council.

_____

Dr. Vijay K. Varadan
Dissertation Director

_____

Dr. Randy Brown
Committee Member

_____

Dr. Linfen Chen
Committee Member

_____

Dr. Thomas Costello
Committee Member

ABSTRACT

Cardio Vascular Disease (CVD) leads to sudden cardiac death due to irregular phenomenon of the cardiac signal by the abnormal case of blood vessel and cardiac structure. For last three decades, there is an enhanced interest in research for cardiac diseases.. As a result, the death rate by cardiac disease in men has been falling gradually compared with relatively increasing the death rate for women due to CVD. The main reason for this phenomenon is due to the lack of seriousness to female CVD and different symptoms of female CVD compared with the symptoms of male CVD. Usually, because the CVDs for women accompany with ordinary symptoms not attributable to the heart abnormality signal such as unusual fatigue, sleep disturbances, shortness of breath, anxiety, chest discomfort, and indigestion dyspepsia, most women CVD patients do not realize that these symptoms are actually related to the CVD symptoms. Therefore, periodic ECG signal observation is required not only for women who have been diagnosed with heart disease but also for persons who want to examine their heart activity. Electrocardiogram (ECG) is used to diagnose abnormality of heart. Among the medical checkup methods for CVDs, it is very an effective method for the diagnosis of cardiac disease and the early detection of heart abnormality to monitor ECG periodically. This dissertation proposes an effective ECG monitoring system for woman by attaching the system on woman's brassiere by using augmented chest lead attachment method. The suggested system called "E-Bra system" in this dissertation consists of an ECG transmission system and a computer installed program called "E-Bra pro" in order to display and analyze the ECG transmitted from the transmission module. The ECG transmission module consists of three parts such as ECG physical signal detection part with 3 stage amplifier and two electrodes, data acquisition with AD converter, and data

transmission part with GPRS (General Packet Radio Service) communication, and it has very compact size that is attachable at the bottom layer of a brassiere for women. However, the ECG signal measured from the transmission module includes not only pure ECG components information; P waves QRS complex, and T wave, but also a motion artifact component (MA) due to subject movements. The MA component is one of the reasons for misdiagnosis. Therefore, the main purpose of the E-Bra system is to provide a reliable ECG data set identical to the quality of an ECG data set collected in hospital. Unfortunately, removing MA is a big challenge because the frequency range of the MA is duplicated on the frequency range of the pure ECG components, P-QRS-T. In this dissertation, two motion artifact removal algorithms (MARAs) with adaptive filter structure and independent component analysis concept are suggested, and the performance of the two MARAs will be evaluated by correlation values and signal noise ratio (SNR) values.

ACKNOWLEDGEMENTS

I would like to take this opportunity to express my deepest gratitude to Dr. Vijay K. Varadan, my major advisor and the graduate committee chair, for giving me an opportunity to work under him. He was a fabulous advisor: sharp, cheery, perceptive, and mindful of the things that truly matter.

Dr. Randy L. Brown, for his patience, support and guidance in my research and coursework.

Dr. Thomas Costello, for his critical reviews, suggestions, constant encouragement and his time.

Dr. Linfen Chen for his enthusiasm and making me ponder over engineering applications with civic sense and societal cause.

I would like to extend my thanks to my research group members – Dr. Gyanesh Mathur, Prashanth Shyamkumar, Pratyush Rai, Mouli Ramasamy, and Sechang Oh.

I was fortunate to have Sunggil Hwang, Sameer Thalappil, and Younglim Choi. My sincerest thanks represents to them for their friendship and support.

I offer my sincerest thanks to my parents, brother, and parents-in-law for their support. I am also grateful to sister-in-law family parents for their encouragement.

Last but not the least, I would like extend my sincerest thanks to my family, my lovable wife, my princess Soonbi Kwon, and my Jr Taewook Kwon. It would have been very difficult for me to concentrate on my research without their love, affection, and support.

TABLE OF CONTENTS

LIST OF FIGURES

Chapter 1: Introduction

1.1 Development motivation of electrocardiogram(ECG) measurement system for women

Globally, as the average life span of the humans is continuously increasing, accelerating an aging society, and increasing the desire for healthy lifestyles, health care expenditure is clearly on the rise. Figure 1 shows that the United States spent 15.2% of GDP for health care in 2006 and has consistently ranked number one in the world. The expenditure gap between the U.S. and the second biggest spender, Switzerland, was around 4%. Among the other high-income countries, the gap is even larger [1] [2].

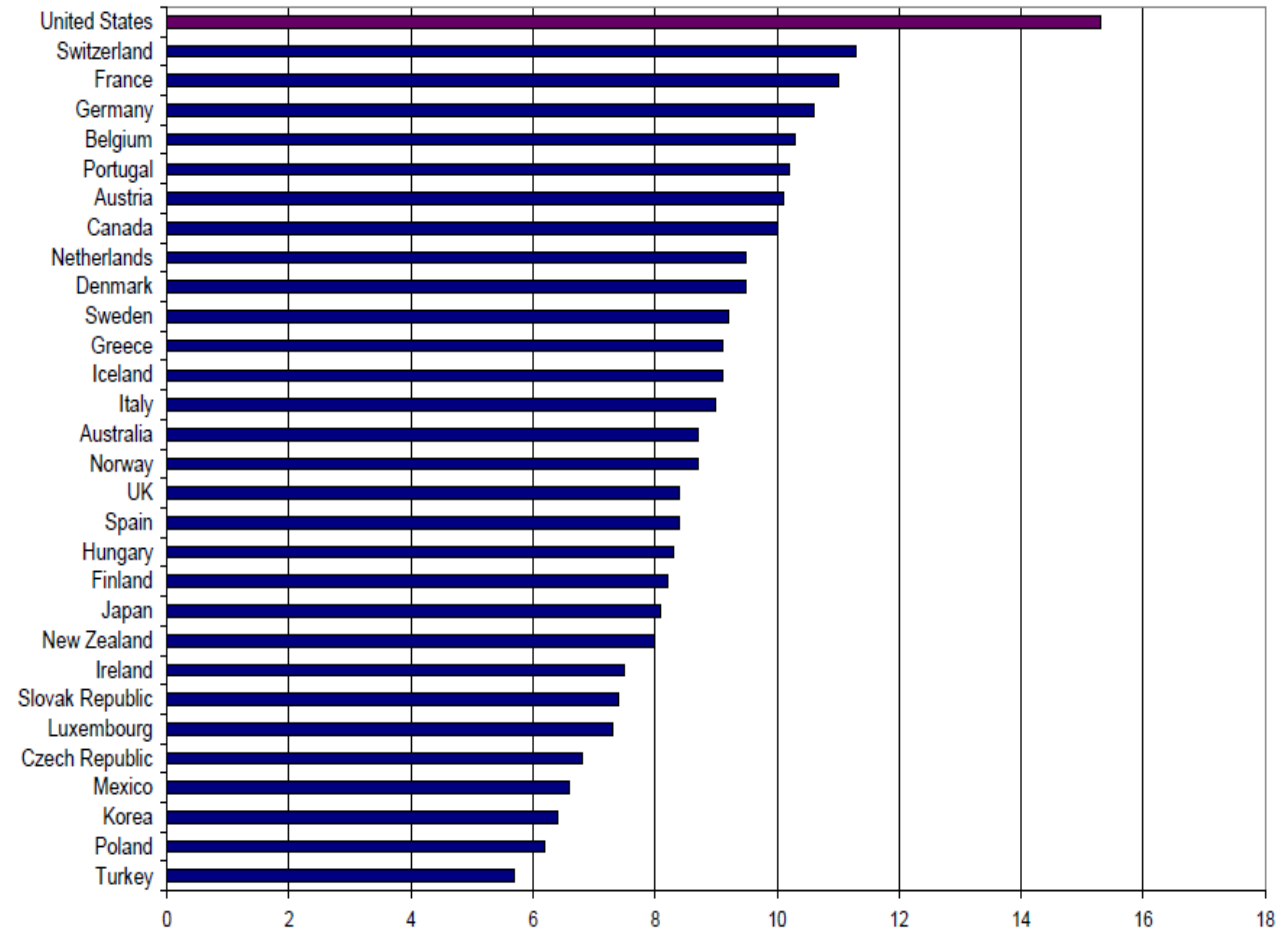

Figure 1. International comparison of health care expenditure as a share of GDP, 2006 [1]

In terms of incremental health care spending, the age-adjusted death rate has declined by 16% among males and 11% among females during the last 10 year period as shown in Figure 2 [3].

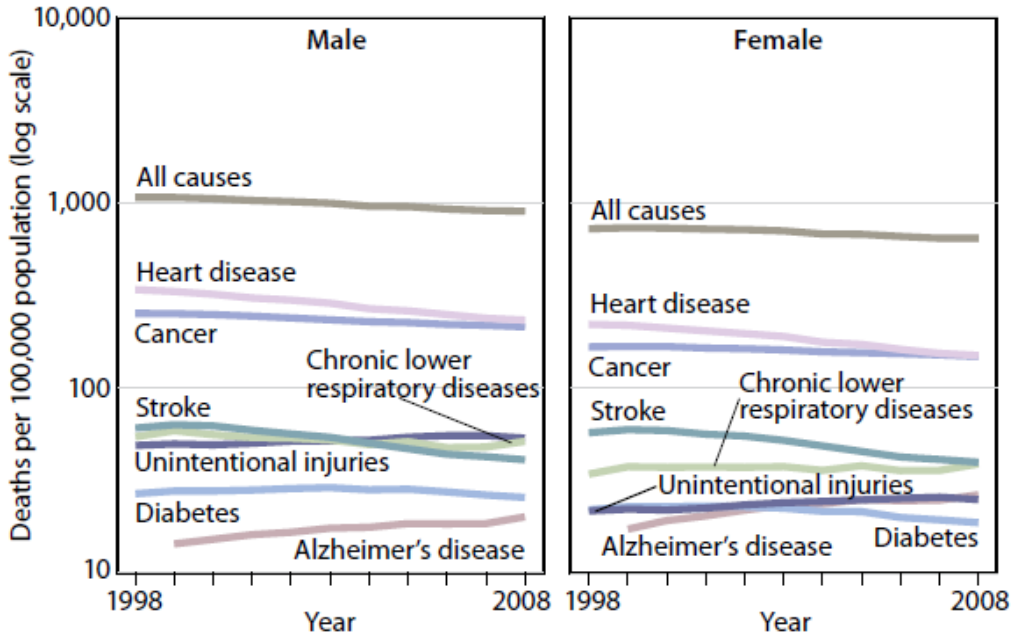

Figure 2. Death rate for selected causes of death for all ages, by sex in the United States [3]

However, even though the number of deaths due to popular diseases such as heart disease, cancer, stroke, etc has decreased over the past 10 years, people are still suffering from these fatal diseases. Among the lethal diseases affecting people today, heart disease resulting from abnormal cardiac function or irregular cardiac structure is the main cause of mortality. According to the National Center for Health Statistics as shown in Figure 3, heart disease has ranked as the leading cause of death in 2009 among males and females [4]. There are several reasons why heart disease is the major disease that threaten people's lives. Several references are showing the cause and reason. The Mayo clinic center explains that heart disease is known as cardiovascular disease(CVD), and the primary reason of heart attack and sudden death is due to narrow and blocked blood vessels which are often accompanied with CVD [5]. According to the UW

Medicine Center [6], heart disease usually includes coronary artery disease, and it occurs when the blood that flows in the vessels is blocked. This is the most common feature of heart disease.

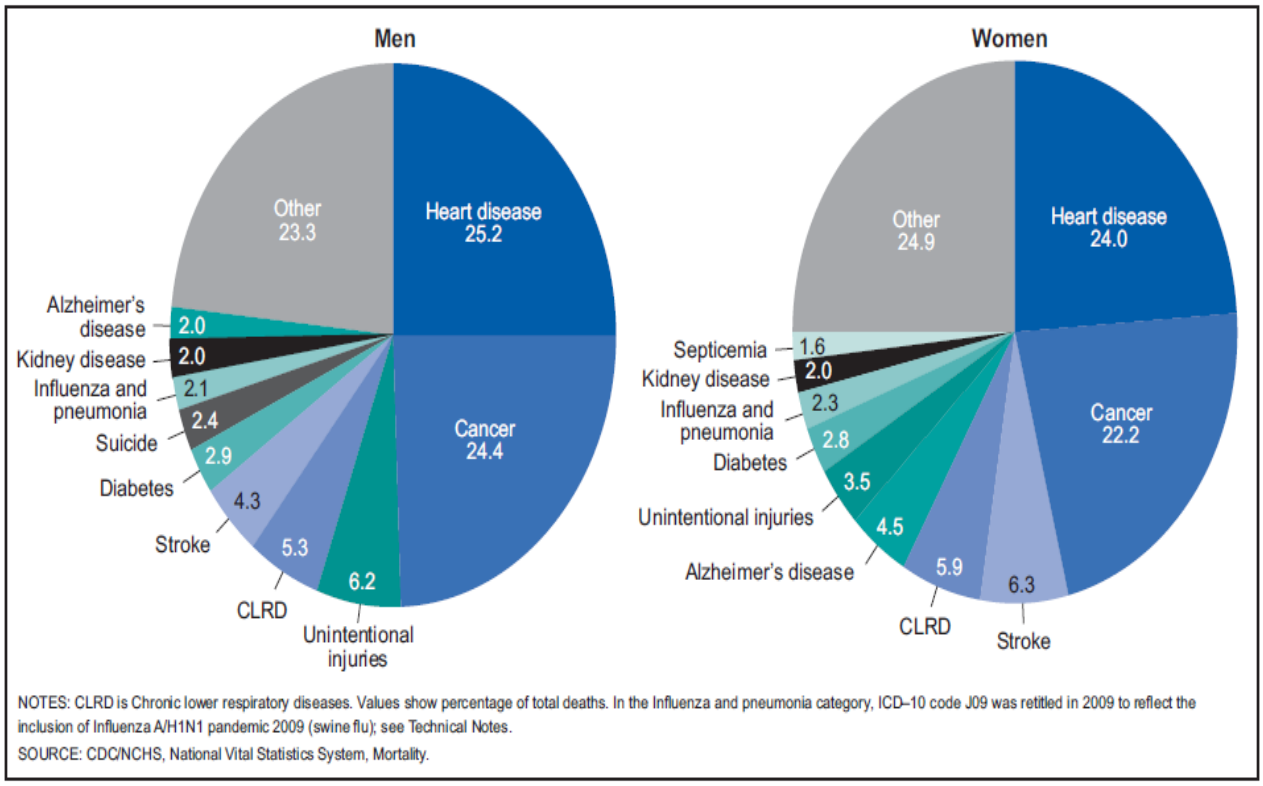

Figure 3. Percent distribution of the 10 leading causes of death by sex in 2009 [4]

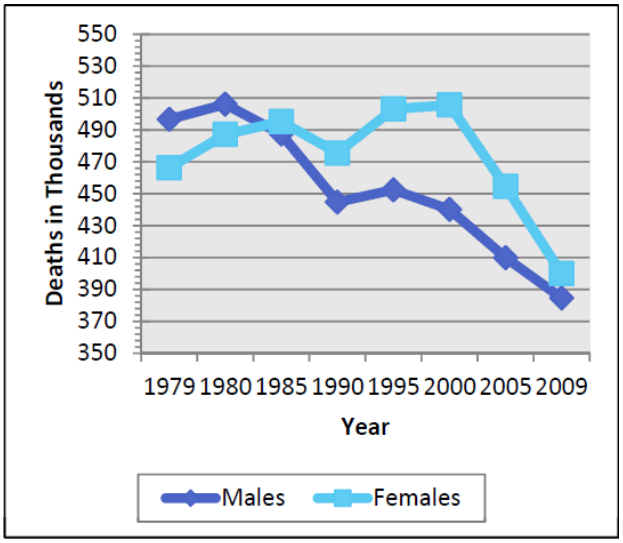

Figure 4. Cardiovascular disease mortality trend for males and females in the United States [7]

An interesting fact for medical researchers and for engineers who are involved in ECG measurement systems is that during the past one decade, women's mortality rate due to CVD is higher than men's rate as shown in Figure 4 [7]. Moreover, a study shows that female adults age 40 and over have a higher death rate than men in one year after having heart attack (23% versus 18%) [8]. As shown in Figure 3 and 4, although both women and men are equally exposed to heart disease, women's death rate due to CVD is higher than men. In spite of this, heart disease is usually recognized as a man's disease. It is a serious issue that even though the occurrence rate of female heart disease has been increasing over the past 10 years, the awareness of this problem is not quite enough. A study has tried to explain the reason of higher death rate of women due to heart disease, and the study shows that the female hormone, estrogen, has been considered one of the most effective causes of blood clot [9]. However, other study mentioned that the effect is minimal in post menopausal women [10], and a survey shows appropriate reason. According to the American Heart Association [11], the survey was performed between 1997 and 2009 in order to investigate the trend in awareness of the leading causes of death among women. Only 54 % of respondents recognized that cardiovascular disease has ranked as the first leading cause of mortality among women. At this point, we need to consider why the female death rate due to CVD is higher than men's and why there is a wide spread lack of awareness of female heart disease. We can discover the reason in a study explaining that the symptoms of a female heart attack differ from that of a male heart attack. There are several common heart attack symptoms depending on the type of heart disease such as chest pain, shortness of breath, weakness or coldness in the legs or arms, a racing heartbeat, a slow heart beat, unusual fatigue, indigestion, sleep disturbance, dizziness, etc [5] [12]. Among these symptoms, chest pain is the most

common symptom recognized as a prodromal symptom of a heart attack in both men and women, but often women do not experience severe chest pain, as if an elephant was sitting on the chest, during a heart attack. They described that it is just a feeling of discomfort, not pain. Among 515 case studies of female patients who had experienced a heart attack, 43% of the patients responded that they did not experience chest pain during the heart attack [2]. Given that the reasons behind the lack of awareness about heart disease differing symptoms and the high possibility of sudden death due to heart disease in women, it is very important to develop an ECG measurement system for women.

1.2 Portable and ambulatory concept for ECG measurement system

As we have already seen in chapter 1.1, people are more interested in their health management in terms of spending huge amounts in order to increase their quality of life. A new concept of health management based on early and self-diagnosis has been expanding from the traditional concept which was focused more on post-diagnosis treatment. Also, there is another recent preclusive health management concept that is focused on user centered health management. Over the past 10 years, in the user centered health management system, a new coinage called U-Health or E-Health, a combination of 'U for ubiquitous or 'E' for electronic, has been spotlighted [13], and a device with this new trend is naturally recognized as a convenient device which includes many advantages such as comfortableness and un-limitation of time, space, and place. The E-Health concept is realized by several wireless communication technologies which are able to share or provide patient's data to clinicians who want to treat diseases or people who want to check themselves with ease, anywhere and anytime. Using such a device instead of visiting a hospital to check physical status prevents an uncomfortable measurement situation where subjects need to lie on a hospital bed for several hours. The combination of wireless communication technology and this comfortable measurement concept leads to the development of an ambulatory and portable ECG measurement system. In other words, users themselves who suffer from CVD and have very active lifestyles can monitor ECG signals continuously with a portable and ambulatory ECG measurement system that includes wireless communication technology.

1.3 Motion artifact removal algorithm requirement

Based on the concept of an ambulatory and portable ECG measurement system as explained in section 1.2, the system has to be able to provide reliable ECG data continuously and periodically identical to the quality of the ECG data set collected at hospital in sedentary measurement environment. In the traditional ECG measurement system, acquiring reliable ECG data is not a big challenge because patients usually lie down on the bed for several hours to measure their ECG data. However, measuring reliable ECG data in the ambulatory ECG measurement system is not easy because of several noise components that are a part of the measurement environment of the subject's active actions. Actually, there are several noise components in the ambulatory ECG measurement system such as system operation noises, and noises due to the subject's movements. The noises due to system operation are classified as high frequency component noises, and the noises due to the subject's respiration and movement actions are classified as low frequency component noises. Among these noise components, removing the noises including high frequency components is not a big challenge in the ECG measurement system because the distribution of frequency range between pure ECG signal and the noise components is clearly different. Usually, the frequency range of ECG components; P wave, QRS complex, and T wave, is distributed from 0.1 to 35 Hz as shown in Figure 5 [14], and the frequency range of noises including high frequency components exceeds 100Hz. Therefore, by using liner a band pass filter or low pass filter, the high frequency components can be removed without any effect on pure ECG components.

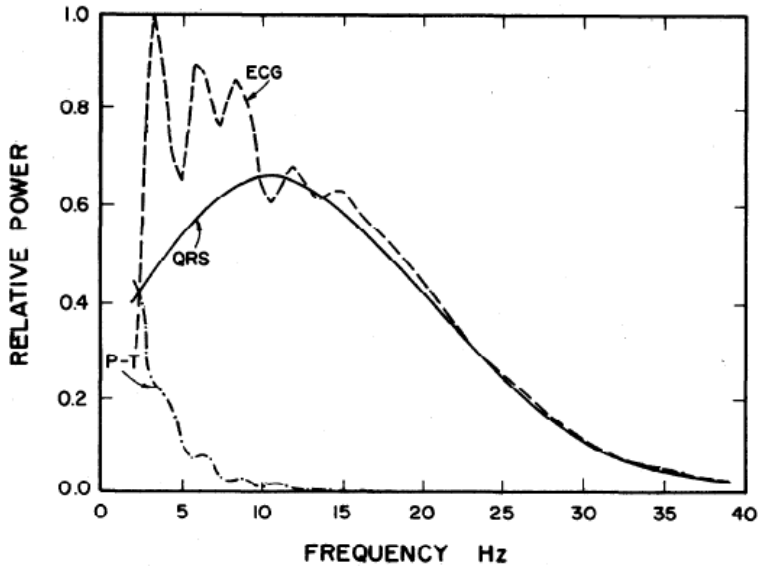

Figure 5. Power spectra of ECG, QRS complex, P and T waves [14]

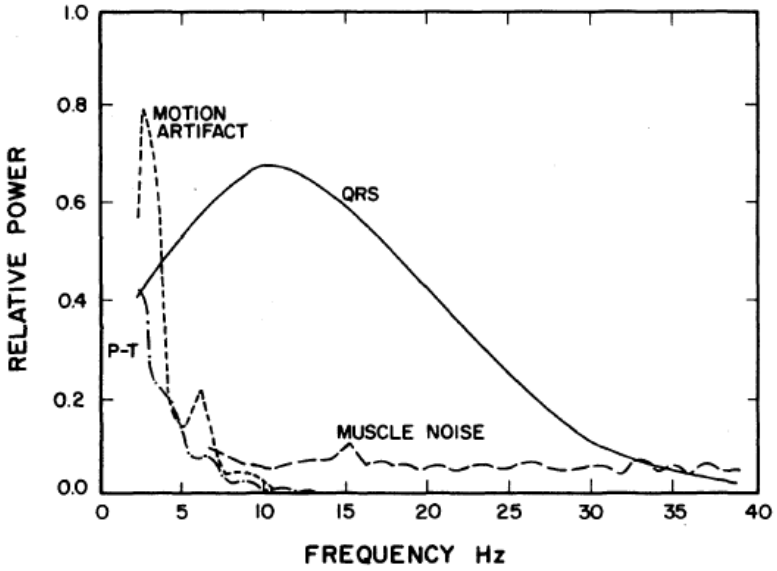

Figure 6. Power spectra of motion artifacts [14]

However, removing the noises including low frequency components, called motion artifact (MA), is a big challenge because the frequency range of the MA component is generally distributed from 0.1Hz to 10 Hz as shown Figure 6 [14]. It is very common that the frequency duplication has a severe effect on distortion of the ECG components; P-QRS-T, because the high noise amplitude due to MA component can produce the amplitude modification of the ECG

components. The phenomenon leads to one of the reasons for misdiagnosis, and it is not an exaggeration to say that the quality of an ambulatory ECG measurement system depends on how much the system can remove the MA components. Therefore, the problem of the MA in the ambulatory ECG measurement scenarios should be solved in order to acquire reliable ECG signal because the main purpose of the ambulatory ECG measurement system is to provide a reliable ECG signal identical to quality of an ECG signal that is detected in any hospital under controlled conditions.

1.4 Other studies for removing motion artifact components

As we discussed in the section 1.4, MA components must be removed in order to acquire reliable ECG data from the ambulatory ECG measurement system. There is a lot of study dedicated to developing an algorithm to remove motion artifact. One early approach was to use a linear FIR filter to remove a baseline wandering noise component included in a measured ECG data set [15]. However, the study showed the limited definition of the baseline wandering noise frequency component. The study assumed that the frequency range of baseline wandering noise is under 0.7Hz, so the noise that might be possible in the range between 0.7Hz and 10Hz as shown Figure 6 was not considered. Many current researchers have put in the effort of solving the frequency duplication problem, and as a result, an adaptive filter(AF) theory [16] and independent component analysis (ICA) theory [17] [18] [19] have been introduced as the representative theories for separating a signal from frequency overlapped signals. However there are two considerations to utilize the two theories in the ambulatory ECG measurement system.

The first consideration reveals on the applications of the AF theory. The concept of adaptive noise cancellation has been introduced [16] [20] [21] , and the adaptive signal processing is known as the free technique from the distortion problem of origin signal. A study shows that it is possible to remove ECG interference in brain waves by using noise cancellation theory [22]. Monitoring fetal ECG for early diagnosis of heart abnormalities is one of the applications of the adaptive noise cancellation concept [23]. In addition, the adaptive noise cancellation algorithm has been used in the industrial product to remove echo cancellation for a microphone system [24]. There are several papers dedicated to removing MA components in ECG measurement scenarios by using the adaptive filter theory. A study shows one of the

adaptive filtering applications to remove baseline wandering noise and 60Hz power noise interference [25], but the frequency range of the baseline wandering noise was assumed to be under 1Hz in this paper. A paper was dedicated to reducing motion artifacts and interference in ECG measurement scenario [26], but a reference which is considered to be the MA component in ECG measurement situation was measured by a pair of electrodes separated from the primary signal which is considered to be the measured ECG signal. This method is not suitable for ambulatory ECG measurement because it would increase the system cost and complexity. In recent investigations, researchers have developed their own chipset including a motion detect sensing part, and they suggested the combination of the chipset usage and adaptive filter theory to extract clear ECG signal without MA [27]. Other study suggested a moving average filter for reference input of the AF algorithm [28]. In this application, the noise patterns were created by a subject's limited actions in order to produce the low frequency component. As we saw in the above other papers, to utilize the AF theory, a reference signal the same as MA components in ECG measurement scenarios has to be acquired. To overcome the problem of acquiring the reference signal in the applications of the AF, several papers have focused on the definition and characterization of the MA components involved in the measured ECG signal. Two studies showed the identification of the MA component on the ECG signal with wavelet transform and a neural network [29] [30], but the applications have a limitation in that the wavelet algorithm is not good at detecting such a noise which includes a smooth and continuous low frequency sinusoid. Another paper has suggested attaching a 3-axis accelerometer on the E-textile ECG measurement system in order to detect MA components [31], but the method leads to an increase in the system cost because of attaching the 3-axis accelerometer.

The second consideration reveals on the applications of the ICA algorithm. The ICA algorithm has generally been focused on as one of the solutions for the cocktail party problem involving the separation of individual voices from mixed voices in a conversation situation. It is known as the best technology that can separate source signals from mixed signals which are linearly combined with each independent source signal by using several statistical theories [32] [33]. There are several studies using ICA theory to look at pure ECG components in the ECG measurement scenarios. An early ICA approach to ECG measurement systems, a paper was dedicated to separating an ECG signal from 3 channel ECG signals mixed with noise components by using optimized Kurtosis theory which is one of the statistical theories for ICA implementation [34]. A recent paper tried to evaluate the performance of the ICA and adaptive filter algorithms in a measurement situation where the system can detect 3 channel ECG signals [35], and another paper used principle component analysis (PCA) and ICA to reduce noise components in 8 channels for ECG measurement [36]. However, those applications are not suitable to adapt the ICA algorithm for an ambulatory ECG measurement system which can provide only a single channel because at least two measured ECG signals are needed to adapt the ICA algorithm.

As discussed in this section, there are two big considerations to use the AF and the ICA in the ECG measurement system. The former is how to acquire noise component as the input of the reference signal for AF noise cancellation structure, and the latter is how to solve the requirement of two measured ECG signals to remove MA component by ICA theory. In this dissertation, two augmented motion artifact removal algorithms (MARAs) are suggested as the solutions of the two considerations in chapter 4.

1.5 Objectives and organization

As there is increasing the demand and requirement of the ambulatory ECG measurement system, researchers are increasingly interested in developing a wearable, light-weight, comfortable, flexible, and portable ECG measurement device. As a part of the trends, an ECG measurement device of one of the ambulatory ECG measurement systems for women was developed in our lab, and the system is named as “E-Bra system”. The E-Bra system is able to monitor an ECG signal periodically and continuously for women, and it is designed with very a compact size as small as it can be attached at the bottom layer of women’s brassiere. Now that the E-bra system is ambulatory device type, removing MA component is critical issue in order to acquire reliable data as mentioned in section 1.3. This dissertation is totally dedicated on designing the E-bra system structure and implementing the performance evaluation for the suggested two MARAs including several theories and technologies such as adaptive filter, ICA algorithm, and a noise component extraction algorithm (NCEA).

The organization of this dissertation is as follows. The fundamental background to understand this dissertation including ECG components information, AF theory, and ICA theory will be explained in chapter 2, and the hardware structure and software architecture for the E-Bra system will be discussed in chapter 3. In chapter 4, there are several crucial algorithms such as a calculation method of the signal and noise ratio (SNR) for the E-Bra system, a noise component extraction algorithm (NCEA) to acquire noise components from an ECG data set collected by the E-Bra system, a motion artifact removal algorithm (MARA) with adaptive filter (AF) structure, and a motion artifact removal algorithm (MARA) with independent component analysis (ICA) structure. The performance evaluation and comparison between the two MARAs with AF and

ICA structure will also be explained in chapter 4 by using three ECG data sets obtained from the website which is freely accessible; www.physionet.org. 30 ECG data sets were collected from three women volunteers in the different test scenarios such as a stationary test case with exaggerated deep breathing to produce respiration MA component, a walking test case, and a running test case. Among 30 results estimated by implementing the two MARAs, one result will specifically be discussed in chapter 5, and other results will also be shown in a chart which reveals the variation of the correlation and SNR values. The conclusion is given in chapter 6.

Chapter 2: Fundamental background for ambulatory women ECG measurement system

2.1 Fundamental background of electrocardiogram(ECG)

2.1.1 Electrocardiogram(ECG)

The electrocardiogram (ECG) is a graphic recording of the electrical currents of the cardiac cells detected by the body's surface. The electrical forces are produced by cardiac contraction and relaxation, and electrical forces are converted to the potential voltage value by electrode sensors. The potential voltages reveal a waveform feature, and observing the waveform is useful for investigating the heart disease such as cardiac dysrhythmias, myocardial infarction, and cardiac hypertrophy and for evaluation of the effectiveness of cardiac medication because the waveform includes heart activities information. The detailed explanation of the heart waveform features will be discussed in section 2.1.5.

2.1.2 Physiology of the heart

The heart is a muscular organ to supply blood and nutrients to all parts of organs and tissue in human body through blood circulation. Two-thirds of the heart is situated to the left of the midline of the body and one third is located to the right in thoracic cavity. It consists of four chambers in thoracic cavity. Two upper chambers called atria are separated by interatrial septum. The lower chambers named ventricles are also divided by interventricular septum. There are several elements in the heart chamber to prevent back flow of the blood such as two atrioventricular valves, the tricuspid valve, and the mitral valve. The valves are located between each atria and ventricles. The right atrium receives deoxygenated blood from the body via the superior and inferior venacava. The right ventricle receives blood from the right atrium, and the right ventricle pumps it to the lungs via inferior venacava. The oxygenated blood is received

from the lung through four pulmonary veins the left atrium propels to the left ventricle. The largest and most muscular left ventricle pumps oxygen rich blood into the systemic circulation via aorta. The left ventricle‘s vigorous contraction generates blood pressure. The cardiac cycle is repeated time after time whenever heart is beating.

2.1.3 Conduction system

The chambers contract and relax in a regular sequence which is controlled by an electrical impulse. This impulse begins in the heart’s natural pacemaker (the sino-atrial node), which is situated in the upper part of the wall of the right atrium of the heart. The electrical impulse generated by the SA node travels from cell to cell through the heart until it reaches the atrioventricular node (AV node). The AV node is situated in the center of the heart, at the bottom of the right atrium, between the atria and ventricles. The AV node receives the electrical impulse produced by the SA node, and the AV node makes a small delay and regulates the electrical impulse. The regulation process not only prevents rapid conduction such as atrial fibrillation, but also allows the blood to travel through the atrioventricular valves, and the blood enters ventricles before contraction. After the delay regulated by the AV node, the electrical impulse passes through AV Bundle into the Bundle of His located between the right and left ventricles. These bundles then innervate the ventricular walls via the Purkinje fibers. When the signal reaches the Purkinje fibers, ventricular contraction occurs. The blood flows from the right ventricle into the lungs, and the blood flows from the left ventricle through the aorta to whole body. This process then repeats for the next heartbeat.

2.1.4 12 Leads placement for ECG measurement scenarios

2.1.4.1 Introduction

While the myocardium is activated, the electrical impulse is diffused in diverse route. These electrical currents can be detected from the body with electrodes placed on the skin and recorded in the waveform of an ECG. The electrocardiographic lead, constitute of a positive and a negative electrode, is the basic component of monitoring and recording devices. The waveform recorded by the leads placed various positions represents different deflections which are a series of positive and negative features for the ECG. These differences result from corresponding to the heart's electrical activity. There are twelve universal ECG measurement scenarios for recording the heart activities; Six limb leads (I, II, III, AVR, AVL, AVF) and six chest leads (V1-V6) as shown in Figure 7.

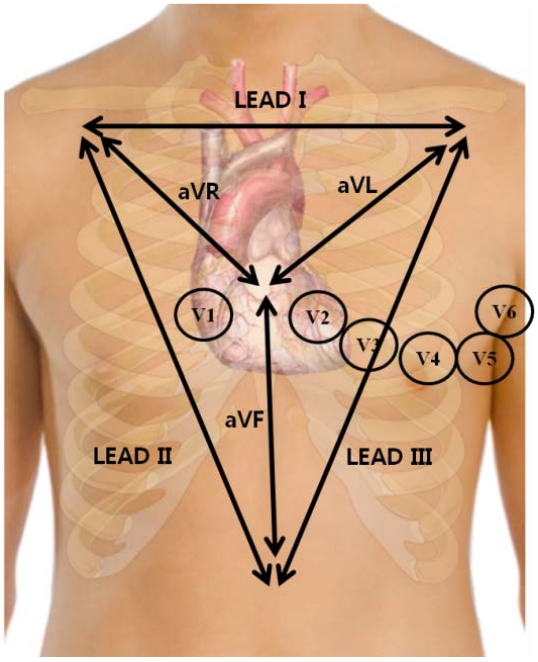

Figure 7. 12 leads ECG measurement

2.1.4.2 The limb or extremity leads

Limb leads consist of 4 leads placed on the limbs. An electrode is located on the four limbs, which are left, right wrist and left, right ankle. The lead connected to the right ankle is a neutral lead, but it plays no role in the ECG itself. The limb leads are classified as standard limb leads –three and Augmented limb leads three.

2.1.4.3 The chest or precordial leads

The chest leads are labelled from V1 through V6 in a row, from the patient's right to his left side successively. The chest leads cover the heart in its anatomical position in designated areas.

- Lead V1 is located in the fourth intercostal space just to the right of the sternum
- Lead V2 is located in the fourth intercostal space, just to the left of the sternum
- Lead V3 sits on midway between V2 and V3
- Lead V4 is located in the fifth intercostal space in line with middle of the clavicle
- Lead V5 is located below the beginning of the axilla, at the same level as the fifth intercostal space
- Lead V6 is located below the mid-axillary line, which is further than the fifth intercostal line.

2.1.5 ECG waveform features

2.1.5.1 ECG rhythm

Each portion of a cardiac cycle generates a different deflection on the ECG. These deflections are recorded as a series of positive (upward) and negative (downward) waves. A

normal ECG shows five visible wave forms. One cardiac cycle is represented by the P wave, QRS complex, and the T wave. The cycle is repeated continuously and periodically. A cardiac cycle is represented by systole, ventricular contraction, and the resting stage between each beat. Each lead detects cardiac electrical activity from a different direction. Although the diagram consists of 5 waves (P wave, QRS complex, and T wave), the Q wave or S wave sometimes are not visible an ECG waveform. Figure 8 shows an ECG waveform composed of 5 waves.

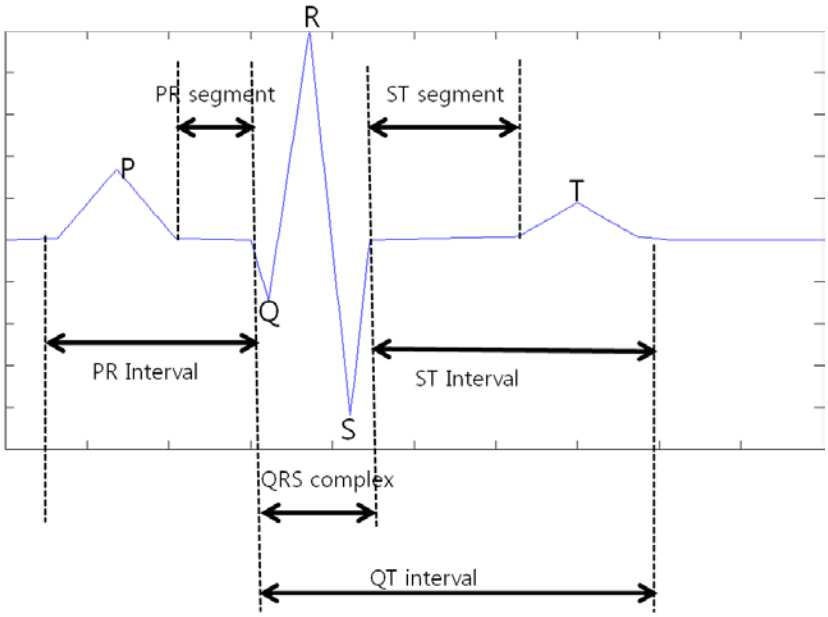

Figure 8. An ECG waveform

2.1.5.2 P wave

The P wave which is the first wave on ECG represents atrial depolarization from SA node near top of the atrium, and it is usually 0.08 to 0.1 seconds (80 – 100ms) in duration, and the duration of the P wave is also usually between 0.08 to 0.1 seconds (80 – 100ms). The amplitude of P wave is not more than 2.5 mm in height and gently rounded, not sharped. Elevated shape of P wave may indicate right atrial enlargement. Wider morphologies may result from left atrial enlargement.

2.1.5.3 QRS complex

The QRS complex represents the ventricular depolarization. The wave consists of a first downward deflection (Q wave), a large upward deflection (R wave), and a second downward deflection (S wave). The duration of the QRS complex is normally less than 0.12 second.

2.1.5.4 T wave

The T wave results from a propagated current during ventricular repolarization. It is normally upright, rounded, and slightly asymmetric. The amplitude of the normal T wave is less than 5mm in the limb leads and 10mm in the chest leads. Its morphology will change in case of breath holding and digitalis toxicity. The T wave may be inverted or flat with conditions such as myocardial ischemia, bundle brach block, ventricular hypertrophy. The T wave is flat and notched in case of pericarditis, hypothyroid, and cardiomyopathies and flat with hypokalaemia.

2.1.5.5 P-R interval

The P-R interval is measured from beginning of the upslope of the P wave to the beginning of the QRS wave. Normally, the PR interval is between 0.12 and 0.20 second in duration.

2.1.5.6 Q-T interval

The Q-T interval is measured from the beginning of the QRS complex to the end of T wave. Generally, the Q-T interval represents the duration of activation and recovery of the ventricular myocardium. The duration of the QT interval varies in accordance with heart rate, gender, and age. The QT interval should be greater than half of the preceding R-R interval. The Q-T interval is shortened at fast heart rate and lengthened at slow heart rates. For that reason, the

Q-T interval should be corrected at a heart rate of 60bpm. The corrected QT interval is calculated by dividing the QT interval by square root of the preceding R-R interval. Normally it is 0.42 second.

2.1.5.7 P-R segment

The P-R segment is the flat, usually isoelectric line between the end of the P wave and the beginning of the QRS complex. The PR segment signifies the time taken to conduct through the slow AV junction.

2.1.5.8 S-T segment

The ST segment is the flat, isoelectric line of the ECG between the end of the S wave and the beginning of the T wave. It represents the interval between depolarization and repolarization of the ventricular musculature. The most important cause of ST segment abnormality (elevation or depression) is either myocardial ischemia or myocardial infarction.

2.2 Adaptive filter theory

The ECG signal measured by the E-Bra system includes not only pure ECG information but also noise components due to subject's body movement related to different activities. The noise component is unknown and unpredictable component in time variance. In other words, the MA components are created in time varying measurement environment. Therefore, to extract pure ECG signal from the measured ECG signal mixed with noise component, a filter have to be satisfied with the adaptive feature to deal with the noise in the face of changing measurement environment. AF can adjust and track their coefficient in terms of minimizing an error signal between a reference signal and a desired signal in time variance. It can be realized with transversal finite impulse response (FIR) filter structure or infinite impulse response (IIR) filter structure. In this dissertation, the AF composed of transversal FIR structure and least mean square (LMS) algorithm is used. Figure 9 shows block diagram of transversal filter structure.

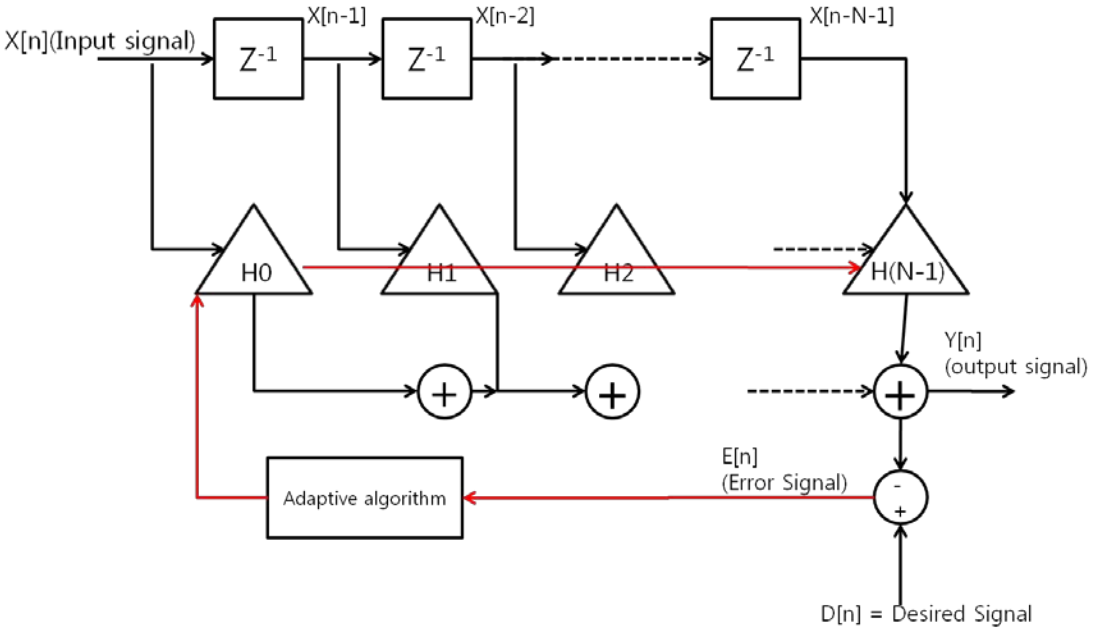

Figure 9. Adaptive filter with transversal filter structure

In Figure 9, at each time n, the output Y⌊n⌋ can be computed from the summation of H coefficient which is updated by LMS adaptive algorithm and input signal samples, where X[n], X[n-1],…,X[n-N+1]. The equation for Y[n] can be formulated as the below equation.

$$Y[n] = \sum_{k=0}^{N-1} H[n]\, X[n-k]$$

The H[n] is a varying coefficient depended on time variance, and the value is adjusted on each calculation step in order to minimize the error signal.

2.2.1 Least mean square(LMS) adaptation algorithm

The LMS algorithm has been introduced by Widrow [37] [16] [38]. The purpose of LMS algorithm is to acquire H[n] coefficient minimizing a cost function. The cost function for LMS algorithm is selected by the $E\{error^2(j)\}$, where E denotes a expectation operation, the error value, $error_j = D_j - Y_j$, is the estimation error, D_j is the desired response, and Y_j is the actual filter output.

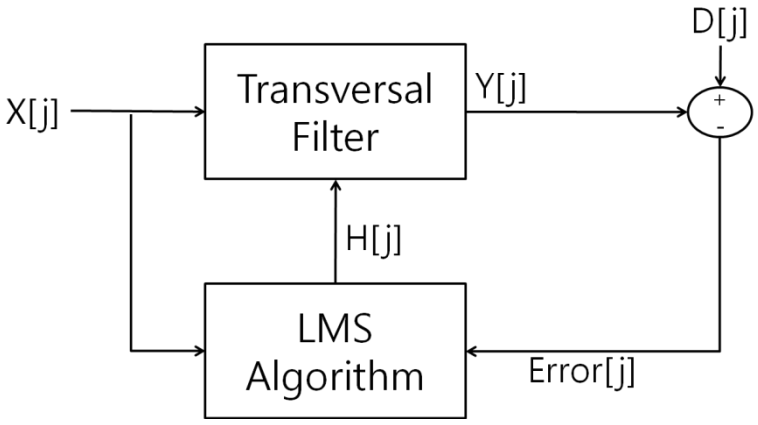

Figure 10. Block Diagram of Adaptive Filter with LMS algorithm

From Figure 10, we can acquire Y_j from the summation of X_j^T and H_j as shown in the below equation.

$$Y_j = X_j^T H_j = H_j^T X_j \quad (2.1)$$

The purpose of the LMS is to acquire H[j] coefficient values minimizing the expected value of the error signal, and the error equation can be written as shown in the equation (2.2).

(Error) $$error_j = D_j - Y_j = D_j - X_j^T H_j = D_j - H_j^T X_j \quad (2.2)$$

By taking squared error concept, $(error_j)^2$ and the expectation value, the $error_j$ can be written as shown in the equation (2.3) and (2.4).

(Error Square) $$(error_j)^2 = (D_j - X_j^T H_j)^2$$

$$= (D_j)^2 - 2D_j X_j^T H_j + H_j^T X_j X_j^T H_j \quad (2.3)$$

(Mean Square Error) $$\varphi_j^2 = E[error_j^2] = E[D_j^2] - 2E[D_j X_j^T] H_j + H_j^T E[X_j X_j^T] H_j$$

$$= E[D_j^2] - 2PH + H^T R H \quad (2.4)$$

The expected value in equation (2.4), $E[D_j X_j^T]$ is the cross-correlation function between D_j, the desire signal and X_j^T, input signal, and another expected value $E[X_j X_j^T]$ is the auto-correlation function of input signal. The expected values can usually be estimated by large sampling number, but in case of short sampling number of the LMS algorithm, the expected values can be considered the same as $E[D_j X_j^T] = D_j X_j^T$ and $E[X_j X_j^T] = X_j X_j^T$. By taking gradient descent concept, which is able to find a position on the error surface of the equation (2.4) in terms of steepest descent, the equation (2.5) can be acquired [39]. In other word, the minimum (optimum) value of the mean square error shown in equation (2.4) can be estimated in the direction of the negative gradient of the cost function of $E\{error^2(j)\}$ with respect to the H coefficient.

(Gradient of Mean Square Error with respect to H coefficient)

$$\frac{\partial \varphi_j^2}{\partial H} = \frac{\partial}{\partial H}\left(E\left[D_j^2\right] - 2p^T H + H^T R H\right)$$

$$\frac{\partial \varphi_j^2}{\partial H} = \nabla = -2P + 2RH \qquad (2.5)$$

where, $E\left[D_j X_j^T\right] = D_j X_j^T = P$ and $E\left[X_j X_j^T\right] = X_j X_j^T = R$.

The equation (2.5) can be written as the equation (2.6).

(Estimated Gradient) $$\tilde{\nabla} = \frac{\partial er_j^2}{\partial H} = 2(D_j - X_j^T H_j)X_j$$

$$= -2er_j X_j \qquad (2.6)$$

To find current H coefficient by using the equation (2.6), as mentioned the theory of steepest decent method, the current H coefficient can be updated at every sampling time as shown in the equation (2.7)

(Steepest descent theory) $X_{j+1} = X_j + \mu(-\tilde{\nabla})$, where (μ is step size for convergence)

(Estimated H coefficient) $$\therefore H_{j+1} = H_j + 2\mu er_j X_j \qquad (2.7)$$

2.2.2 Noise cancellation concept by adaptive filter

The basic idea of noise cancellation concept by AF theory is that an output signal can be acquired by subtracting between a noise signal and a source signal, where the noise signal is MA component and the source signal is the ECG components collected from the E-bra system. Figure 11 shows the block diagram of the traditional adaptive noise cancellation concept.

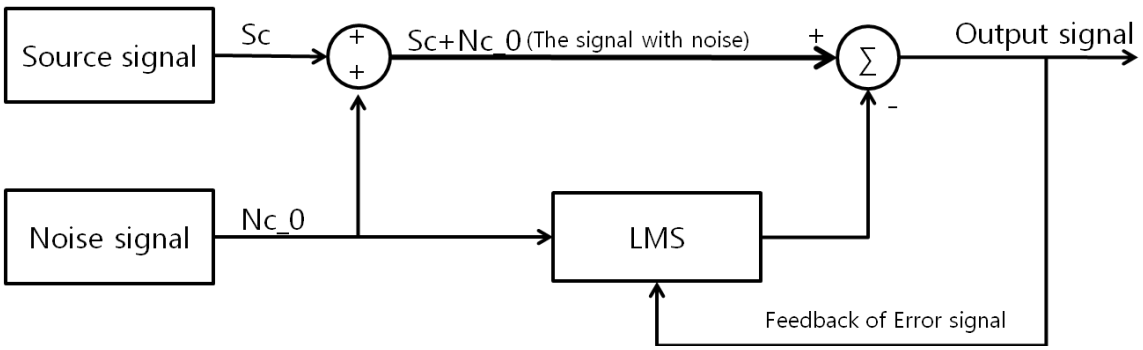

Figure 11. Block diagram of adaptive noise cancellation concept

The basic assumption to use the adaptive noise cancellation concept is that the original noise component Nc_0, which is a MA component included in an ECG component, is basically uncorrelated with source signal Sc, which is a pure ECG components without MA component. However, an ECG signal collected by an ambulatory ECG measurement system includes in both components; the source component and the noise component, and the ECG signal can be represented as Sc+Nc_0. In terms of uncorrelation assumption, the expected values between source signal Sc and noise signal Nc_0 can be written as $E[S_j Nc\_0_j] = 0$. The output signal Y produced by AF process then can be expressed by the combination of a noise reference, Nc_0 and H coefficient as the equation below.

$$Y_j = \sum_{k=0}^{N} Nc\_0_k(j) H_k(j-k)$$, where Y_j is output.

The error signal is defined by subtracting the output signal, Y_j , and $D_j = S_j + Nc\_0_j$ as shown in the equation below.

$$Error_j = D_j - Y_j$$

Then, solving the noise cancellation problem becomes the same as estimating the minimum (optimum) error value as we discussed in session 2.2.1.

2.3 Independent component analysis(ICA) theory

ICA (Independent Component Analysis) is an algorithm whose the purpose is to separate independent signals from signals mixed by linear combination of independent signals and an unknown mixing vector. In other words, an arbitrary signal mixed by linear combination of source signal components and unknown mixing vector can be separated to the source signals by multiplying an estimated unmixing vector W that includes minimum statistical dependency of the mixed signals. The unmixing W vector can be estimated by using several statistical theories: kurtosis, entropy, maximum likelihood, complexity, and so on. ICA is being spotlighted as one of the solutions in the voice recognition and separation research area: cocktail party problem. These days, usage of ICA algorithm is gradually spreading to other areas of application. Especially, the requirement of ICA is increasing in the bio signal analysis research area. In this dissertation, we mention an algorithm based on the ICA that can extract ECG feature information from a mixed signal including the ECG components and motion artifact components.

2.3.1 Independent component analysis

The purpose of the ICA is to recover source signals from signals that are linearly combined by unknown mixing vector A and source signals. The basic concept is as follows. In Figure 12, the observed variables x_i denotes as an observed vector $X = [x_1, x_2, \dots, x_n]^T$, and the source variables s_i denotes as $S = [s_1, s_2, \dots, s_n]^T$.

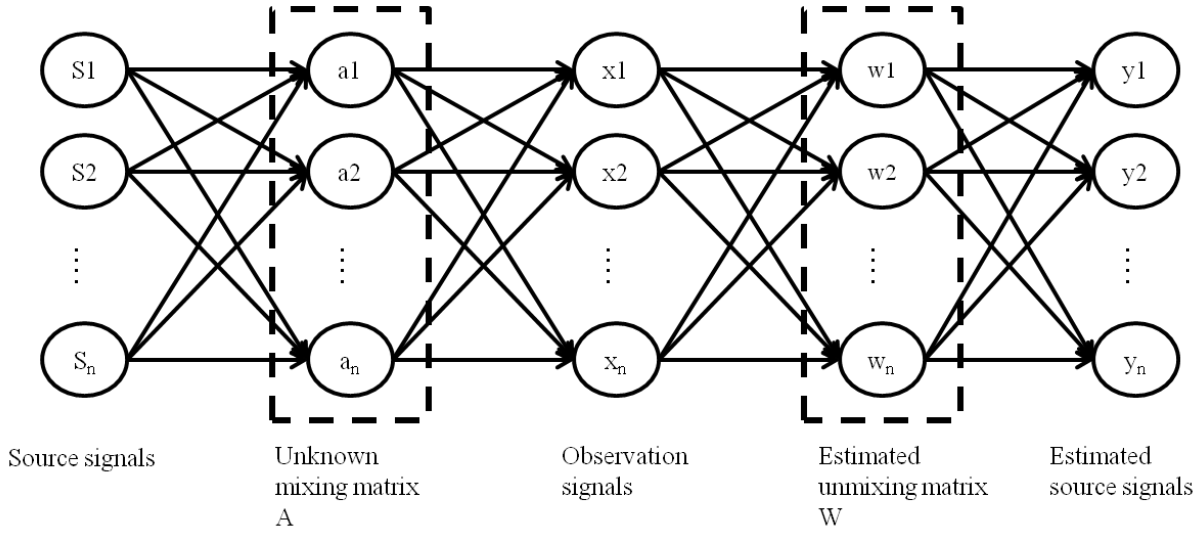

Figure 12. Data structure of independent component analysis.

Linear combination of source signals and unknown mixing matrix A can be represented by observation signals as shown in equation (2.8). In this paper, the observation signal, X is the measured ECG signal from the E-Bra system.

$$x_1(t) = a_{11}s_1(t) + a_{12}s_2(t)$$

$$x_2(t) = a_{21}s_1(t) + a_{22}s_2(t)$$

$$X = AS = \sum_{i=1}^{n} a_i s_i \tag{2.8}$$

The estimated source signal then can be acquired by the combination of a weighted unmixing vector W and the observation signal X as shown in equation (2.9).

$$y_1(t) = w_{11}x_1(t) + w_{12}x_2(t)$$

$$y_2(t) = w_{21}x_1(t) + w_{22}x_2(t)$$

$$Y = WX = \sum_{i=1}^{n} w_i x_i \tag{2.9}$$

By observing the equations (2.8) and (2.9), we can recognize that if we can estimate the W vector which has the characteristic of $A^{-1} = W$, the weighted unmixing vector W can be estimated by the equation below.

$$Y = WAS$$

$$\therefore Y = S \text{ , where } A^{-1} = W$$

In this dissertation, source signals are a pure ECG signal and an MA component due to subject's movements. Here, we just know only the observation signals X, which is an ECG signal collected by the E-bra system, and the collected ECG signal includes both source signals which are the pure ECG component and the MA component. With the collected ECG signal, if we can find unknown unmixing matrix W which includes in the characteristic of the inverse matrix of unknown mixing vector A, we can estimate source signals S by equation (2.9). There are a variety of statistical algorithms to estimate the weighed vector W: Entropy, Kurtosis, maximum likelihood, FastICA and so on [40] [41] [32] [42]. Among the statistical theories, Entropy and FastICA theories will be explained in next two sections.

2.3.2 Entropy

The purpose of the ICA is to extract the unmixing weighted vector W. We can estimate the independency of a set of the mixed signals by using a statistical quantitative value, which is entropy [43]. The unmixing vector W that maximizes the entropy value of the extracted signal can also maximize the degree of the independence between source signals. The extracted signal involving the weighted vector W with maximum entropy value can be considered a source signal. Informax concept is known as the process of finding independent signal by maximizing entropy value [42]. The entropy can measure the uniformity of distribution of a set of values, and complete uniformity means maximum entropy. We can drive equation (2.10) by definition of entropy, where y=WX , Z=g(y), and g is cdf(cumulative distribution function). Equation (2.11) can be expressed by the pdf y of the estimated signal y = WX , the pdf Pz of cdf y, and the

Jacobian[10]. Here, Jaccobian can be replaced by the pdf p_s assumed as the source signal [11]. Therefore, the function p_s can be considered to the pdf of source signals of the mixed signal because the weighed vector W that maximizes entropy value of the collected ECG signal can make the pdf $p_y(y) = p_s(y)$, so equation (2.10) can be rewritten as equation (2.12) by substituting equation (2.11) to equation (2.10). The denominator of (2.11), $\left|\frac{\partial y}{\partial x}\right|$, can be written by mapping y=WX as $\left|\frac{\partial y}{\partial x}\right| = |W|$, where $|W|$ is the absolute value of the determinant of the weighted vector W, and the (2.9) can be driven by putting the above equation to (2.13). By the combination of the concept of gradient ascent, tanh function for extracting cdf value, and entropy value of (2.13), the final equation to estimate weighted vector W that maximize entropy of the measured signals can be extracted as equation (2.14)

$$H(Z)= -\frac{1}{N}\sum_{t=1}^{N} \ln p_Z(Z^t) \tag{2.10}$$

$$P_Z(Z)= \frac{P_y(y)}{\left|\frac{\partial Y}{\partial y}\right|} \Rightarrow P_z(Z)= \frac{P_y(y)}{P_s(y)} \tag{2.11}$$

$$H(Z)= -\frac{1}{N}\sum_{t=1}^{N} \ln \frac{P_y(y)}{P_s(y)} \tag{2.12}$$

$$H(Z)= -\frac{1}{N}\sum_{t=1}^{N} \ln \frac{P_x(X)}{|W|P_s(y)} \Rightarrow H(Z)= -\frac{1}{N}\sum_{t=1}^{N} \ln p_x\left(X^t\right)+ \ln|W| + \frac{1}{N}$$

$$\therefore H(Z)= H(X)+ \ln|W| + \frac{1}{N}\sum_{t=1}^{N} \ln p_s(y^t) \tag{2.13}$$

$$W_{new}= W_{old}+\mu \left(W^{-T}- \frac{2}{N}\sum_{t=1}^{N} \tanh(y^t)\left[X^t\right]^T\right) \tag{2.14}$$

2.3.3 FastICA algorithm

2.3.3.1 Approximations of negentropy

The differential entropy H is defined with random vector y with density f(y) as shown in equation (2.15) [44].

$$H(Y)= -\int f(y) \log f(y)\, dy \tag{2.15}$$

According to information theory [44], entropy has the smallest value in the distribution of concentrated data, which has a probability density function(pdf) that is very “peaky”. It means that uniform data distribution has maximum entropy. The negentropy is defined as shown in equation (2.16).

$$J(y)= H\left(y_{(gauss)}\right) -H(y) \tag{2.16}$$

where $y_{(gauss)}$ is a gaussian random variable of the same covariance matrix as y. The equation (2.16) is to obtain the degree of nongaussianity, and it is always nonnegative value and zero under the condition that y has a gaussian distribution. However, the estimation of the negentropy is not easy computationally, so a simple approximation is suggested as shown in equation (2.17) [45].

$$J(y)\approx \left[E\{G(y)\}-E\{G(v)\}\right]^2 \tag{2.17}$$

where, y is variable assumed to be of zero mean and unit variance, v is a gaussian variable of zero mean and unit variance, and G is a nonquadratic function. In particular, choosing below two G functions as shown in equation(2.18) are very useful for negentropy.

$$G1(u)= \frac{1}{a1}\log\cosh(a1u),\ G2(u)= -e^{(-\frac{u^2}{2})}$$

$$g1(u)= \tanh(a1u),\ g2(u)= ue^{(-\frac{u^2}{2})} \quad (2.18)$$

where, $1 \leq a1 \leq 2$ is a suitable constant. By maximizing the function of J(y), the sources can be decomposed from the mixed signal.

2.3.3.2 Newton method

Newton-Raphson method is known as the fast approximation to find the true root of a real valued function of the nonlinear equations. Figure 13 shows the second order Newton's method.

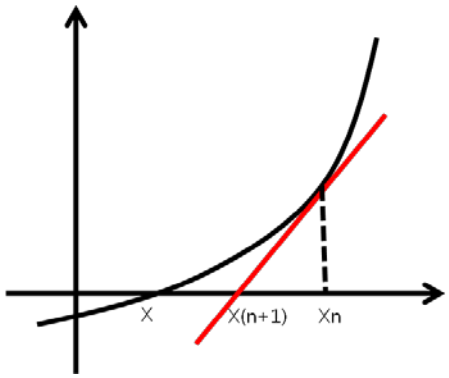

Figure 13. Second-order Newton's method

The process is started on the initial assumption that a position is reasonably close to the true root, and the nonlinear function is approximated by the tangent line such as the red color line. The x(n+1) in the tangent line can be considered as a better approximation root than the original assumption x(n), so the differentiation of the function f(x) can be written as followed in equation (2.19).

$$f'(x)= \frac{\Delta y}{\Delta x} = \frac{f(x)- 0}{x_n - x_{n+1}} \quad (2.19)$$

We can rewrite the equation (2.19) as equation (2.20).

$$x_{n+1} = x_n - \frac{f(x)}{f'(x)} \quad (2.20)$$

2.3.3.3 FastICA algorithm

A fixed-point algorithm has been introduced under the condition that the data is sphered [46]. The basic assumption to use it is that the maxima of the equation (2.17), where $y= w^T x$, is obtained at certain optima of $E\{G(WT)\}$, and the optimum value of $E\{G(WT)\}$ can be acquired under the constraint $E\{G(WT)\}^2=\|W\|=1$ at the under the points of equation (2.21).

$$E\{xg(w^T x)\}-\beta w=0 \quad (2.21)$$

where, β is a constant as $\beta=E\{w^T x g(w^T x)\}$. In here, we can solve the equation (2.21) by Newton's method explained in the session 2.4.3.2 and Jacobian matrix in terms of w. The below equation (2.22) is acquired by taking the Jacobian matrix in equation (2.21).

$$JF(w)=E\{xx^T \acute{g}(w^T x)\}- \beta I \quad (2.21)$$

The approximation of the first term of the equation (2.21) can be written as $E\{xx^T \acute{g}(w^T x)\}=E\{xx^T\}E\{\acute{g}(w^T x)\}= E\{\acute{g}(w^T x)\}$ by the initial assumption that data is sphered. From the equation (2.21), the approximated value of equation (2.21), and the Newton's method of equation (2.20), we can acquire the estimation equation for w value as shown in equation (2.22).

$$w_{new} = w_{old} - \frac{E\{xg(w^T x)\} - \beta w}{E\{\acute{g}(w^T x)\}} \quad (2.22)$$

Chapter 3: E-bra system structure: A women ECG measurement system

3.1 Introduction

The demand of an ambulatory ECG measurement system for women is increasing as shown in the section 1.1, and providing a reliable ECG data set is the main key for the ambulatory ECG measurement system. The electrocardiogram(ECG) is the diagnostic test which is able to provide the waveform of ECG components, P wave, QRS complex, and T wave as shown in Figure 8. By observing the characteristics of the ECG waveform, it can provide the probability of diagnosis of a heart abnormality, and several relevant characteristics of the ECG waveform components such as RR interval, PR interval, QRS duration, and T wave alternans and amplitude can be indicators and parameters to investigate the possibility of heart disease. For instance, the observation of the amplitude and duration of the ST segment can be used in the diagnosis of asymptomatic myocardial ischemia, which is one of the reasons of the decrease of blood supply [47]. In addition, the T wave alternans due to T wave variation is considered to be an indicator of heart attack due to ventricular arrhythmias [48]. Monitoring ECG components provides ECG components information related to heart disease such as myocardial ischemia. Continuous monitoring of ECG signals requires subjects to wear the sensor system throughout the day, and the concept is the same as portable and ambulatory concept as explained in section 1.3. In order to make unobtrusive and wearable the system every day, the ECG acquisition system for women, “E-Bra system”, was developed in our lab. The E-Bra system consists of two parts. One is a transmission module which includes two electrodes, 3 stage amplifiers, data acquisition, and a GPRS communication module. The other is a display and analysis program which includes a MARA and display function. The physical ECG signal detected by two

electrodes converts a potential ECG signal, and the potential ECG signal is amplified through the 3 stages amplifier because the amplitude of the potential is only a few mili-volt. The amplified signal is converted to a digital signal in the data acquisition section, and the digitalized ECG data set is sent to a computer installed with the display and analysis program through GPRS communication module. Finally, the program installed in the computer acts as a server to collect the digitalized ECG data transmitted by the transmission module, and the ECG data set is saved in the computer, and is analyzed by the MARAs. This chapter gives the details for E-Bra system.

3.2 E-Bra system architecture

To achieve the function of continuous ECG monitoring, the ambulatory concept should be included in the E-Bra system, so two considerations have been adapted to the process of developing the E-Bra system. The first consideration was the continuous wearing of the system, and the second consideration was how to provide an ECG signal collected from the E-Bra system to clinicians who are eligible for examining ECG abnormality or to people who need daily checkup instead of visiting hospital.

The former consideration was realized by developing a transmission module which consists of data acquisition, data conversion, and data transmission functions. Moreover, the size of the system had to be compact because the ECG measurement system should be portable and ambulatory type. Figure 14 shows the exterior of the transmission module of the E-Bra system, and the size of the transmission module is quite small in the sense that it is attachable to the bottom layer of a female brassiere.

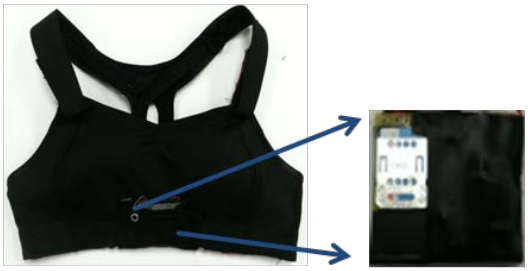

Figure 14. Exterior of the transmission module of the E-Bra system

There are 12 lead ECG test scenarios such as standard limb leads, augmented limb leads, and chest leads as described in section 2.1. However, detecting heart signal by using all 12 lead ECG test scenarios is needed for only high risk CVD patients, so the E-Bra system with the augmented placements of V1 and V2 is used to acquire continuous diagnostic information as

shown in Figure 15. The augmented V1 and V2 positions which are used in the E-Bra system are located in a little bit under compared to the standard V1 and V2 positions of the 6 chest leads because the dry sensors are located in the bottom layer of the women's brassiere.

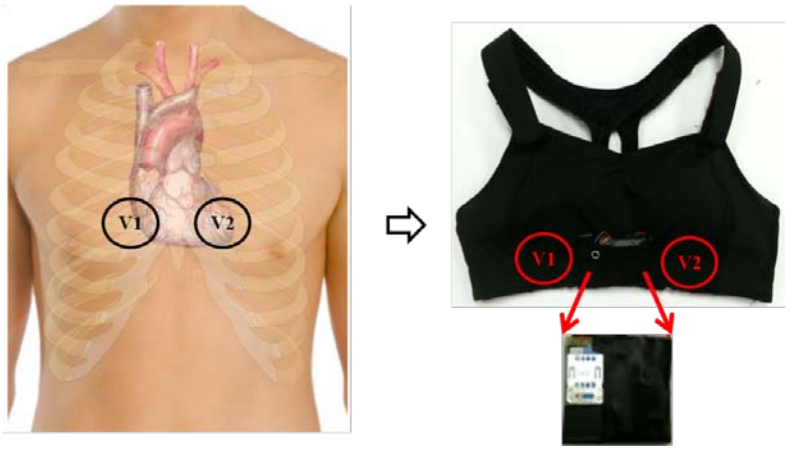

Figure 15. V1 and V2 lead placement on the E-Bra system

The ECG signal detected from the difference between standard V1 and V2 includes in R wave, QRS complex wave, and T wave that are created by activities of left ventricle of heart, and the difference between V1 and V2 provides rich information of the ECG components, P-QRS-T, as shown in Figure 16 (a).

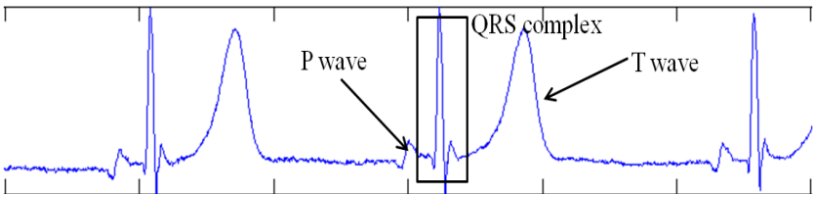

(a) An ECG waveform detected from the standard V1 and V2 positions

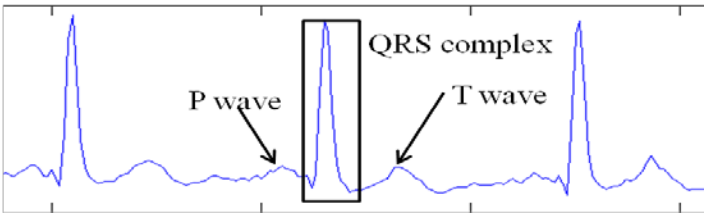

(b) An ECG waveform detected from the augmented V1 and V2 positions of the E-Bra system

Figure 16. ECG waveforms detected from V1 and V2 positions

The ECG signal shown in Figure 16 (a) was collected from the website, www.physionet.org, which offers free web access to large collections of recorded physiologic signals. The ECG data shown in Figure 16 was collected on August 23th in 1994 from a woman 35 years old who has healthy condition. The ECG waveform shown in Figure 16 (b) is one of the ECG signals detected from the augmented V1 and V2 positions of the E-Bra system, and normal ECG components; P wave, QRS complex, and T wave are also shown in the ECG waveform detected from the augmented V1 and V2 positions. Therefore, the ECG waveform measured by the E-Bra system can be used as the ECG signal providing enough ECG information; P-QRS-T.

The latter concern was realized by adapting GPRS communication technology and developing a software program which is able to collect data through TCP/IP protocol. It is mandatory factor to adapt wireless communication technology for ECG measurement systems in order to realize convenient, useful, and accessible portable ECG measurement system. Several representative wireless communication technologies have been adapting on ambulatory ECG measurement systems such as Bluetooth(IEEE 802.15.6), Zigbee(IEEE 802.15.4), Wi-Fi(IEEE 802.11), and GPRS. These technologies can be classified into two groups based on the data transmission range. Bluetooth, Zigbee, and Wi-Fi can be classified as short communication group which is able to send a data set in a local area measurement environment covering to a few hundred meters. Bluetooth and Zigbee have a big advantage of small power consumption rather than Wi-Fi, but the communication distance is usually available less than 100 meters. In case of Zigbee, even though it can provide just less than 250Kbps data transmission speed, it is very useful technology in multi connection application. Moreover, in the view of energy efficiency, Zigbee technology is the best solution among other wireless communication technologies.

GPRS can be classified into remote communication group which can be used under data transmission environment where mobile phone use is available. Bluetooth, Zigbee and Wi-Fi have several advantages such as low power consumption, multi connection, and small size as compared to GPRS, but those technologies can't realize wide area network (WAN) service without supporting additional devices such as a router. In other words, it is not an exaggeration that GPRS is one of the best solutions for ambulatory type device that must not be limited by time and space. Given that reason, GPRS technology is implemented on the E-Bra system, and Figure 17 shows the data service structure of the E-Bra system.

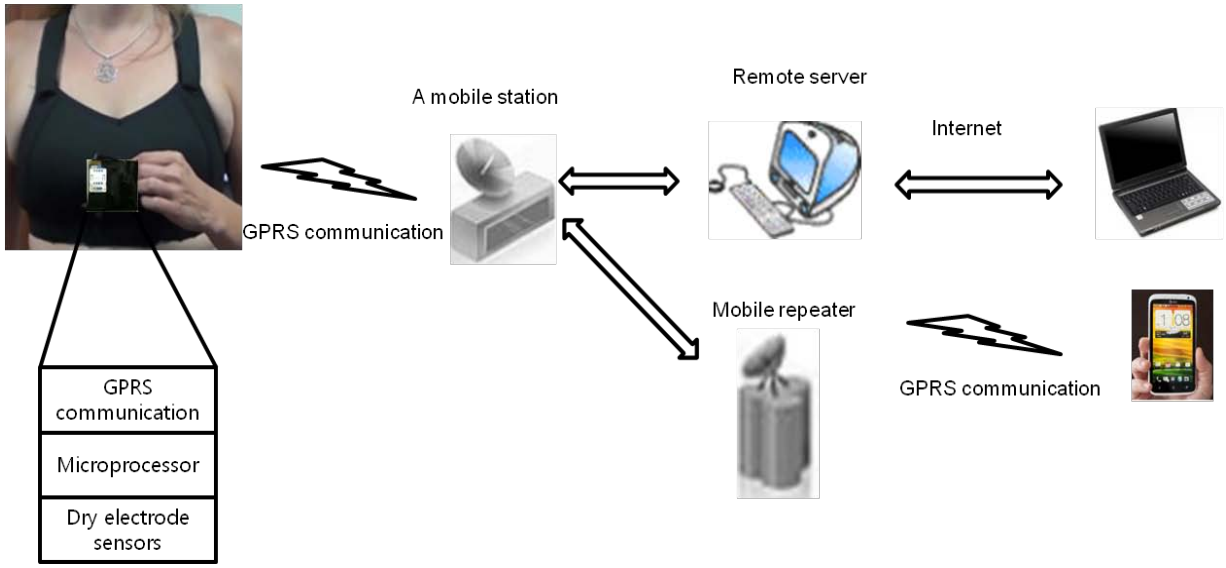

Figure 17. The E-bra system data service structure

3.2.1 Hardware structure of the transmission module

The E-bra system comprises of a transmission module and a computer located in remote area, and software including display and analysis is installed in the computer. The transmission module consists of sensors, 3 stage amplifier, power management part, and GPRS communication module as shown in Figure 18. The total size of the transmission module is 50 mm x11mm x 45 mm. Various hardware components such as resisters, semiconductor chips,

capacitors, etc are stacked on the double sided PCB to reduce size. In this section, hardware structure of the transmission module is explained.

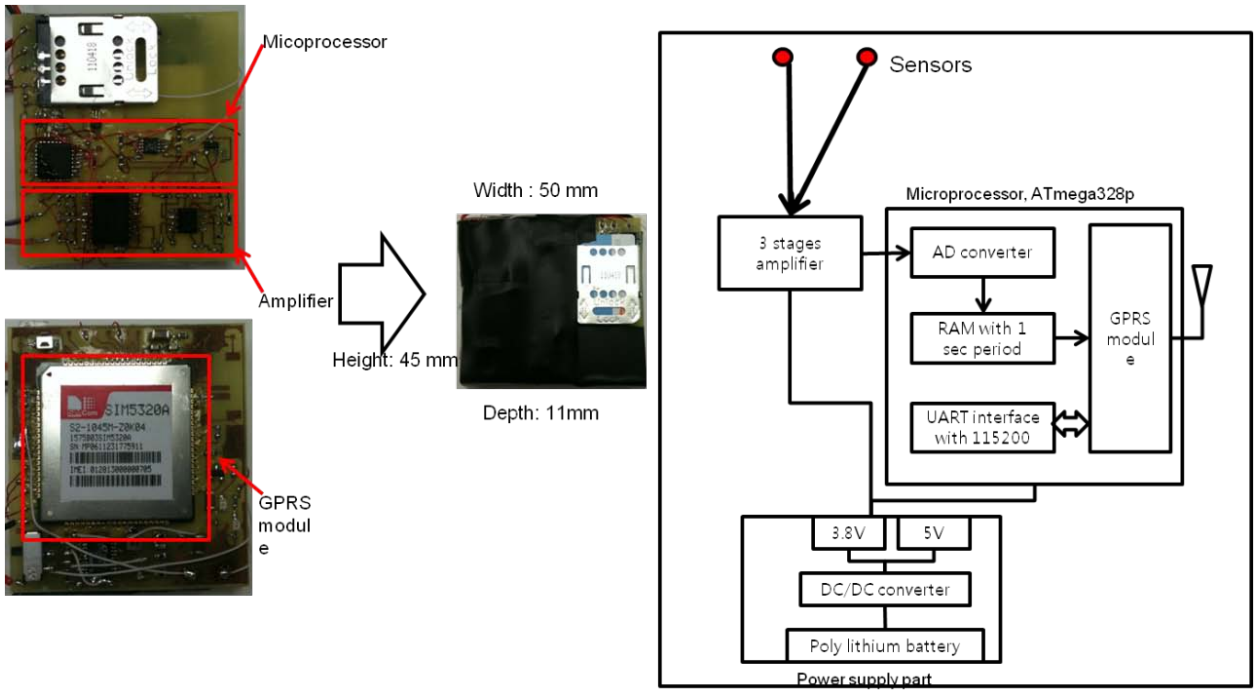

Figure 18. Hardware composition of the transmission module

3.2.1.1 Sensor

ECG signals are detected from electrodes that are placed on the skins. Generally, commercial Ag/AgCl electrodes are used for ECG measurement by using conductive gel to minimize the contact impedance between skin and electrodes. Conductive gels not only increases the noise in the acquired ECG signal when the gel dries, but also causes inconvenience and skin irritation when attached for a long time. Due to these problems, we had proposed to the use of gold nanowire and conductive textile electrodes which performed comparably as demonstrated in our previous work [49], and the gold nanowire electrode has a gold nanowire structure aligned in vertical direction on a Titanium foil. Those electrodes are dry type electrode, so using conductive

gel is not required to measure ECG waveform. Figure 19 shows gold nanowire electrodes and conductive textile electrode along with their size and shape.

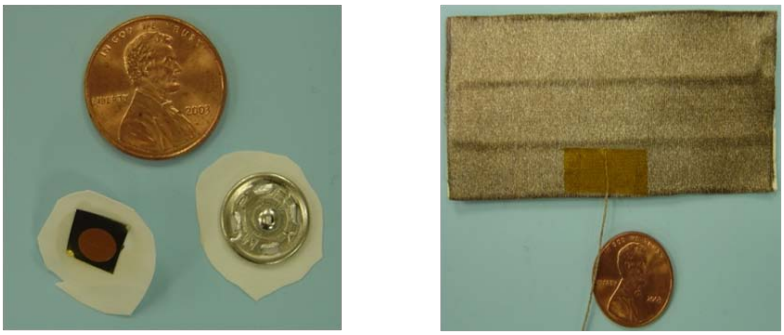

Figure 19. Dry type electrodes

3.2.1.2 Amplifier

The physical ECG signal measured by electrodes is an analog signal which has a few micro-volt or a few milli-volt amplitude. The measured ECG signal needs to be amplified to 5 voltage level in order to be digitalized by A/D conversion, so a 3 stage amplifier is implemented in the transmission module. The schematic of the 3 stage amplifier is shown in Figure 20.

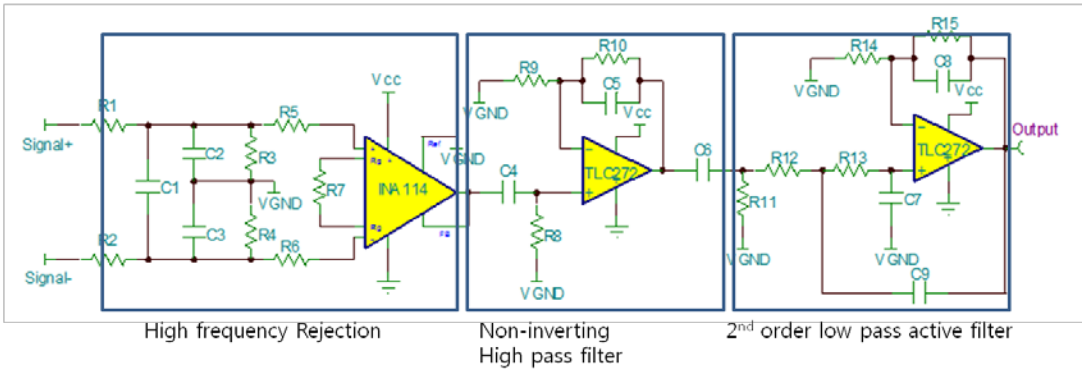

Figure 20. The circuit schematic diagram for 3 stage amplifier

An instrumentation amplifier is implemented with differential inputs and high common mode rejection ratio (CMMR) in the first stage. The second stage includes a high pass filter 0.16 Hz cut-off frequency in order to remove DC offset. Finally, the last stage of the amplifier is an active low pass filter of 2nd order Sallen-Key low pass filter, and the overall gain and bandwidth

for this amplifier are 76db and 0.3Hz ~ 35Hz. The bandwidth range is decided by the investigation of the ECG frequency range referred at the Thakor's research [14].

3.2.1.3 Microprocessor and power management

A microprocessor, ATmega328p, is used for data acquisition using the onboard 10 bit AD converter and for controlling the GPRS communication module. The microprocessor has 32kB flash memory, 2-kB internal SRAM, UART interface, and 6 channels AD converter including in 10 bit resolution. A poly-lithium battery with a capacity of 1800mAh and 3.7V output is stacked for power management of the E-Bra system. The 3.7V output is converted to 3.8V and 5V by using DC/DC converter (LTC3113, Linear Technology), and the amplified 3.8V and 5V are used for GPRS communication module and microprocessor separately. Figure 21 shows the circuit schematic diagram for power management.

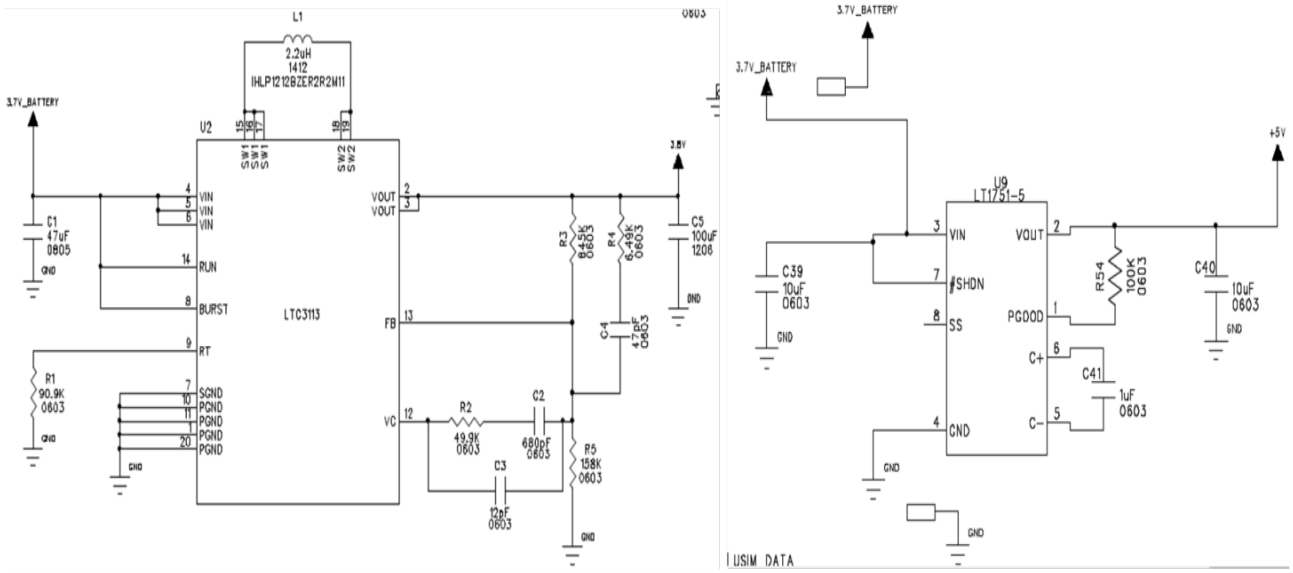

Figure 21. The circuit schematic diagram for power management

3.2.1.4 GPRS module

Commercial GPRS communication module (SIM5320, SIM Com) is implemented in the transmission module to realize WPN communication. The GPRS communication module is connected to the ATmega328p microprocessor by UART interface with 115200 bps (bit per second) baud rate, and the module provides several GPIO (General Purpose Input Output) pins as status indicators such as network indicator LED and power status indicator LED.

3.2.2 Software structure

3.2.2.1 Software structure for the transmission module of the E-bra system

The main purpose of the E-Bra system is to provide an ECG data continuously and if required periodically. The process of providing continuous ECG data is started by acquiring the physical ECG data from two electrodes. The physical heart signal detected by two electrodes is amplified by the 3 stage amplifier, and the amplified ECG signal is digitalized by an A/D converter that is stacked in the microprocessor(ATMEGA 328, ATMEL) with 10 bit resolution. In terms of the Nyquist-Shannon sampling theorem, 100 Hz sampling rate is enough a sampling rate to represent the ECG components, P-QRS-T, occupying from 0.1Hz to 35Hz frequencies. Therefore, 100Hz sampling rate is fixed to convert the amplified analog physical ECG signal to digitalized ECG signal. The data acquisition function is performed in a microprocessor (ATMEGA328, ATMEL), and a timer interrupt task is the main key for the data acquisition function. The timer interrupt task has an important role in managing user specified time stamp on timer interrupt, so to realize a 100Hz sampling rate, the timer callback is performed every 10 ms because 100Hz sampling rate means 10msec time stamp. After called timer interrupt, A/D conversion start signal is called in the timer callback. The AD conversion function is noticed by a flag which is specified on a function register, and then software AD conversion interrupt

callback function is called by the flag. The digital ECG signal is saved on an internal buffer whose size is allocated in as much as the amount of 1 sec at internal RAM. The data saved in internal RAM is sent to a GPRS module (SIM5320, SIMCOM) through UART interface, which is an interface method between GPRS module and the microprocessor. The GPRS module is configured to be a client mode on TCP/IP protocol, and the configuration of the client mode is operated by ATmega328p with several AT commands provided by chip provider (SIMCOM). Continuous connection maintenance function is required for the E-Bra system in order to detect unexpected disconnection status due to signal unreachable environment. The connection maintenance function is realized on every data transmission time. Figure 22 shows the software flow chart for the transmission module of the E-Bra system.

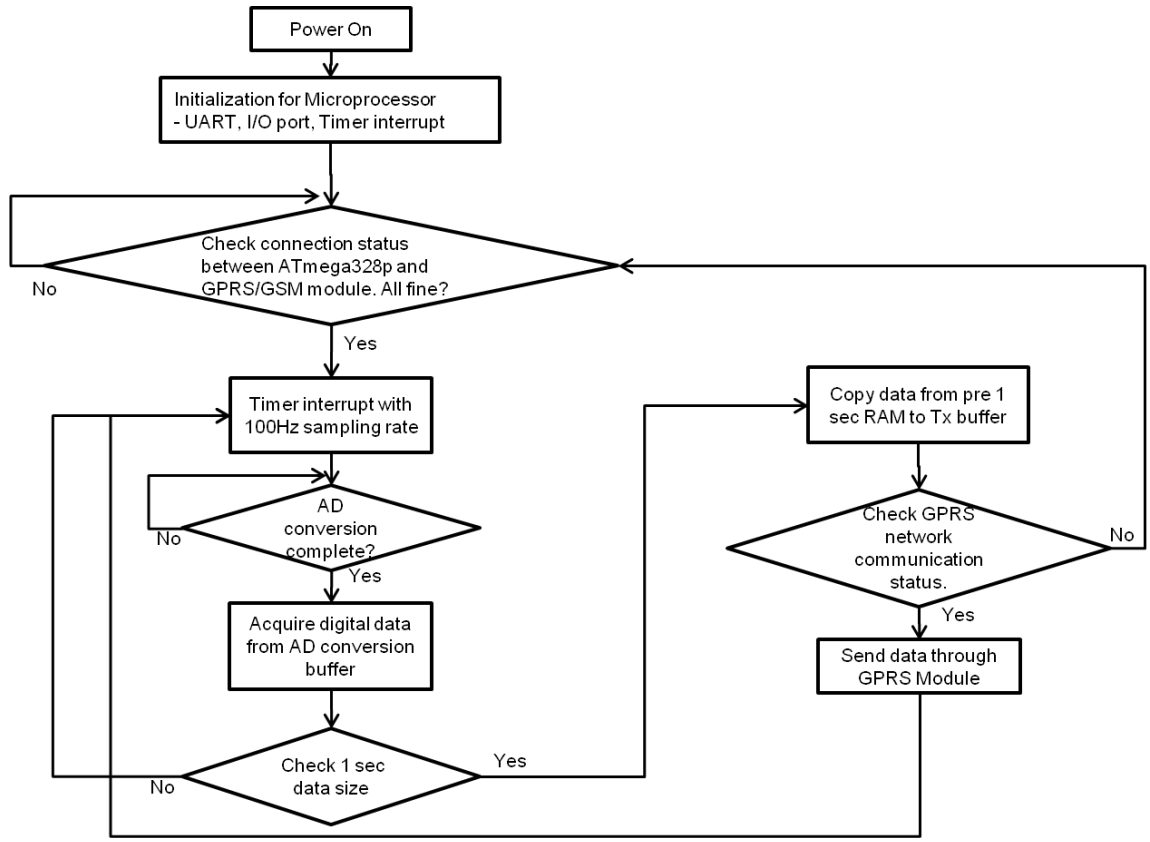

Figure 22. The software flow chart for the transmission of the E-Bra system

3.2.2.2 Reliable data transmission guarantee

Data transmission between the transmission module and the remote computer is accomplished through GPRS communication technology. While data transmits, there is a possibility of disconnection between the transmission module and the remote computer as discussed in section 3.2.2.1. From a transmission module point of view, connection consistency is the most important part, but a remote computer point of view, data loss recognition is the most vital part. If data loss occurs in certain unexpected communication status, the data displayed in the remote computer is not able to keep the sequence in a row. Therefore, the displayed data in the computer screen can be cut off. The suggested idea in this dissertation to prevent discordance of data is that, if it is possible for the remote computer to provide sequence numbers of data transmission, a remote computer will be able to detect data loss point. The other purpose of the protocol is to distinguish criteria between a measured ECG data and headers that include several pieces of information of the data measurement environment such as the number of channels, the transmission module name, messages, etc. The requirement of the protocol is to be able to distinguish a starting point of ECG data if the ECG data is sent in a row on every 1 sec. Therefore, a data protocol named ″E-Bra protocol” was developed for the E-Bra system as explained in Figure 23.

Start	Data length		Type	ID	Payload	Checksum
1 byte	High (1 byte)	Low (1 byte)	1 byte	1 byte	1~1000 byte	1 byte

Figure 23. Data protocol between transmission module and remote computer

1. Start Field : The value is 0x7E, which means a start position of data transmission

2. Data Length Field: The field consists of 2 bytes which have data length information from type to payload field. It doesn't include checksum and data length fields.
3. Type Field: The field indicates meaning message as an identifier. The most significant 3 bit represented the data identifier, and the least significant 2 bits represent the number of channels. Below is a list which shows the meaning of the most significant 2 bits:
    1) 001 : Data transmission
    2) 010 : Connection check request
    3) 011 : Connection check response
    4) 100 : ID check request
    5) 101 : ID check response

    Ex) Connection check request and there are 3 channels (X: don't care)

7 bit	6 bit	5 bit	4 bit	3 bit	2 bit	1 bit	0 bit
0	1	0	X	X	X	1	1

4. ID Field : A unique number that is included in the transmission module
5. Payload Field: The field is reserved for data information. The size can be from 1 to 1000 bytes.
6. Checksum Field: A checksum byte can be calculated and verified to check data integrity by exclusive OR operation.

The first 1 byte is to provide a start point whenever the transmission module sends an ECG data on every 1 sec. A program installed in a remote computer, called "E-Bra Pro", can then recognize the start point by checking a value, 0x7E. The data length filed will notice the

amount of data that is sent from the transmission at one time. The length is changed under the measurement environment such as number of channels in the transmission module, and the length does not include the check sum field and data length field itself. The E-Bra protocol is considered not only for the E-Bra system but also for multi-channel bio potential measurement systems that are developed in our lab. Therefore, the remote computer operates as a server, and the transmission module operates as a client. The type field and the ID field are considered able to make multi-channel connections between a remote server and several transmission modules in order to deliver meaning messages and to notice the transmission ID name. The actual ECG data in the E-Bra system or the measured bio potential data is included in the payload field. The maximum size of the payload is 1000 bytes, so in case of 5 channel transmission modules, the amount of data with 100Hz, 16bit resolution, and 1 sec period can be included in the payload filed at one time. The final check sum field is to check data loss between the type field and the payload field by exclusive OR operation.

3.2.2.3 Software structure for a remote computer of the E-bra system

Another main composition of the E-Bra system is a remote computer including the E-Bra pro. Key functions of the program are to display, to save, and to provide more reliable ECG data from an ECG data transmitted from the transmission module through GPRS communication. The transmitted ECG data through GPRS communication from the transmission module is delivered by TCP/IP protocol. Therefore, when the remote computer program operates, a TCP/IP server mode task is basically performed in the E-Bra program. The TCP/IP task keeps operating until a connection request is reached from the transmission module, and the operation of delaying the request is called “listening”. When the listing operation is done by connection request, a

transmission data capsulated by the protocol described in section 3.2.2.2 is delivered in a receive buffer on the remote computer. The receive buffer is filled every 1 sec, and a data parse task is then operated. The data parse task will separate only ECG data from the data capsulated by the protocol and will acquire basic information about measurement conditions such as the number of channels. The extracted ECG data from the capsulated data is saved on each display buffer with channel information. Finally, the data is displayed on the computer screen. When ECG data is displayed, motion artifact algorithm can be selected by user option as shown in Figure 24.

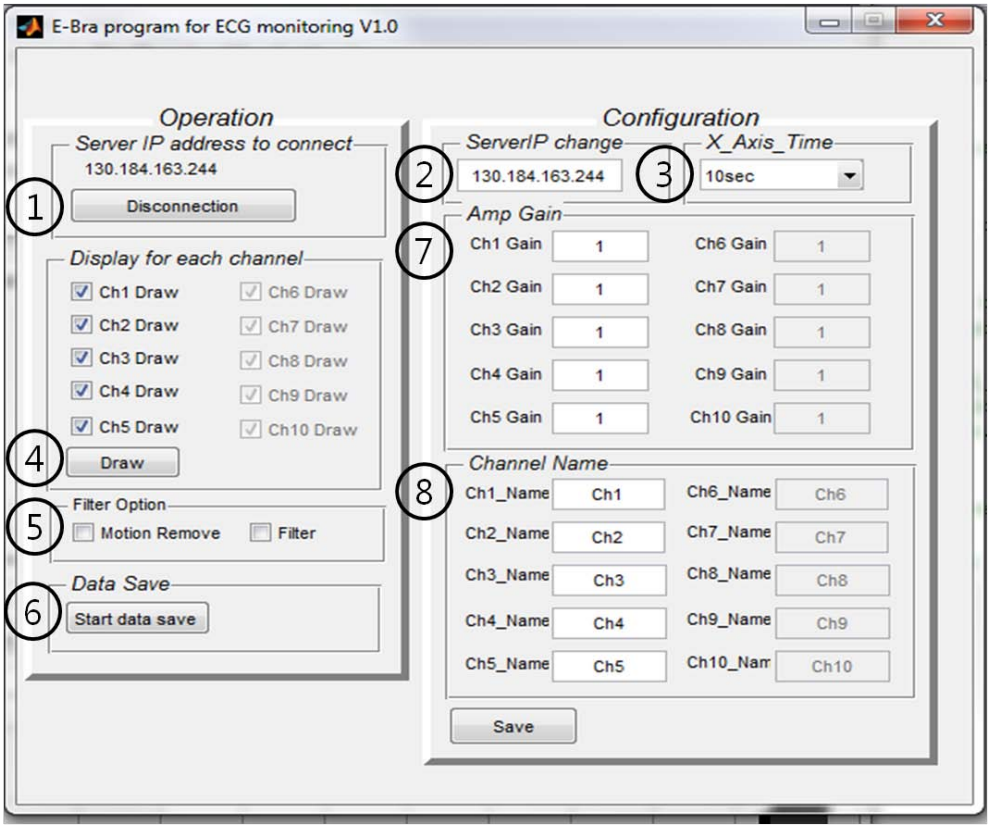

Figure 24. The E-Bra program

① Connection button

- When the button is pressed, the program starts the wait connection request from the transmission module. When connection is completed, connection status is displayed at the center of the button.

② IP address field

- This field deciphers an IP address for a remote computer. The transmission module tries to connect to the IP that is displayed in this field.

③ Display X axis time scale

- X axis time scale is decided by this field option. The time scale is from 30 sec to 10 sec.

④ Display option button

- When the button is pressed, ECG data starts to be displayed on the screen.

⑤ Filter option field

- There are two options in this field. The first option is for motion artifact remove option, and the second option is for 30 Hz low pass filter option.

⑥ Data save button

- When this button is pressed, the data starts to save in the computer folder, and the name of the saved data is not duplicated because the name is created by the time sequence.

⑦ Gain option field

- This field adds gain values that are decided on the hardware amplifier.

⑧ Channel name option field

- Each channel can be named through this field

Chapter 4: Motion artifact removal algorithm architecture

4.1 Motion artifact

As mentioned previously, the need for long term ECG monitoring for women is increasing, and the optimal systems will have to be compact and portable. Moreover, the accessibility to the measured ECG data should be unrestricted in order to realize the long term monitoring function. The E-Bra system is obviously one of the ambulatory ECG monitoring systems which meet the requirements. The E-Bra system continuously can provide an ECG data set not only to a clinician who can treat heart disease but also people who have been diagnosed with heart disease. When observing the long period ECG data acquired from the E-Bra system, it is possible to find irregular heart activities that occur intermittently. The purpose of the E-Bra system is that it should provide a reliable ECG data identical to an ECG data set detected from a stationary measurement environment such as in a hospital measurement environment. However, as described in chapter 1, there are several severe noise impacts in the ambulatory ECG monitoring system, so the E-bra system is also not free from the noise components. The noises can be classified by a range of the frequency distribution such as noises with high frequency range and noises with low frequency range. There are several noise components in the E-Bra system such as device operation noise, power line interference noise, baseline wandering noise due to respiration, and noises components produced by subject's movements. Among the noise components, the device operation noise and power line interference noise are classified as noises with high frequency range, and the baseline wandering noise and noise due to subject movement can be classified as noises with low frequency range. The noises with low frequency range are known as motion artifact (MA).

Usually, the device operation noise such as DC-DC element noise occupies the high frequency range over one hundred Hz, and the power line interference noise occurs at 50Hz or 60Hz. By using a linear band pass filter, the noise frequencies can be removed without any affect to ECG components; P-QRS-T, because the frequency range between ECG components and the noise components are not duplicated. However, severe impact factors in the E-Bra system are MA components. The MA components are created by contact impedance change between electrodes and skin due to subject actions; respiration and movements, and the frequency range is distributed from 0.1Hz to 10Hz as explained in chapter 1. The contact impedance change leads usually to ECG signal distortion because the frequency range of MA components is unfortunately overlapped in the part of the frequency range of ECG components distributed between 0.1Hz and 35Hz frequency as described in chapter 1. ECG signal distortion due to MA components is one of the main reasons for misdiagnosis. Specifically, heart disease diagnosis is based on the investigation of ECG waveform modification such as checking a sharp increase and decrease of the amplitude and period of the P wave or T wave. However, the feature examination of the ECG waveform is influenced by the MA component because the MA components can have a severe impact on the waveform change. In other words, the ECG waveform can be changed by MA components, and this effect is one of the reasons why there is heart disease misdiagnosis. Therefore, it is not an exaggeration to say that the performance evaluation of an ambulatory ECG monitoring device is entirely determined by elimination ability of the MA components. Figure 25 represents several contaminated ECG waveforms in terms of different motion artifact level, and the graph is an example of why motion artifact is an important key factor in the ambulatory measurement system.

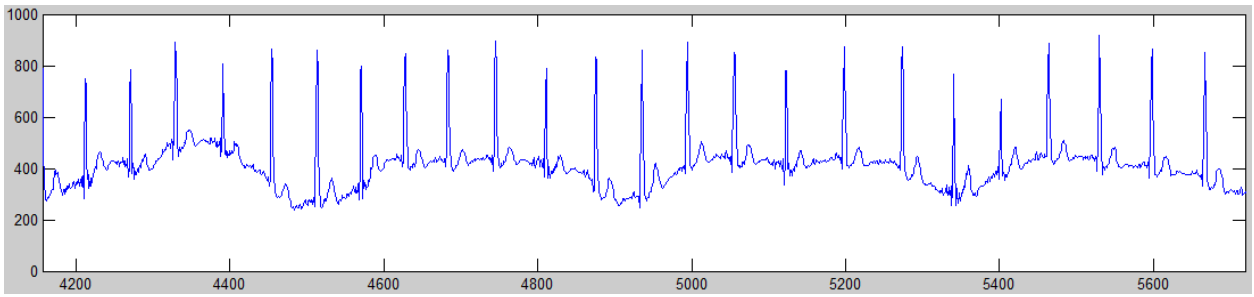

(a) The first level ECG signal: An ECG including baseline wandering noise components

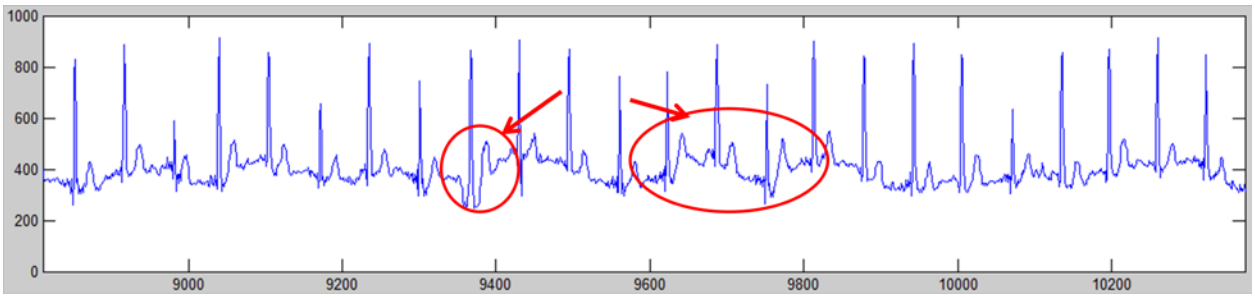

(b) The second level ECG signal: An ECG distorted by MA component, but R waves exist

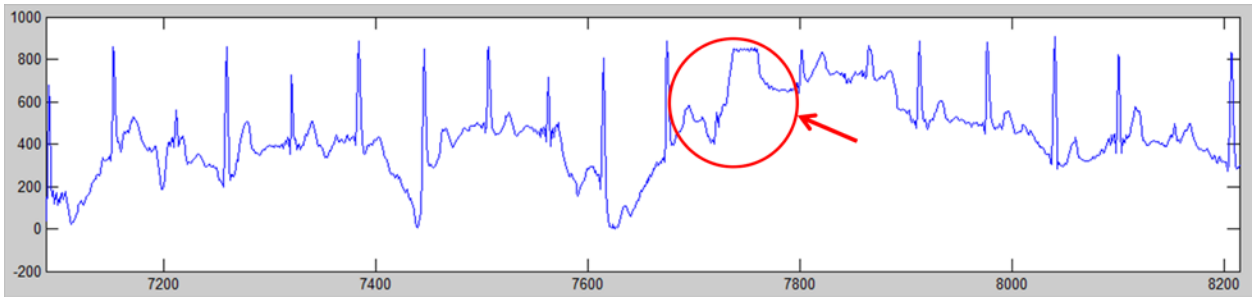

(c) The third level ECG signal: An ECG that is not included in the P wave, QRS complex, and T wave information.

Figure 25. Examples of ECG signals affected by different level motion artifacts

In this dissertation, there are three ECG classifications in the measured ECG signals detected from the E-Bra system as shown in Figure 25, and the ECG classifications are distinguished by the degree of contamination due to MA components.

The first case of MA is the first level motion artifact (FLMA). The FLMA contains a MA component, also known as baseline wandering noise components. Generally, respiration action of a subject has an effect on an impedance change between two electrodes due to variance of air

volume. The slow movement of two electrodes leads to the motion artifact. In this period, the measured ECG signal is influenced by just low noise level as shown in Figure 25 (a). Therefore, the MA component, baseline wandering noise, has an effect on the fluctuation of the measured signal without severe signal distortion of ECG components; P wave, QRS complex, and T wave. This means that the ECG signal collected in the FLMA measurement environment usually doesn't lose the ECG component information; P-QRS-T. Even though the degree of distortion in the ECG signal due to baseline wandering noise is weak, the baseline wandering noise component has to be removed. The frequency range of the baseline wandering noise is usually less than 2 Hz. However, it is impossible to remove the noise components without ECG signal distortion by using a linear low pass filter because the frequency range of P and T waves is widely distributed from 0.5Hz to 2Hz. The duplication of the frequency between those components causes the ECG signal distortion as shown in Figure 26. The first graph shown in Figure 26 (a) shows an ECG waveform including baseline wandering noise due to respiration, and the second graph in Figure 26 was estimated by using linear low pass filter with 2Hz cutoff frequency. The black color circle shows normal T wave case, but the red color circle shows T wave distortion due to elimination of all 2Hz components in a measured ECG signal. The extraction of the wrong result might cause misdiagnosis.

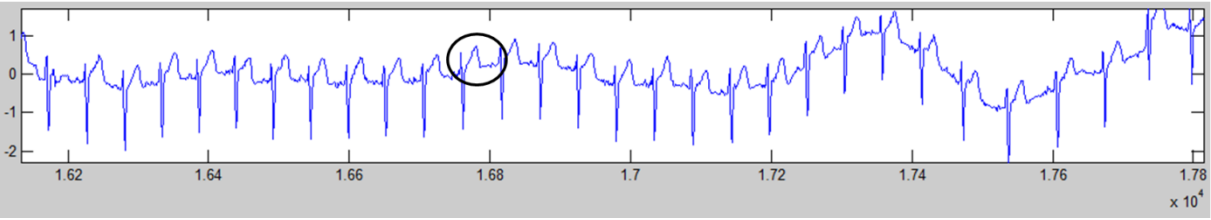

(a) An ECG data set

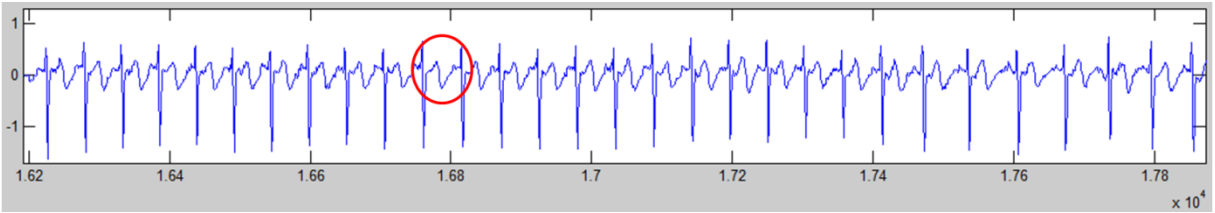

(b) The ECG data set extracted from (a) by a linear low pass filter with 2Hz cutoff frequency

Figure 26. Noise removal trial by using linear low pass filter with 2Hz cutoff frequency

The second case of MA is the second level motion artifact (SLMA). The SLMA contains a MA component due to subject movements. The noise level produced by the SLMA is quite higher than that produced by the FLMA because the contact point between electrodes and subject skin might be widely moved by subject's actions rather than the movement of human respiration. Unfortunately, the noise level due to the SLMA cannot be predicted, and it has a deleterious effect on all of the ECG components; P wave, QRS complex, and T wave. As shown in Figure 25 (b), the red color circles show parts of ECG component distortion. Because the noise level of the SLMA is not predictable, the degree of the distorted signal due to the SLMA is also unpredictable. Therefore, many studies are dedicated to recovering the ECG signal contaminated by the SLMA, and the quality of an ambulatory ECG monitoring system is usually evaluated by the quality of the recovered ECG data set contaminated by the SLMA. This dissertation is also dedicated to finding a technique that is able to remove not only SLMA but also FLMA. The suggested technique in this dissertation is based on detecting R peak value in the entire measured ECG signal because the R value usually dominants even in the period contaminated by the SLMA. For instance, as shown in the Figure 25 (b), the ECG components in the period of the red color circle are distorted by the SLMA, but there are still R peak values in the contaminated period. The most important part for the suggested MARAs in this paper is a possibility of detecting R peak value in the measured ECG signal. The availability of detecting R peak plays a

very important role in removing MA components. The detailed explanation of the suggested MARA will be discussed in the next chapter.

The third case of motion artifact is the third level motion artifact (TLMA). It contains a motion artifact with very high noise amplitude which the ECG components information, P-QRS-T, cannot be found in the period where is contaminated by the TLMA. Figure 25 (c) shows one of the examples due to the TLMA. As shown in Figure 25 (c), ECG components; P-QRS-T are not shown in the period marked with red color circle. Therefore, the period will be considered as garbage data period, and the signal in the period is just removed without any ECG component extraction trial in this dissertation. However, other parts including the R wave in Figure 25 (c) will be analyzed by two motion artifact removal algorithms (MARAs).

4.2 Noise component extraction algorithm(NCEA)

4.2.1 Introduction

As described in the section 4.1, motion artifact (MA) is a mandatory factor that has to be removed in an ambulatory ECG monitoring system, and developing the motion artifact removal algorithm (MARA) is a main key to improve the quality of the ambulatory ECG monitoring system in order to provide reliable ECG data. Given that purpose of the ambulatory ECG monitoring system, in the initial step of the E-Bra system development, considering development of a MARA with high performance was main issue for the E-Bra system. In this dissertation, adaptive filter algorithm (AFA) has been suggested to be one of the MARAs, and independent component analysis algorithm (ICAA) has been suggested to be the other of the MARAs. The detail explanation for the two algorithms will be discussed in the section 4.3. In this section, the requirement of the noise component extraction algorithm (NCEA) will be explained.

As early discussion, AFA is known as an algorithm that can estimate an output signal which includes a minimum error value between a reference input and a desired input. The advantage of the AFA is that the extracted output signal can be free from the signal distortion when the reference signal is well acquired on their purpose. In opposite point of view, it means that if the reference signal is not well defined by some reason, the ECG signal estimated from the AFA included the wrong reference signal will be distorted and be lost the ECG component, P-QRS-T. A traditional noise cancellation concept by AFA has introduced in section 2.3.2. In the concept, a noise signal regarding as the reference signal has to be acquired from certain method, and there are many research investigations to find the noise component that is included in the collected ECG signal such as usage of the another motion detection sensor, 3 axis accelerometer

sensor, usage of wavelet algorithm, etc. Those methods have several disadvantages such as cost impact, size impact, and limited noise component extraction as discussed in section 1.4. As a result, it is not exaggeration to say that a method to extract the reference signal without including pure ECG components is main key for a noise cancellation application by AFA. In this dissertation, to improve and to let loose of the signal distortion problem, a noise extraction algorithm is suggested, and the NCEA is not only for MARA with AF structure, but also for MARA with ICA structure. The detail explanation will be discussed in the section 4.3.

The basic idea of the suggested noise extraction algorithm is based on a modified noise cancellation concept of AFA. Figure 27 shows the block diagram for the suggested the NCEA. In thin block diagram, D(n) is a measured ECG signal detected from the E-Bra system, which includes MA components and pure ECG component, and R(n) is a reference signal. To acquire the reference R(n), several pre-processing steps such as R-R interval detection algorithm and R-R time period synchronization are needed. The steps will be explained in next two sections. The R(n) signal acquired from the pre-process is composed of a pure ECG signal which is acquired in the stationary measurement environment. Therefore, as earlier mentioned the traditional noise cancellation concept in section 2.3.2, E(n) can be extracted by R(n) – Y(n), and the Y(n) is updated by new weighted coefficient values, $H = [H_0, H_1, \dots, H_{N-1}]^T$, at every sample. The coefficient H values are estimated on each sample by LMS algorithm. For instance, the j^{th} coefficient H_j is estimated by equation (2.7) with the error value, E(j), which is signal acquired by difference between D(j) and R(j). The error signal estimated from all samples represents the MA component because it is extracted by minimum value between D(n), the measured ECG signal, and R(n), the approximated pure ECG signal.

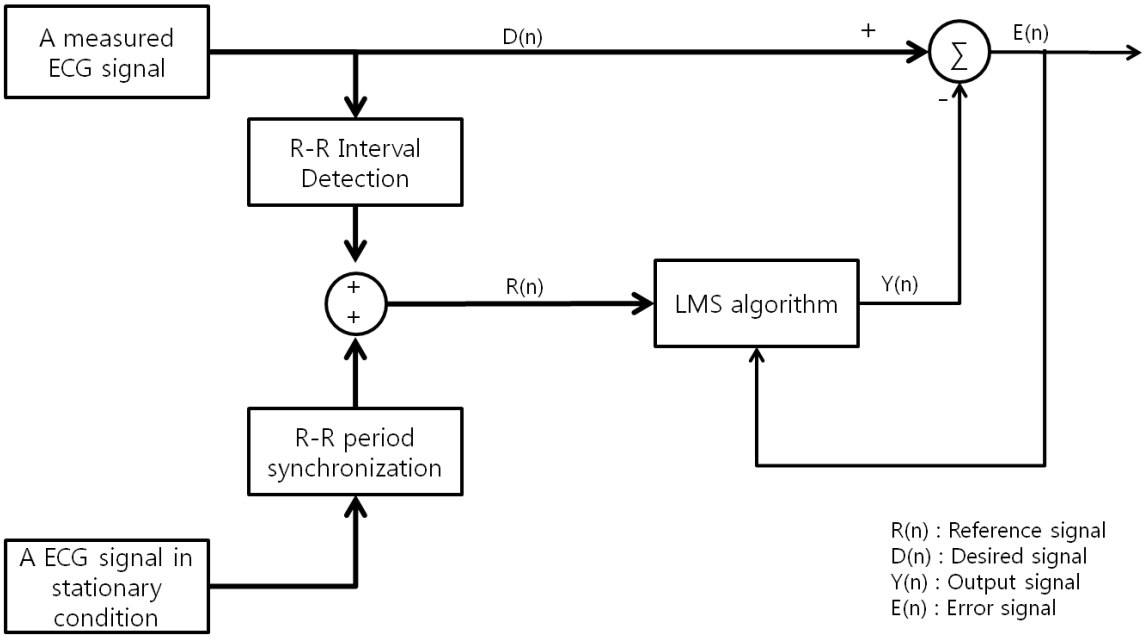

Figure 27. A block diagram for the NCEA

4.2.2 R-R peak detection

The NCEA is to estimate the noise components that are included in a measured ECG signal from the E-Bra system. As earlier explanation, utilizing the MARA has a meaning in a period where it was possible to show the ECG components; P wave, QRS complex, and T wave as shown in Figure 25 (a) and (b). Among the ECG components detected from two electrodes attached between augmented V1 and V2 positions of the E-Bra system, the R waves are shown in the any cardiac cycle as the dominant wave even in the contaminated period that P wave, T wave, and ST segment are distorted by MA as shown in Figure 25 (b). Therefore, tracking R waves in entire recorded data is usually used to detect heart rate.

The suggested the NCEA is based on tracking R intervals between previous R position and current R position. The R-R interval is used to synchronize the time scale between the reference signal, R(n), and the desired signal, D(n), as defined in previous section. The time

synchronization method and the requirement will be explained in next section. R wave detection usually uses a characteristic of steep slope and amplitude variation in a period where QRS complex components are included. However, detecting R wave position is difficult because the QRS complex components can be corrupted by MA component. A study suggested an algorithm to detect R wave position in the real time [50]. In this dissertation, by modifying the algorithm suggested by Pan and Tomkins, the algorithm to detect R wave position is realized by MATLAB software. Figure 28 shows the block diagram of processing flow chart for R wave detection algorithm.

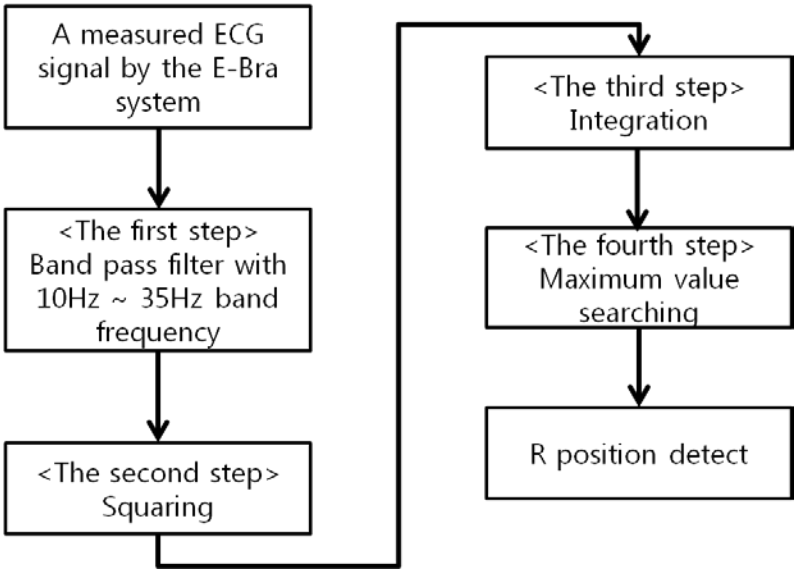

Figure 28. The block diagram of processing flow chart for R position detection

To detect R wave position, it is the first step to apply a band pass filter with 10Hz ~35Hz band pass frequencies. As explained in section 1.3, the frequency range of the MA components usually distributed from 0.1Hz to 10Hz, so the frequency range between 10Hz ~ 35Hz doesn't includes the MA components. Figure 29 shows QRS complex positions between the measured ECG signal and a ECG signal filtered with the 10Hz ~ 35Hz bandwidth frequency.

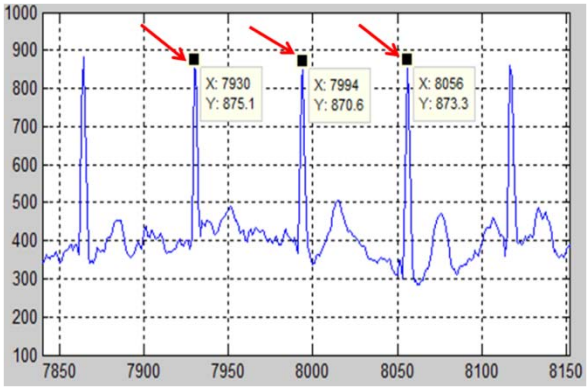

(a) R wave positions detected from a measured ECG signal.

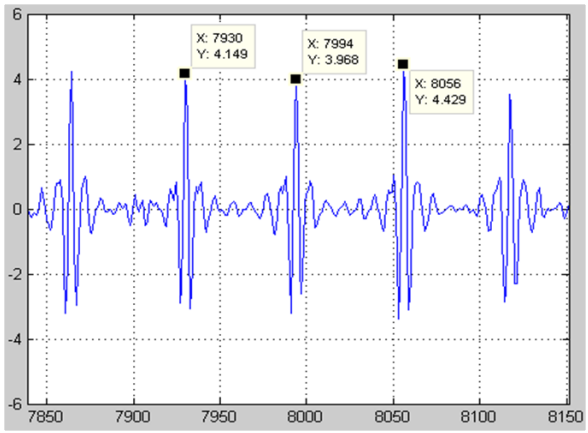

(b) R wave positions detected from a filtered signal by bandpass filter

Figure 29. A comparison between a measured ECG signal and a filtered signal

The extracted QRS wave positions marked with 3 red color arrows as shown in Figure 29 (a) are exactly same as the QRS wave positions estimated from the filtered signal as shown in Figure 29 (b). Moreover, the derivative signal by band pass filter includes enough slope information of QRS complex as seen in Figure 29 (b), so the difference equation existed in the algorithm suggested from Pan and Tomkins in order to emphasize the QRS complex slope is omitted in this dissertation.

The second step is to make all data samples to be positive values by using equation (4.1).

$$y(k) = [x(k)]^2 \tag{4.1}$$

Figure 30 shows a result graph after the squaring operation.

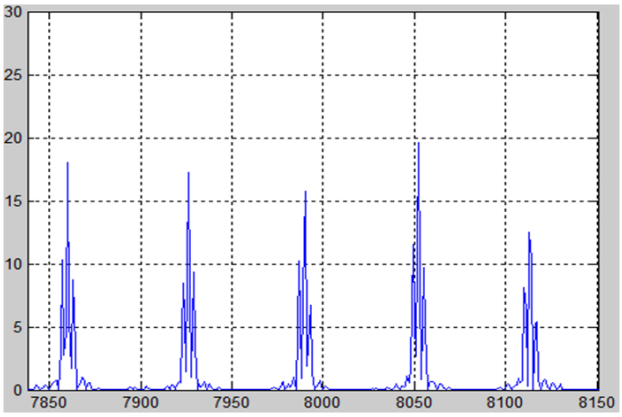

Figure 30. A result graph after the squaring operation

The third step is to acquire an integrated signal from the squared signal, and the process has an important role in reconstructing all QRS features within 1 peak feature. Figure 31 shows a result graph after integration.

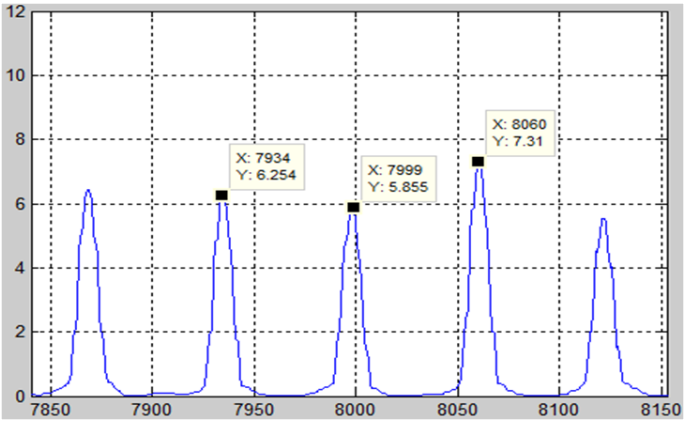

Figure 31. A result graph after integration

The last step for R wave detection is to search R wave position. The R wave position is detected by searching the maximum value in a period between 85% and 115% from the peak value position acquired by integration step.

4.2.3 R-R Interval synchronization

The key point for NCEA is how to extract a reference signal, R(n), which includes pure ECG components. As discussed in the previous section, R-R interval provides a time stamp the same as an interval of 1 cardiac cycle, so tracking R-R interval not only provides heart rate information but also can be used as an indicator to be a standard point between unsynchronized signals. Each R-R interval between current R position and previous R position can be written as RR(j), and the entire RR values consists of vector space as $[\mathrm{RR}(1), \mathrm{RR}(2), \ldots, \mathrm{RR}(n)]^{\mathrm{T}}$. Therefore, the number of cardiac cycle is the same as the number of RR values. Unfortunately, the duration of cardiac cycle is frequently changed in the ECG measurement scenarios, and the RR interval time stamp is also changed by cardiac cycle fluctuation. To extract noise component from the single channel ECG signal collected by the E-Bra system, the traditional noise cancellation concept by AFA is modified as shown in Figure 27, and the modified concept is to obtain noise components instead of the original purpose of noise cancellation by changing the reference signal as pure ECG signal. The reference signal is synchronized with the R-R intervals which are detected from the measured ECG signal, and as a result, the dimension of the reference signal can be the same as the dimension of the measured ECG signal. Figure 32 shows an ECG cycle to be a standard cardiac cycle, so the ECG cycle is selected in a period where there is no MA effect. Figure 33 shows the time synchronization between the measured ECG signal and the reference signal.

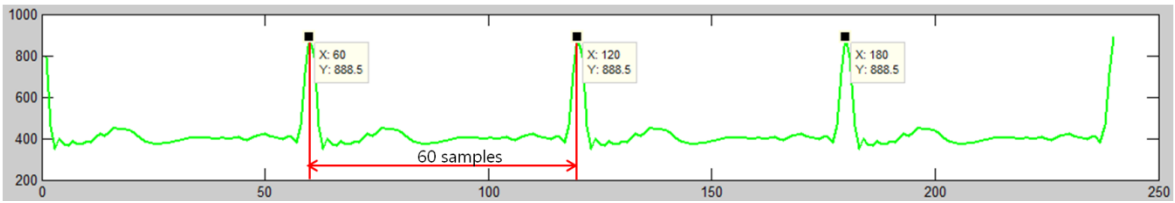

Figure 32. A selected standard pure ECG signal no affected from the MA component

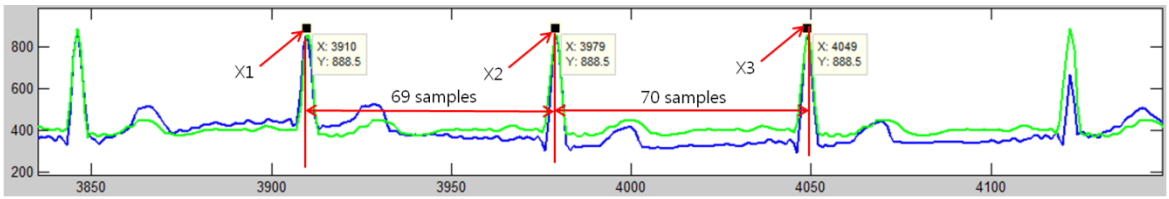

Figure 33. R-R interval synchronization between the reference signal and the desired signal

In those two graphs, the signal with green color is the reference signal; R(n) = an pure ECG signal not affected from MA, and the signal with blue color is the desired signal, D(n) = an collected ECG signal. The time stamp of the reference ECG cycle in Figure 32 is 60 samples (600msec), and time stamps among X1, X2, and X3 in Figure 33 are 69 samples (690msec) and 70 samples (700msec). As seen in the time stamp values, the R-R interval times are varied on every cardiac cycle, so the variation of the R-R interval time stamp measured in the collected ECG data sets leads a necessity of time synchronization between the reference signal and the ECG signal collected from the E-Bra system. The time synchronization is achieved by interpolation method which is known as resample technique.

The reference signal synchronized by following R-R interval time stamp is used as the input for LMS algorithm block as shown in Figure 27, and the LMS algorithm block estimates a new coefficient which includes the minimum error value between the LMS output value and the measured ECG value at same sample time. Finally, noise components can be extracted by difference of the measured ECG signal and the LMS output signal. Figure 34 shows a MA signal estimated by using the NCEA.

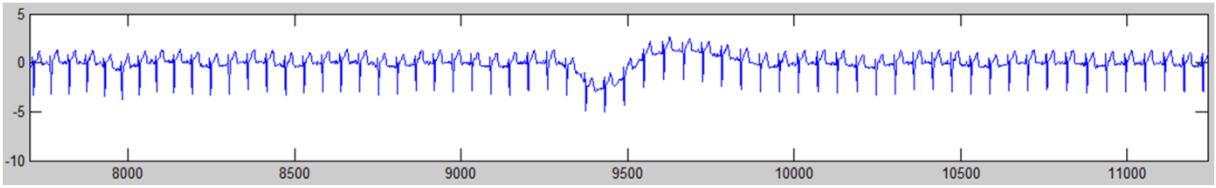

(a) An ECG signal

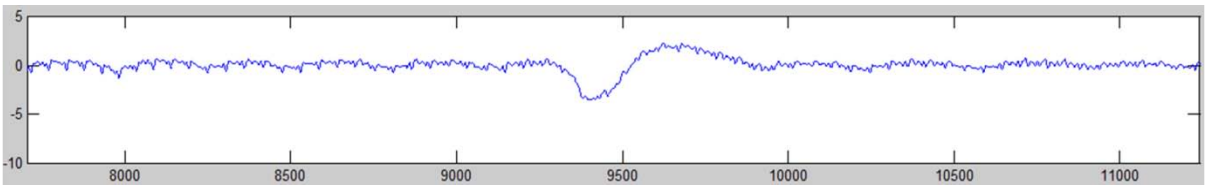

(b) A noise component estimated by the NCEA

Figure 34. An example of a noise component estimated by the suggested algorithm

4.3 Simulation of motion artifact removal algorithm

Electrocardiogram (ECG) is a periodic signal in the sense that the ECG components, P-QRS-T, is periodically shown in following R-R interval because the R wave can substantially be observed among P-QRS-T even in a situation that a period presented the ECG components is contaminated by MA components; FLMA and SLMA defined in section 4.1. Therefore, R-R interval time stamp is used for tracking synchronization time between a reference signal and a measured ECG in the NCEA as mentioned in previous section. The reference signal synchronized with the R-R interval time stamp of the measured ECG signal included in MA components is used as the input signal for LMS algorithm operation block, and the noise component is estimated by the NCEA. The noise components extracted by the NCEA is the main key to implement MARA. In this section, the two algorithms including AF structure and augmented ICA structure will be described, and several simulations are performed to evaluate the performance of two MARAs.

4.3.1 SNR measurement

The signal to noise ratio (SNR) measurement is usually used to evaluate a quality of signal that includes in noise components. The SNR is a value calculated by power values between the measured signal and noise signal that occupies on the background of the measured signal. The SNR value is represented by terms of logarithmic decibel scale as explained in below equation.

$$\mathrm{SNR} = 10 \log \frac{\mathrm{Es}}{\mathrm{En}} \tag{4.2}$$

The Es notice is an average power value of a measured signal included in noise components, and the En notice is an average power value of a noise component occupying the background of the measured signal. However, to use the equation (4.2), it is a necessary process to acquire noise components which are included in the measured signal. However, to adapt the SNR concept in the E-Bra system, extracting noise components from the ECG signal is also big challenge in the E-Bra system with single channel, so as discussed in section 4.2, the NCEA was suggested for extracting noise components including MA components. As a result, using the estimated noise components by the NCEA is not correct way to be a parameter of the En in equation (4.2). Therefore, the concept of the SNR measurement should be modified for ECG measurement system with single channel. The modified concept is based on a ratio value between the reference ECG signal without MA components and the noise components which is included in the ECG signal estimated by a MARA. The main key for the modified SNR is that FFT power level of the noise components can be acquired by difference between FFT power levels of the reference ECG signal and FFT power levels of the ECG signal estimated by a MARA because the noise components can be defined by the contaminated degree of the ECG signal estimated by a MARA. For instance, if the ECG signal estimated by a MARA includes higher noise components than the reference ECG signal, the FFT power levels acquired by the difference between the reference ECG signal and the ECG signal estimated by the MARA will be increased, and the ratio between reference ECG signal and noise components will also be increased. In the modified SNR measurement concept, the Es notice is for an average value of the FFT power levels calculated from the reference ECG signal without noise components including MA component, and the En value can be acquired by the difference between the FFT power levels calculated from the ECG

signal estimated by MARA and the FFT power levels calculated by the reference ECG signal. The below steps explain the process of the SNR measurement in this dissertation.

Step 1. Measure an ECG signal in the stationary test situation so that the ECG signal is not influenced by MA components to acquire 1 cycle of the ECG signal.

Step 2. Measure an ECG signal with any test purpose.

Step 3. Estimate the reference ECG signal by R-R interval synchronization with 1 cycle of the ECG signal acquired in step1 and the ECG signal acquired in step 2.

Step 4. Estimate an ECG signal by a MARA.

Step 5. Calculate FFT power levels of the reference ECG signal.

Step 6. Calculate FFT power levels of the ECG signal estimated by the MARA.

Step 7. Acquire the difference between two FFT power levels acquired at step5 and step6.

Step 8. Acquire the ratio between two values of step 5 and step 7.

Step 9. Acquire SNR value by using equation (4.2)

4.3.2 Motion artifact removal algorithm with adaptive filter structure

To extract a noise component signal from a measured ECG signal included in MA components, the traditional noise cancellation concept with AF structure was modified as described in section 4.2.3. By the NCEA, we can acquire the noise components from the measured ECG signal detected by the E-Bra system without the requirement of another noise detection sensor. The acquired noise components are used as inputs for the traditional noise cancellation concept in order to estimate an ECG signal without the MA components. In other words, the noise cancellation concept with AF structure is used twice as many times in the MARA with AF structure in order to estimate both signals as a reference signal which is a noise

component and an ECG output signal which is not included in the MA component. Figure 35 shows a block diagram for the MARA with AF structure.

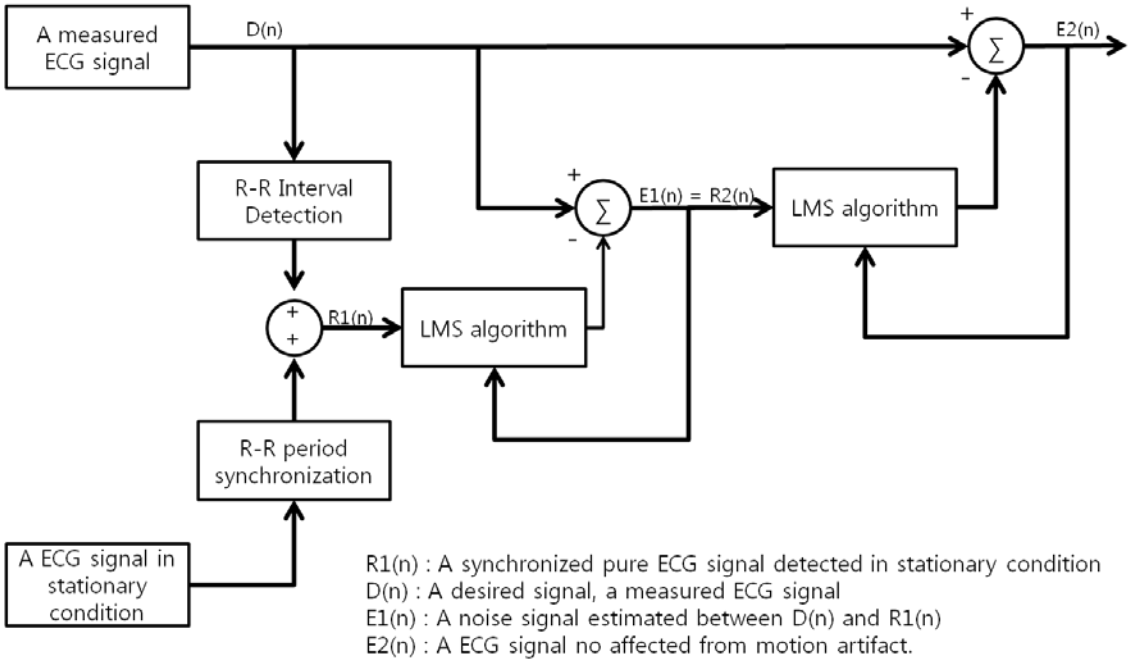

Figure 35. The block diagram for a motion artifact removal algorithm with adaptive filter structure

To use the MARA with AF structure, there is a big assumption. The assumption is that one cardiac cycle, one period including R-R interval, has to be acquired in the stationary measurement condition. In other words, one ECG cycle without MA components in ECG data sets is required in order to be used as a standard point for the reference signal, R1 (n). It is not a big challenge to detect 1 cycle cardiac signal in the stationary measurement system. Actually, by using the suggested MARA concept, it is possible to estimate a pure ECG signal from an ECG signal contaminated by MA component even in the case of a pure ECG signal which includes heart disease feature. To evaluate the MARA with AF structure, several simulations are performed with a couple of ECG data sets that are collected from people who have already been

diagnosed with heart disease and from people with healthy conditions. Those data sets can be freely accessed from a web site (www.physionet.org). There are three simulation cases such as the healthy condition case and two the myocardial infarction cases. Among the data sets, to evaluate the performance of the MARA with AF structure, two simulations were performed with the ECG data set with health condition and the ECG data set with a case of the myocardial infarctions. The collected ECG data sets were not influenced by MA components, so basically the data sets provide the uncontaminated ECG components information. Figure 36 shows the simulation result of the first case which is a healthy condition case. The data was detected from a woman who is 35 years old.

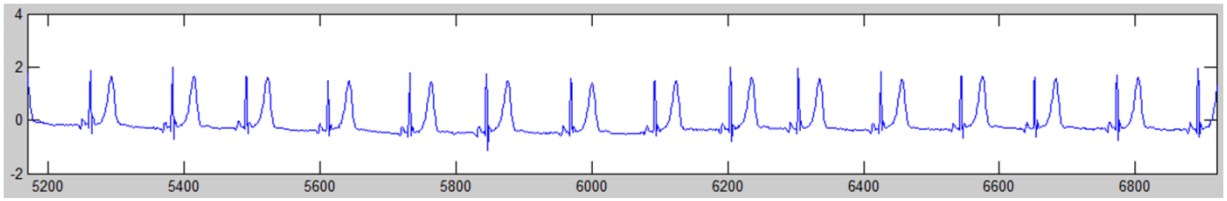

(a) An ECG signal with healthy condition collected from a woman 35 years old

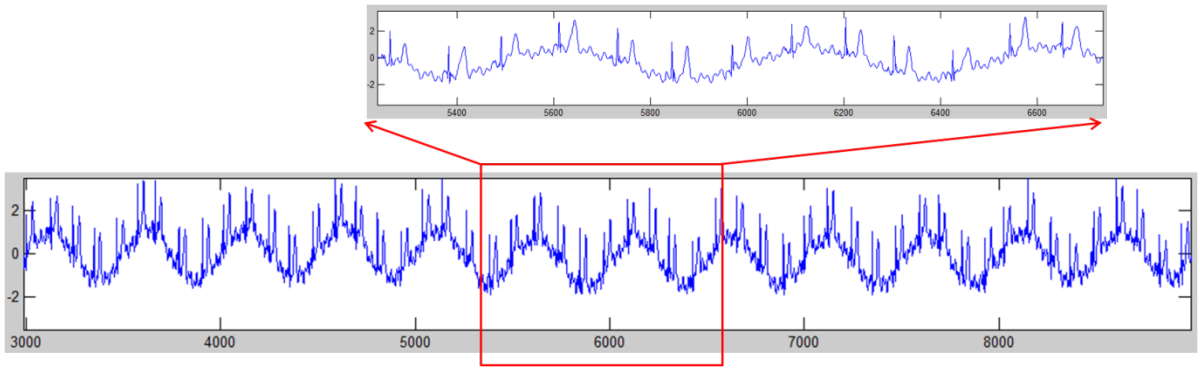

(b) An ECG signal combined with the signal (a) and artificial motion artifacts included in 0.2Hz, 3Hz, and 7Hz

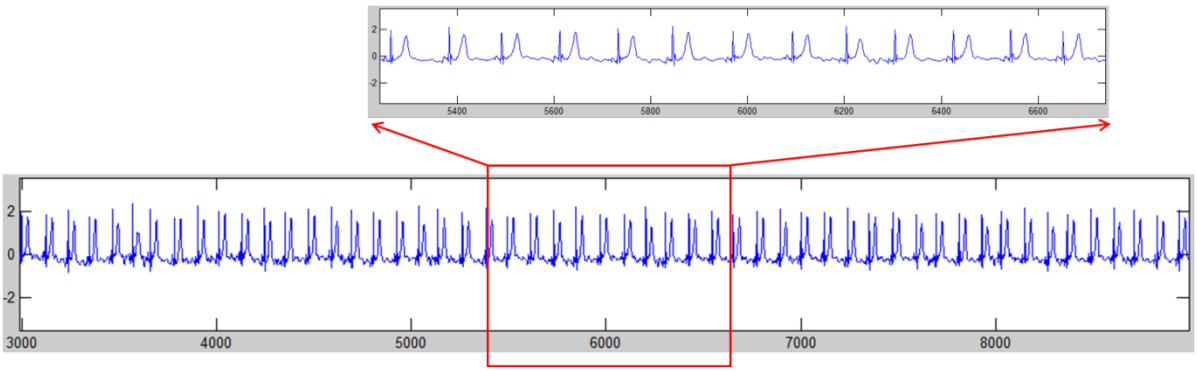

(c) An ECG signal estimated by MARA with AF structure from (b)

Figure 36. A simulation in healthy condition ECG signal for evaluation of the MARA with AF structure

Figure 36 (a) presents an ECG waveform with healthy condition, so there are clear P-QRS-T components in each cardiac cycle. Now that the ECG signal is free from the motion artifact influence, an artificial noise component with 0.2Hz, 3Hz, and 7Hz frequency is created. The selection of those three frequencies is based on three assumptions: 0.2Hz is a noise frequency produced in respiration such as deep breathing, 3Hz is a noise frequency produced in a walking test case, and 7Hz is a noise frequency produced in a running test case. Figure 36 (b) shows the signal waveform which is combined with the collected ECG data (shown in Figure 36 (a)) and the noise signal created by combination of those three frequencies, 0.2Hz, 3Hz, and 7Hz. As we can see in the extended red color area, the original signal is contaminated by the artificial noise components. In detail, there are two big affections by the artificial MA components. The first affection in the collected ECG data sets is by the artificial baseline wandering created by 0.2Hz frequency, and it seems a wave fluctuation. The other affection in the collected ECG data set is by the artificial high level noise component created by 3Hz and 7Hz, and it causes the distortion of the collected ECG data set. Those two big affections in the ECG data sets are elements that must be removed in order to improve the quality of the data sets. The requirement can be accomplished by the MARA with AF structure, and Figure 36 (c) shows the ECG

waveform estimated from the signal of Figure 36 (b) by the MARA with AF structure. From observing the signal in the extended red color area, we recognize that the signal in the extended red color area is very similar to the collected ECG signal shown in Figure 36 (a). The similarity between Figure 36 (a) and (b) is investigated with two techniques, an autoregressive (AR) power spectrum density (PSD) and correlation value.

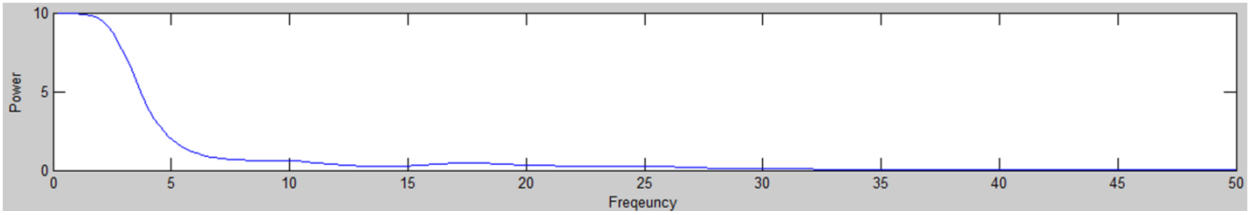

(a) ARPSD analysis on the signal (a) of Figure 36.

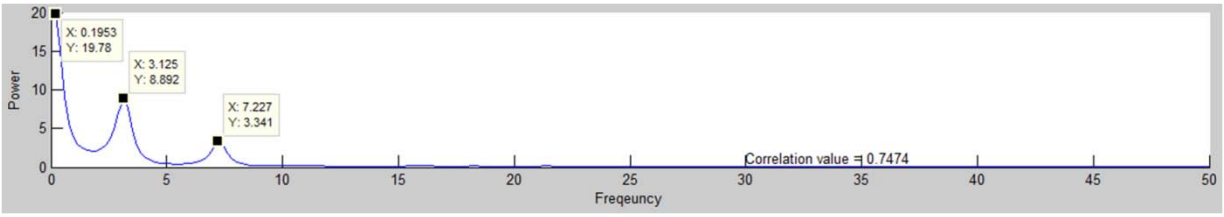

(b) ARPSD analysis on the signal (b) of Figure 36

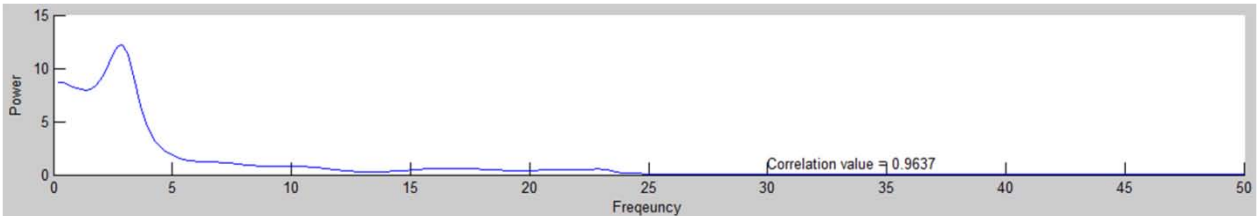

(c) ARPSD analysis on the signal (c) of Figure 36

Figure 37. Autoregressive power spectrum density (ARPSD) of all data sets represented in Figure 36

Figure 37 shows the results of ARPSD analysis performed on all data sets represented in Figure 36. Figure 37 (a) shows the result of the frequency analysis acquired by the ARPSD for the collected ECG data with healthy condition, and Figure 37 (b) shows the result of the frequency analysis acquired by the ARPSD for the contaminated ECG signal due to the artificial MA component. The marked values in the Figure 37 (b) are frequency values that are distributed on the data sets. Among the frequency values, three prominent values, 0.1953, 3.125, and 7.227,

are marked in the graph, and the values is caused by the artificial MA frequency components. Figure 37 (c) shows the frequency components acquired from the ECG signal that is estimated by the MARA with AFA. It is visually easy to recognize which frequency component, (b) or (c), has a higher similarity to the frequency components of the collected ECG signal. However, to provide clear comparison values between (b) and (c), correlation values are marked in each graph (b) and (c). Using a correlation value is one of the best ways to compare the similarity feature of two signals, and it means that the closer the value is to '1', the more each compared signals have high similarity. As we can see in the graphs, the correlation value of the ECG signal contaminated by artificial MA is 0.7474, and the correlation value of the ECG signal estimated by the MARA with AF structure is 0.9637. It means that the ECG components estimated by the MARA with AF structure includes higher similarity to the collected ECG data than the contaminated ECG signal due to artificial MA.

As discussed earlier, there is a high occurrence possibility of the MA component in long term ECG monitoring by an ambulatory ECG monitoring device. The necessity of long term ECG monitoring will be required by people who have been diagnosed with heart disease rather than people with healthy heart conditions. Therefore, it is vital to simulate the performance of the MA suggested in this dissertation with several data sets that are collected from people who have been diagnosed with heart disease. Among a variety of heart disease cases, two myocardial infarction cases have been selected because myocardial infarction is one of the representative heart diseases. The results acquired from one of two myocardial infarctions will be explained in the graphs below, and the other results will be explained in section 4.3.3. The simulation result of

the first case, one of the myocardial infarction cases, is shown in Figure 38. The data set was collected from a woman, 65 years old.

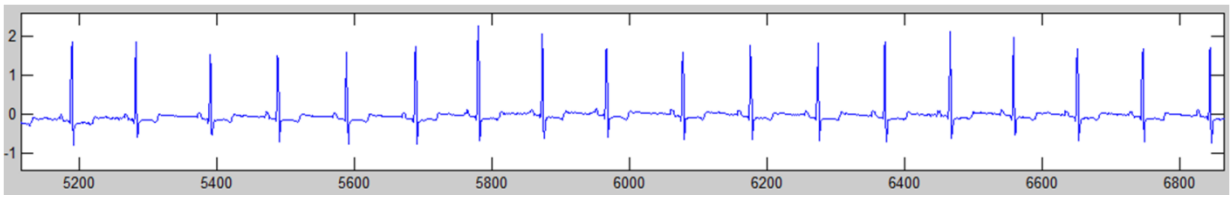

(a) An ECG signal with myocardial infarction

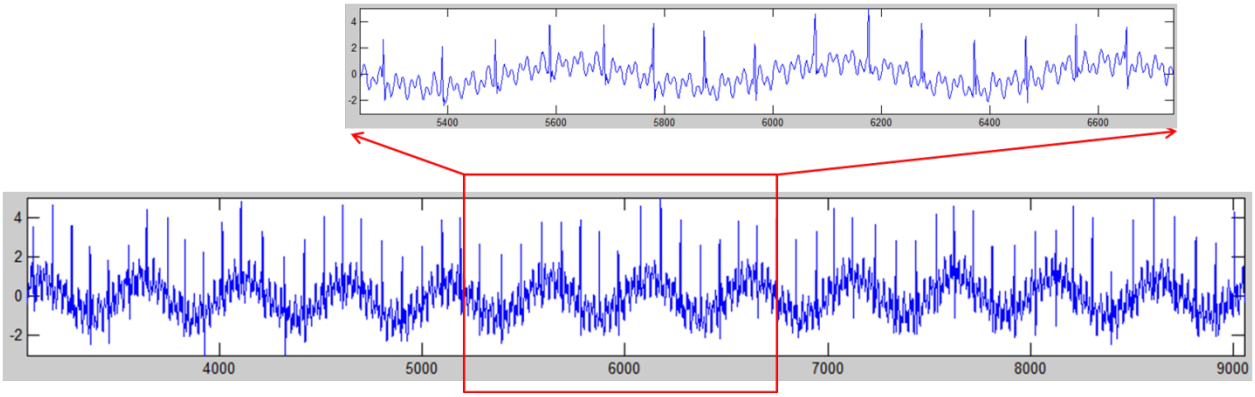

(b) An ECG signal combined with the signal (a) and artificial motion artifacts included in 0.2Hz, 3Hz, and 7Hz.

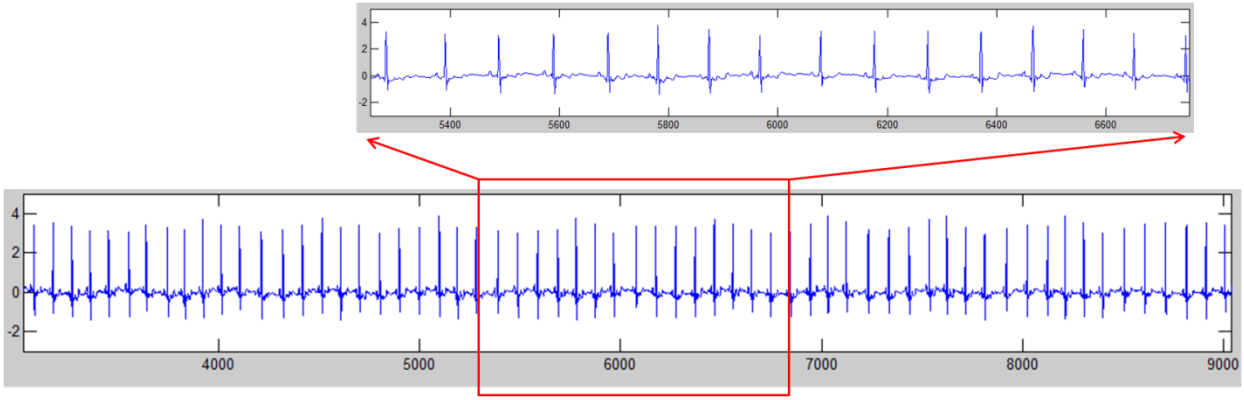

(c) An ECG signal estimated by MARA with AF structure from the data set of (b)

Figure 38. A simulation result of myocardial infarction case

Figure 38 (a) shows the ECG waveform collected from the test subject. The ECG component features are very different compared with the Figure 36 (a) which is the ECG waveform with healthy condition. The simulation processes performed in the simulation of the healthy condition

are performed for this case, so Figure 38 (b) shows the ECG waveform affected by the artificial MA component. Figure 39 (c) shows the ECG waveform estimated from the Figure 38 (b) by performing the MARA with AF structure. As shown in the extended red color box in the Figure 38 (b), we can recognize that the ECG waveform is prominently distorted as if there are no ECG components. This recognition can be proof through the correlation value between Figure 38 (a) and (b) as noticed at the right bottom side in Figure 39 (b). The correlation value is 0.1725. It means that the ECG signal affected by artificial MA components has prominent low similarity to the pure ECG data without artificial MA components. The last two graphs shown in Figure 38 (c) and Figure 39 (c) represent the ECG waveforms estimated by the suggested MARA with AF structure and the result of ARPSD analysis.

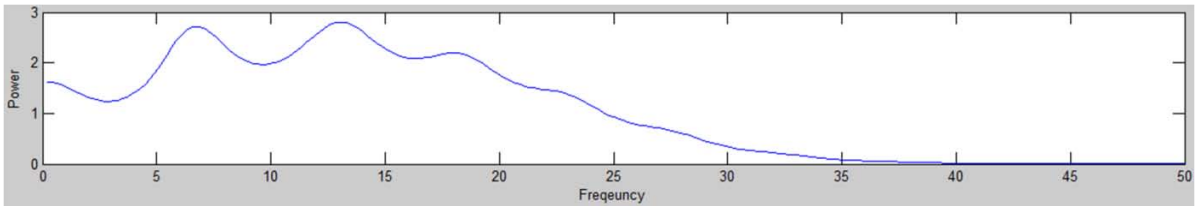

(a) ARPSD analysis on the signal (a) of Figure 38.

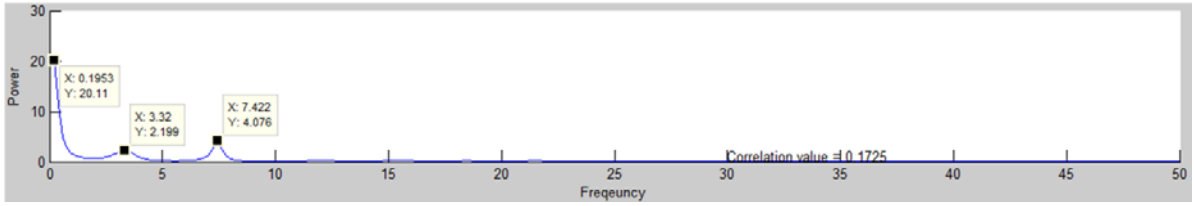

(b) ARPSD analysis on the signal (b) of Figure 38.

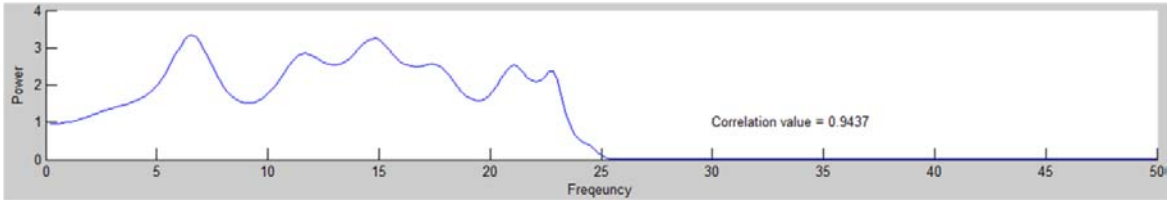

(c) ARPSD analysis on the signal (c) of Figure 38.

Figure 39. Auto aggressive power spectrum density (ARPSD) of all data sets represented in Figure 38

The correlation value between the collected ECG data as shown in Figure 38 (a) and the affected ECG data as shown in Figure 38 (b) due to artificial MA is marked at the right bottom side in the Figure 39 (c), and the value is 0.9437.

4.3.3 Motion artifact removal algorithm with an augmented ICA structure

The ICA algorithm is a representative algorithm for extracting a source signal from a signal mixed with several sources. As described in the section 2.3.1, to adapt the ICA algorithm to an application, there is an important assumption in the ICA algorithm. That is that the sources have to be independent from each other. The representative application of the ICA algorithm is the cocktail party problem, and the basic concept of the cocktail party problem is explained in Figure 40.

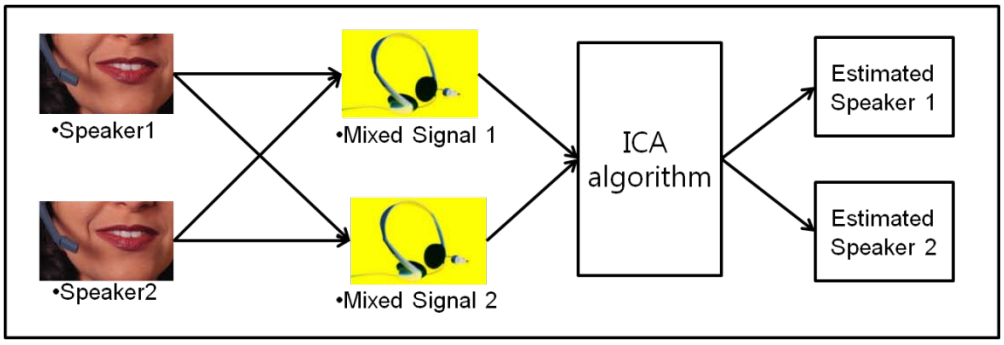

Figure 40. A block diagram of an ICA application: Cocktail party problem

If there are several people speaking on each topic in the same room, one hearing the sounds might be confused because each sound spoken from an individual will be mixed in the same room. As shown in the Figure 40, the signal 1 and 2 mixed from the combination of ach sound spoken by speakers 1 and 2 can be separated into two sounds estimated by the ICA algorithm. In addition, the basic assumption of the ICA algorithm that the sources should be independent of each other is satisfied in the cocktail party problem because the sources are created by each

speaker independently. However, as seen in those applications, at least two mixed signals are required to utilize the ICA algorithm in the application, and it is impossible to adapt the original ICA algorithm concept in the E-Bra system because the E-Bra system provides only one single channel. To solve the problem, an augmented ICA structure is discussed in this dissertation.

As early explained in the section 4.2, noise components including the MA components can be acquired by the NCEA with modified AF structure, and the noise components is used not only for MARA with AF structure but also for MARA with ICA structure. The basic idea for MARA with ICA structure is that if it is possible to create two pseudo signals including two source features, the ICA algorithm can be used for estimating the source signals measured from the E-Bra system. Specifically, there are two sources in the ECG data set collected by the E-Bra system. The first component is pure ECG components; P-QRS-T, and the second component is the MA components. Fortunately, the MA components can be acquired by the NCEA, and by multiplying three elements such as an ECG component collected by the E-Bra system, a noise component acquired by the NCEA, and a random matrix, we can acquire two pseudo ECG signals the identical to the mixed signal 1 and 2 as shown in Figure 40, and the pseudo ECG signals can be used as the input signals for ICA application. In other words, by a concept combined with the modified AF structure for the NCEA and original ICA structure, two pseudo ECG signals can be extracted, and an ECG signal can be estimated by the MARA with augmented ICA structure. Figure 41 shows the block diagram for motion artifact removal algorithm with the augmented ICA structure.

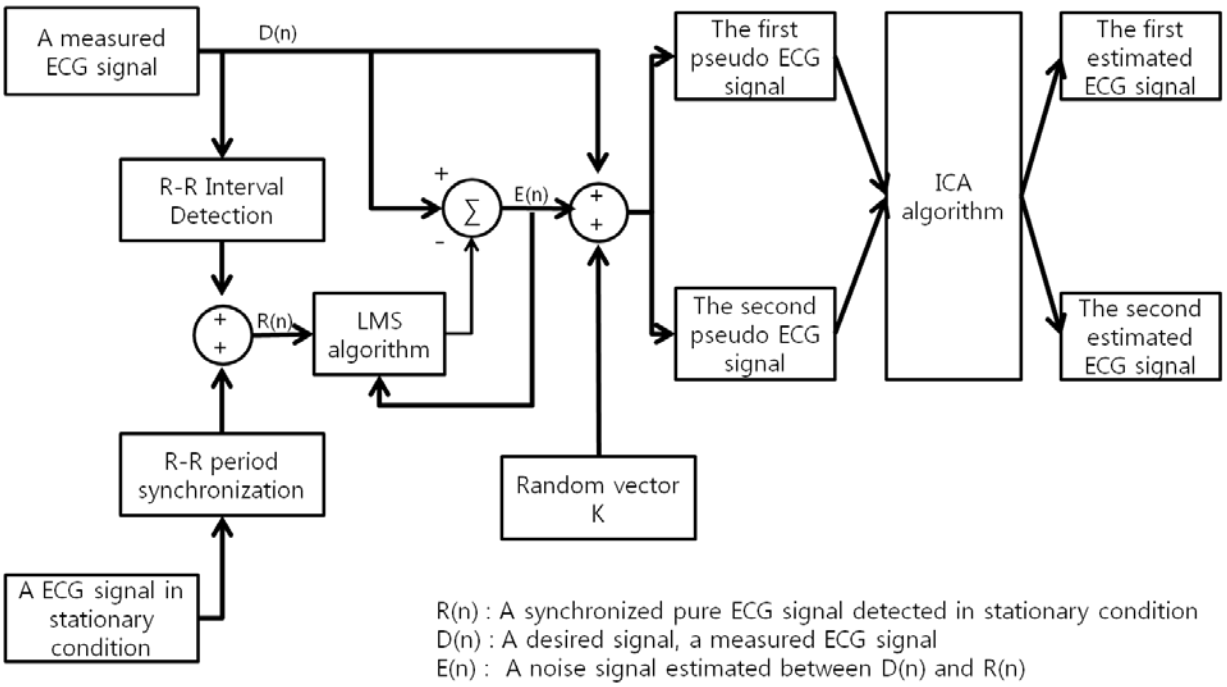

Figure 41. A MARA concept by the augmented ICA structure

Two pseudo ECG signals are created by multiplying three elements; a random matrix K with two dimensions, an ECG signal measured by the E-Bra system, and a noise signal extracted from NCEA explained in section 4.2. The two pseudo ECG signals are used to estimate the un-mixing weighted vector W that includes a maximum independent feature of the measured ECG signal. In detail, the steps below show the process of the block diagram for the MARA with ICA structure.

Step 1: An ECG signal is collected by the E-Bra system.

Step 2: In the period of the ECG signal collected in the stationary situation, one cycle of the ECG signal not affected by MA is detected.

Step 3: A noise signal is extracted by the NCEA including R peak detection and R-R interval synchronization as described in section 4.2

Step 4: A random vector K with two dimensions is initialized.

Step 5: Two pseudo ECG signals are created by multiplying with the noise signal acquired from step 3, the random vector K, and the measured ECG signal at step 1.

Step 5: The two pseudo signals are normalized and considered as the two ECG signals, which are inputs of ICA algorithm.

Step 6: The new signals, Y, are extracted by $Y = WX$ (X consists of the two pseudo ECG signals, W is the un-mixing weighted vector that is estimated by the fast ICA algorithm as explained in the section 2.3.3.3). In addition, one of the Y signals will be an ECG signal without MA components, and the other Y signal will be an MA component that is included in the measured ECG signal at step 1.

To evaluate the performance of the MARA with ICA structure, we utilize the same simulation which was performed in section 4.3.2 with an ECG data set collected from the website of physionet.org. The ECG data is collected for a 66 year old woman who was diagnosed with myocardial infarction disease. Figure 42 (a) shows the collected ECG waveform. As shown in the extended red color box of the Figure 42 (a), the ECG components, P-QRS-T, is not the same as the normal heart activity, and we can recognize that the ECG data is influenced by very low degree of the FLMA components because there is very low fluctuation due to the baseline wandering component.

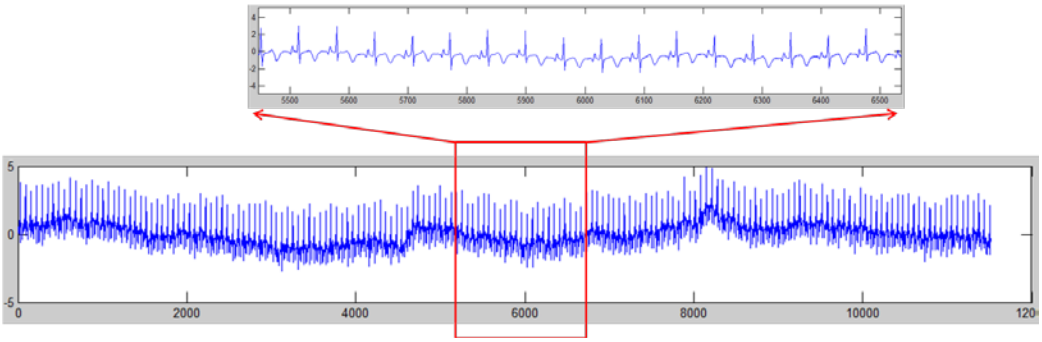

(a) An ECG signal with myocardial infarction

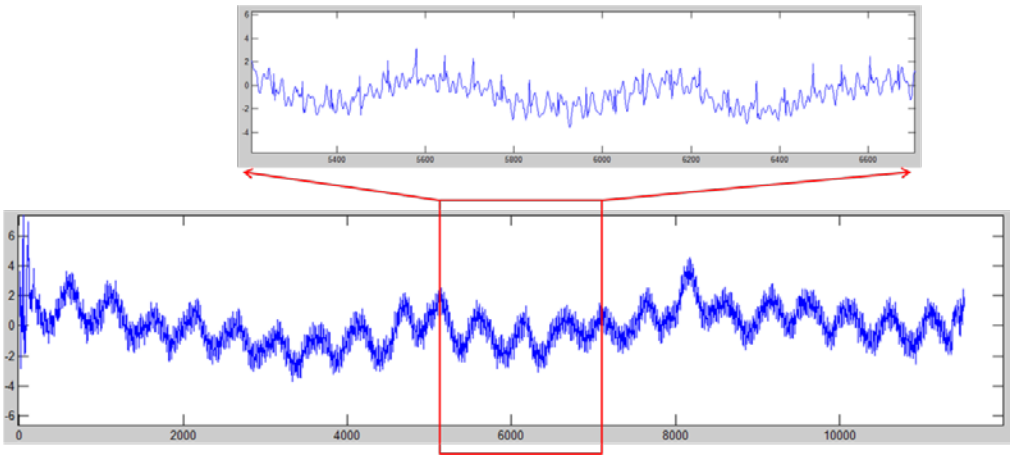

(b) The first pseudo ECG signal contaminated with artificial MA

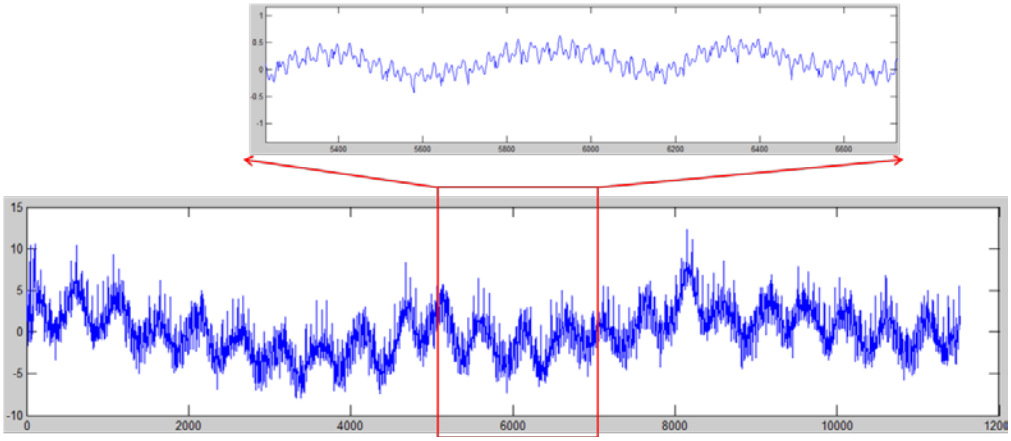

(c) The second pseudo ECG signal contaminated with artificial MA

Figure 42. The signals extracted for the simulation of MARA with ICA structure

To enhance the MA component in the collected ECG data set, the artificial MA component that was used in the simulation which was performed in section 4.3.1 was included in the collected ECG data set, and two pseudo ECG waveforms were created by multiplying a two dimensional random vector K, the ECG signal including the artificial MA component, and a noise component estimated by the NCEA as shown in Figure 42 (b) and (c). The two pseudo ECG waveforms have a severe impact on the artificial MA component as if the signals are not considered ECG waveforms as shown in the extended red color box. Two source signals were estimated by the MARA with ICA structure. The first signal was the ECG signal without the MA component, and

the second signal was the noise components including the MA component. Figure 43 shows each signal that is estimated by MARA with ICA structure.

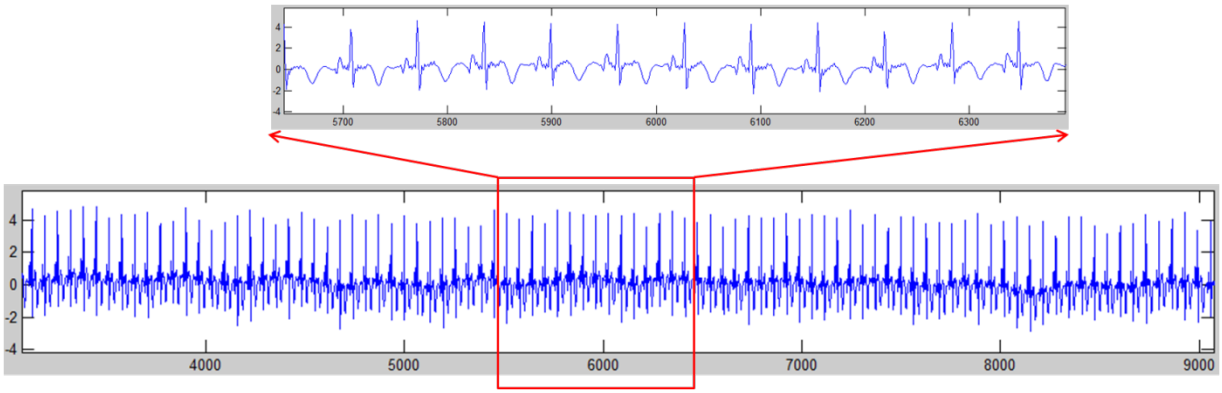

(a) An ECG signal estimated by MARA with ICA structure

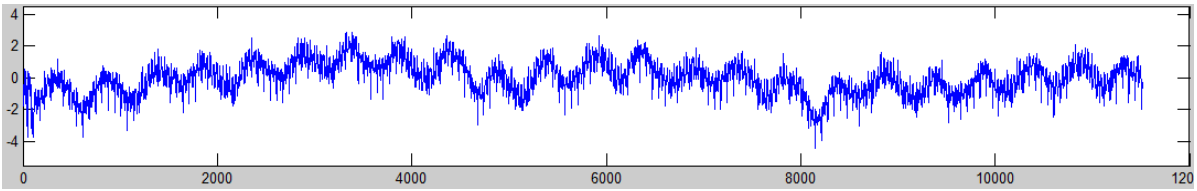

(b) A noise signal estimated by MARA with ICA structure

Figure 43. The simulation result by MARA with ICA structure

The signal shown in the Figure 43 (a) is the ECG signal removed not only of artificial MA but also of the FLMA component that has already been included in the measurement environment.

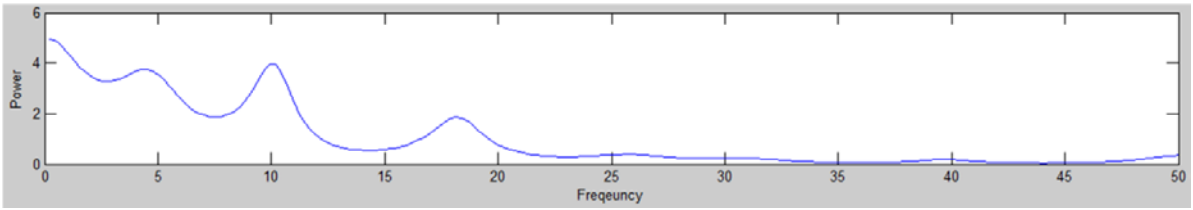

(a) ARPSD analysis on the signal (a) of Figure 42.

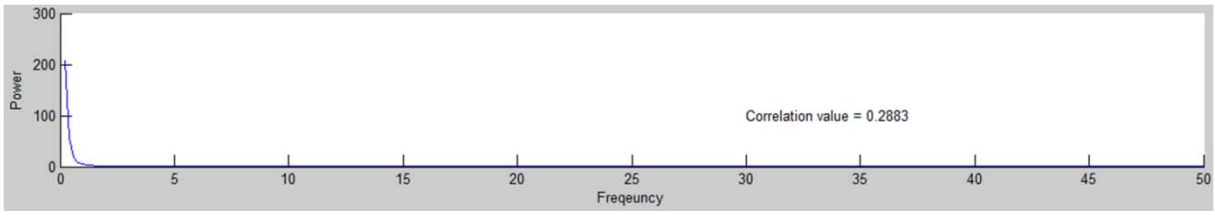

(b) ARPSD analysis on the signal (b) of Figure 42.

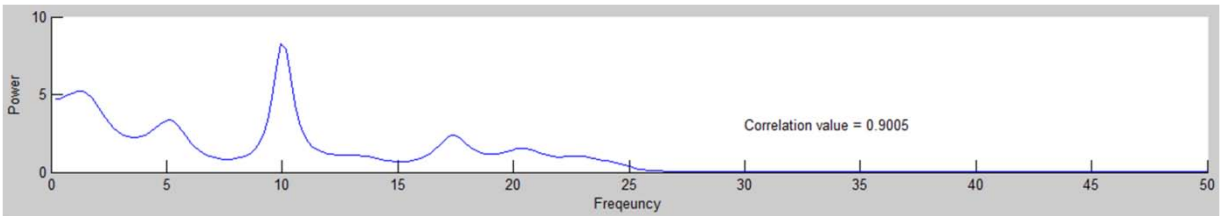

(c) ARPSD analysis on the signal (a) of Figure 43.

Figure 44. Auto aggressive power spectrum density (ARPSD) of all data sets represented in Figure 42 and 43

Figure 44 (b) shows a result of the ARPSD analysis on the ECG signal affected by the artificial MA. The correlation value marked in Figure 44 (b) is 0.2883. It means that the ECG signal has about 78% distortion damage due to the artificial MA component. Figure 44 (c) shows the result of the ARPSD analysis on the ECG signal estimated by using MARA with ICA structure. The correlation value between the Figure 43 (a) and (c) is 0.9005. It means that the ECG data estimated by the MARA with ICA structure was recovered with 90% similarity.

4.3.4 Performance comparison of motion artifact removal algorithm between adaptive filter and ICA

As shown in previous several sections, the artificially created MA components are almost completely removed by the suggested two MARAs with AF and ICA structure, and the ECG data sets used in the simulations are collected from real patients not only who have been diagnosed with myocardial infarctions but also who are in healthy condition in order to verify suitability of the two MARAs and to inspect the performance of the two MARAs. The two suggested MARAs have on important role in improving the quality of the E-Bra system, so it would be very valuable process to investigate the performance comparison between two MARAs. To evaluate the performance of the two MARAs, simulations to estimate ECG components eliminated by linear low pass FIR filter with a cutoff frequency are performed by adding the

cutoff frequency increased with 0.5Hz on each simulation. The idea of increasing 0.5Hz on each simulation is that the performance evaluation can be accomplished by comparison of the coherency degree between the estimated ECG signal and the original ECG signal under the same condition. Therefore, by observing the degree of the distortion under the same condition, the performance evaluation can be accomplished. For instance, when the cutoff frequency is selected as 0.5Hz, the ECG signal estimated by the two MARAs must be distorted because the noise component extracted by the linear low pass filter with the cutoff frequency of the 0.5Hz includes all components related on 0.5Hz frequency component. In other words, the frequency components in 0.5Hz includes not only in noise components but also in ECG components. However, by investigating the correlation values between two ECG signals estimated by MARA with AF structure and MARA with ICA structure, we can recognize which one has less signal distortion, and the less signal distortion indicates that the algorithm which shows a high correlation value reveals a higher performance than the other algorithm. The steps below show the process of the simulation for performance evaluation of the two MARAs.

Step 1: Acquire an ECG data set with healthy condition.

Step 2: Acquire coefficient values with 0.5Hz cutoff frequency compared with the previous cutoff frequency. (Initial value of the cutoff frequency is 0.5Hz)

Step 3: Acquire noise component by using linear FIR filter with a cutoff frequency of the same as the frequency used in step 2 (The extracted noise component must be included not only noise components but also ECG components)

Step 4: Estimate an ECG data by the MARA with AF structure.

Step 5: Estimate an ECG data by the MARA with ICA structure.

Step 6: Acquire correlation value between the estimated ECG data from step 4 and the collected ECG data in step 1.

Step 7: Acquire correlation value between the estimated ECG data from step 5 and the collected ECG data in step 1.

Step 8: Compare with two correlation values to investigate which one of the estimated ECG data sets is closed to the collected ECG data in step 1.

Step 9: Repeat from step 2 to step 8 until the cutoff frequency becomes 4 Hz. (It is not meaningful to investigate the frequency range over 4Hz because the correlation value becomes too low)

Figure 45 shows the frequency analysis result for the collected ECG data with healthy condition. The ECG data set used in this simulation is the same as the ECG data set that was used in the section 4.3.2.

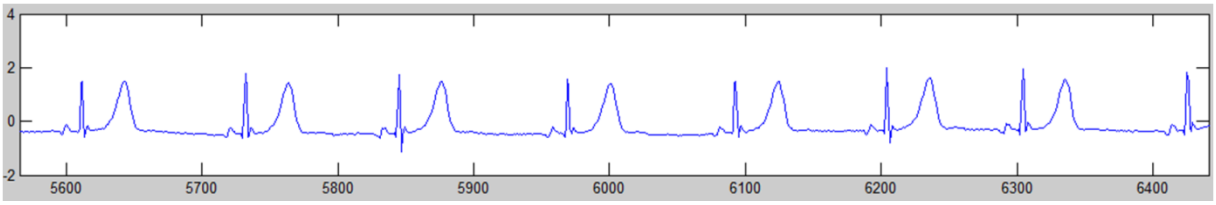

(a) An ECG waveform of the collected data set with healthy condition

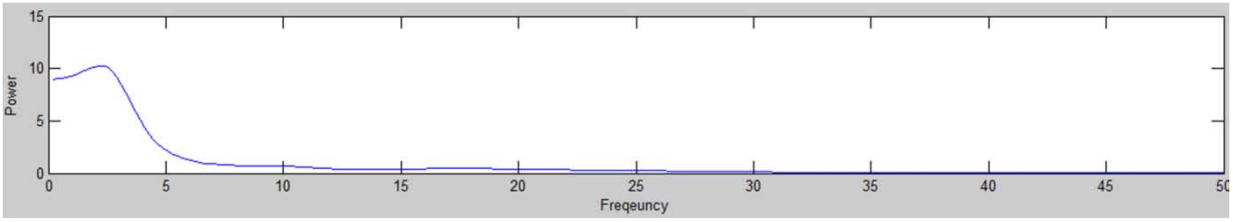

(b) A result of the frequency analysis by ARPSD for (a)

Figure 45. Frequency analysis for a collected ECG data with healthy condition

Figure 46 and Figure 47 show the results of the frequency analysis for two ECG signals estimated by the suggested MARAs with AF structure and ICA structure. Figure 46 shows the

result of the frequency analysis for an ECG data estimated by MARA with AF structure, and Figure 47 the result of the frequency analysis for an ECG data estimated by MARA with ICA structure.

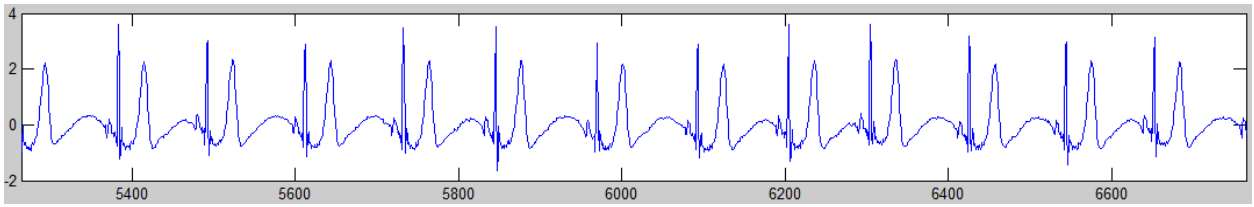

(a) An ECG waveform estimated by MARA with AF structure

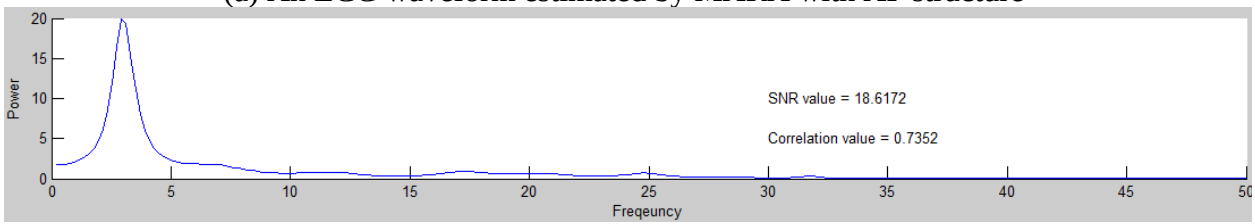

(b) ARPSD analysis of the data set (a)

Figure 46. The frequency analysis for the ECG data estimated by MARA with AF structure under forcibly contaminated situation by the artificial noise component with 0.5Hz frequency

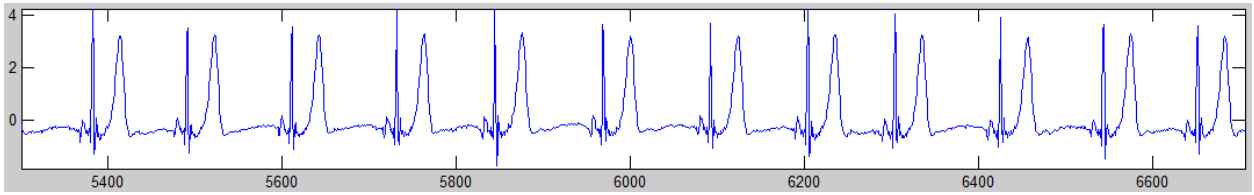

(a) An ECG waveform estimated in the process of step 5 (by MARA with ICA structure)

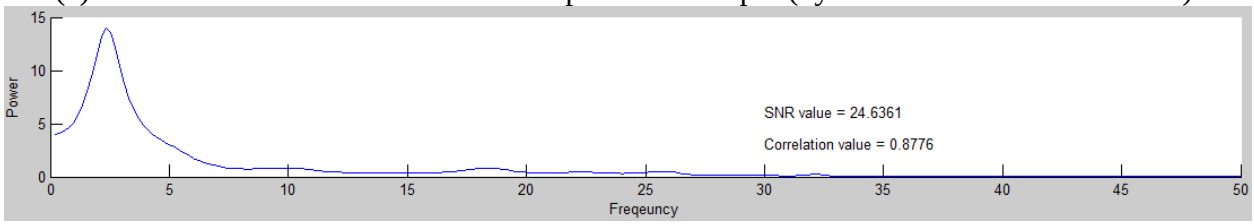

(b) ARPSD analysis of the data set (a)

Figure 47. The frequency analysis for the ECG data estimated by MARA with ICA structure under forcibly contaminated situation by the artificial noise component with 0.5Hz frequency

Figure 46 (a) and Figure 47 (a) are the graphs drawn in time domain for the waveform of the two ECG signals estimated by the suggested MARAs. It is visually not difficult to recognize that

the graph shown in Figure 46 (a) has more fluctuation than the graph shown in Figure 47 (a). It means that the ECG data set estimated by MARA with AF structure is more influenced by the cutoff frequency than the ECG data set estimated by MARA with ICA structure. The more clear difference is visible by the correlation values marked in the each graph. The correlation value marked in the Figure 46 (b) is 0.7352, and the correlation value means the degree of the similarity between the collected ECG data set shown in the Figure 45 (a) and the estimated ECG data set shown in the Figure 46 (a). The other correlation value marked in the Figure 47 (b) is 0.8776, and the correlation value means the degree of the similarity between the collected ECG data set shown in the Figure 45 (a) and the estimated ECG data set shown in the Figure 47 (a). Moreover, the SNR value shown in Figure 47 (b) is higher than the SNR value displayed in the Figure 46 (b). The signs, the correlation factor and the SNR value, reveal that the ECG signal estimated by MARA with ICA structure is less influenced than the ECG signal estimated by MARA with FA structure.

Several simulations identical to the simulation process explained in above paragraph were performed by changing the cutoff frequency such as adding 0.5 Hz on every simulation, and the gap of the correlation value between the ECG signal estimated by MARA with AF structure and the ECG signal estimated by MARA with ICA structure were investigated on every simulation. Figure 48 and 49 shows the alteration process of the correlation and SNR gap between the ECG signal estimated by MARA with AF structure and the ECG signal estimated by MARA with ICA structure. The x axis shows the cutoff frequency component that was used into the low pass filter, and the y axis shows the correlation values that were extracted from the estimated two ECG signals. The alteration with blue color is for the ECG data set estimated by MARA with ICA

structure on every simulation, and the alteration with red color is for the ECG data set estimated by MARA with AF structure.

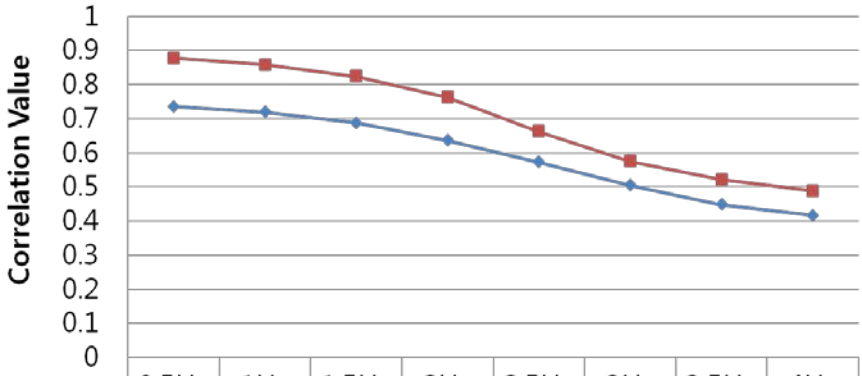

	0.5Hz	1Hz	1.5Hz	2Hz	2.5Hz	3Hz	3.5Hz	4Hz
MARA with AF structure	0.7352	0.7191	0.6878	0.6359	0.5723	0.5047	0.4482	0.4167
MARA with ICA structure	0.8776	0.8582	0.8239	0.763	0.6624	0.5744	0.5211	0.4882

Figure 48. The alteration of the correlation gap in the two ECG signals estimated by two MARAs

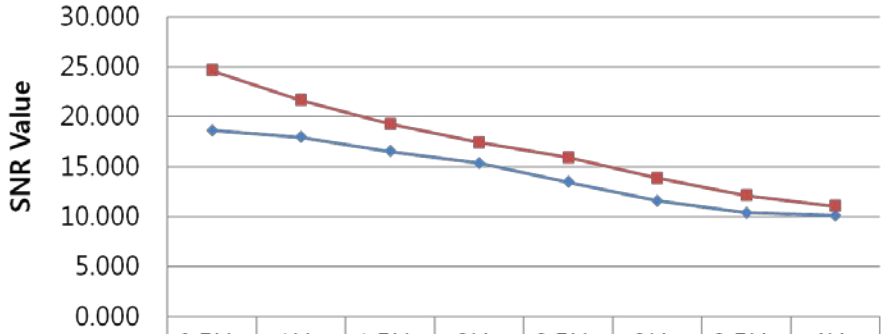

	0.5Hz	1Hz	1.5Hz	2Hz	2.5Hz	3Hz	3.5Hz	4Hz
MARA with AF structure	18.617	17.965	16.537	15.349	13.482	11.594	10.392	10.099
MARA with ICA structure	24.636	21.649	19.283	17.400	15.939	13.856	12.101	11.066

Figure 49. The alteration of the SNR gap in the two ECG signals estimated by two MARAs

As shown in the Figure 48 and 49, the correlation and SNR values estimated by the MARA with ICA structure were higher than the correlation values estimated by the MARA with AF structure under the same test conditions. It means that the ECG signals estimated by MARA with ICA structure has more similarity compared with the ECG signal estimated by MARA with FA structure. In other words, the performance of the MARA with ICA structure is higher than the performance of the MARA with FA structure. At this point, we need to keep in mind that the suggested MARA with AF structure also performs the corrective function with reasonable accuracy and can also be used for an ambulatory ECG monitoring system as described in the section 4.3.2.

Chapter 5: Experimental results of the E-Bra system

5.1 Test procedure

The ambulatory ECG monitoring system is the best solution to provide a continuous and periodic heart signal not only for clinicians who are qualified to treat heart abnormal function but also for people who have been diagnosed with heart disease. However, securing a reliable ECG data set in the ambulatory type measurement system is a big challenge because it is very common for the measured ECG signal to be influenced by MA due to subject movements as explained in previous chapters. The E-Bra system, which is one of the ambulatory ECG monitoring systems for women was developed in our laboratory, is unfortunately not free from the MA component. Two MARAs based on AF and ICA algorithm were suggested to solve the critical issue in the previous section, and several simulations were performed to evaluate the two MARAs' performance. As shown in the simulations, several ECG data sets collected from real patients were combined with an artificial MA including three different frequencies to simulate virtual test cases as regarding deep breathing, walking, and running. The ECG data sets were estimated by implementing the suggested two MARAs. The performance evaluation for the two MARAs was performed by examining correlation difference between an ECG data set detected in a stationary measurement environment and an ECG signal estimated by the suggested two MARAs. In this chapter, the performance evaluation of the two MARAs performed with 30 ECG data set collected from the E-Bra system will be discussed, and 30 ECG data sets gathered from three women volunteers in three age groups wearing a sport brassiere designed so that the transmission module of the E-Bra system can be attached at the bottom layer of the brassiere. The subjects were asked to take three different intentional test actions such as a stationary test

case with exaggerated breathing to produce the baseline wandering noise components due to respiration, a walking test case, and a running test case in order to create different MA components, and each intention test action was performed for 1 minute. The total test time for collecting 1 ECG data set from subject was about 3 minutes.

The ECG data set collected from the transmission module of the E-Bra system was sent to a computer installed with the “E-Bra pro” program through GPRS communication technology, and the ECG data set was saved in the computer. Figure 50 shows the ECG data transmission flow through GPRS communication.

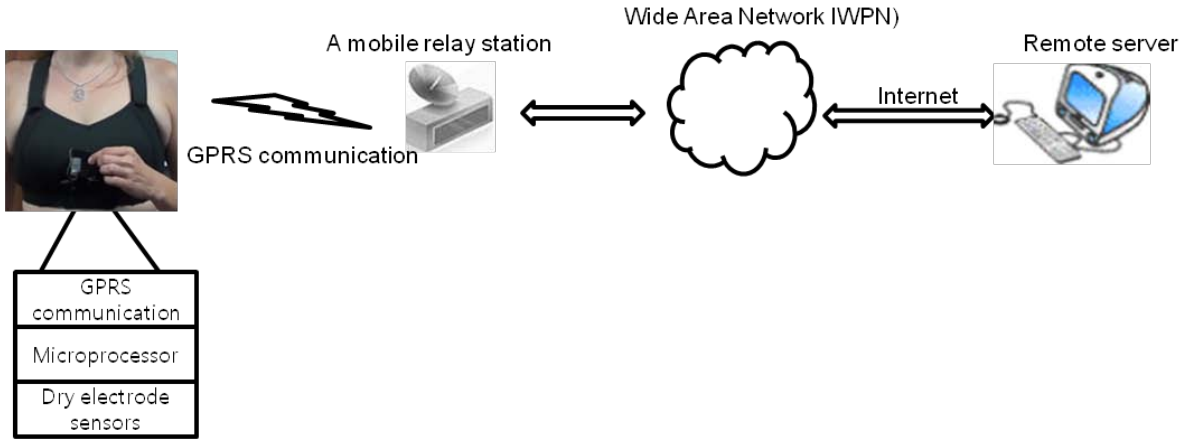

Figure 50. The ECG data set transmission flow of the E-Bra system.

The ECG data set collected in the computer was analyzed by the two MARAs, and the results produced by simulations implemented in each test stage provided the estimated ECG waveforms and correlation values used to evaluate the performance of the two MARAs. Specifically, there are several correlation values in the results. The first correlation value is acquired by comparing the ECG data set collected from the transmission module with MA component and the reference ECG signal which is not affected by the MA, and the second and third correlation values are acquired by comparing the collected ECG data set and the ECG data set estimated by two

MARAs. The examination of the values allows for an evaluation of the similarity of the estimated ECG data set and the reference ECG data set, and also allows for the comparison of the performance difference of the two MARAs. In addition, SNR values were calculated during the simulations, and the SNR values were used as another indicator to evaluate the performance difference between the two MARAs.

5.2 Simulation results in the stationary test case with deep breathing

The 30 ECG data sets were collected from the three subjects, and the ECG data sets were simulated by the two MARAs to acquire correlation values and SNR values. Figure 51 and 52 visually show ECG signal waveforms and frequency analysis graphs which were estimated from the simulation implemented by two MARAs. The results were extracted from an ECG data set among 30 ECG data sets. Other simulation results will be discussed in the section 5.5 to compare the performance of two MARAs. The results shown in Figures 51 and 52 are estimated by the simulation with the ECG data detected in the stationary test action including intentional deep breathing action in order to create a respiration MA component. Figure 51 (a) shows an ECG waveform which is created with 1 cycle of an ECG data set detected from a stationary situation without any movement. It is used as the reference ECG signal.

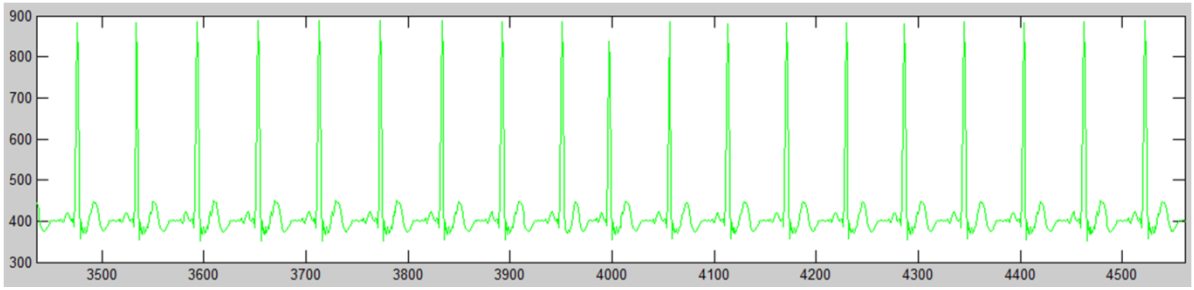

(a) A reference ECG signal detected in the stationary test case without any movement

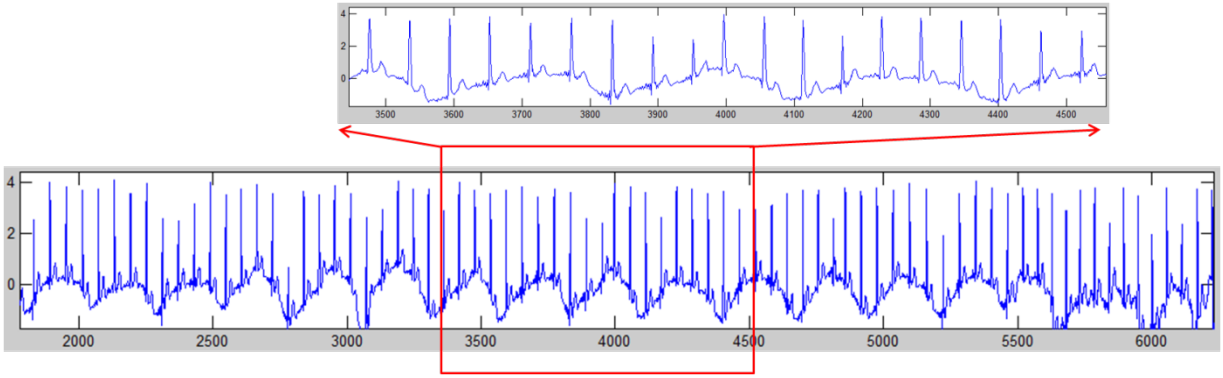

(b) An ECG data set collected from the E-Bra system in the stationary test case with intentional deep breathing action.

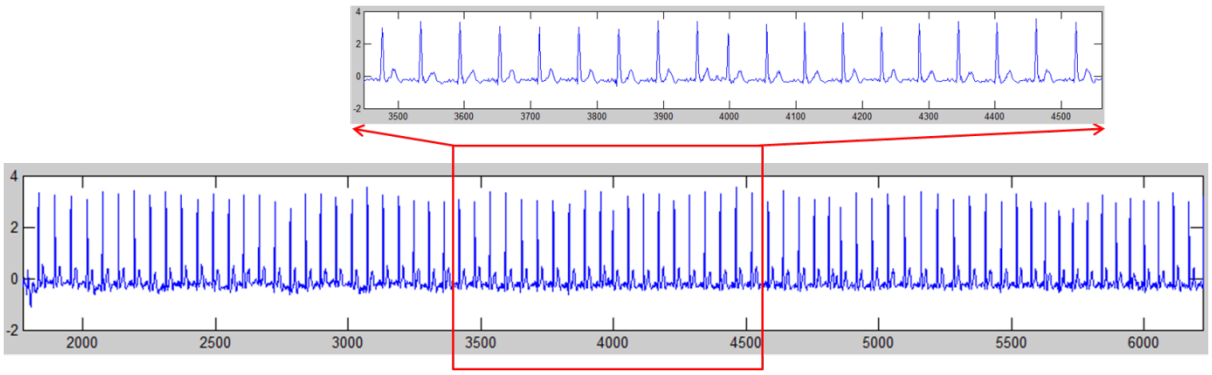

(c) An ECG data set estimated by the MARA with AF structure in the stationary test case

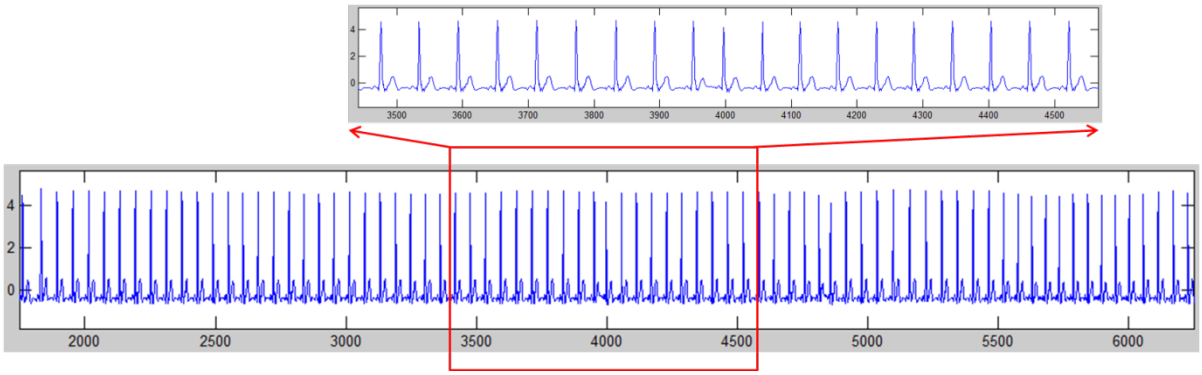

(d) An ECG data set estimated by the MARA with ICA structure in the stationary test case

Figure 51. ECG waveforms estimated by the two MARAs in the stationary test case

As shown in Figure 51 (b), we can see the respiration MA component in the graph as a small fluctuation of the baseline. The fluctuation is produced by the subject's slow chest movement due to air volume change in the respiration action. The ECG signal detected in the test case seems free from the signal distortion influenced by the MA component of the fluctuation because the ECG components, P-QRS-T, appear to keep the original ECG feature in the fluctuation. However, a frequency difference can be observed as shown in the Figure 52 (b). Figure 52 (b) shows the frequency analysis graph for an ECG signal measured by the E-Bra system, and the correlation value marked on the right side of the graph, 0.7214, is acquired by comparing the reference ECG signal and the measured ECG signal. The value, 0.7214, means that there is about

28% difference between the reference ECG signal and the ECG data set collected in the deep breathing test case. In other words, the collected ECG data set is influenced by MA component due to the deep breathing action.

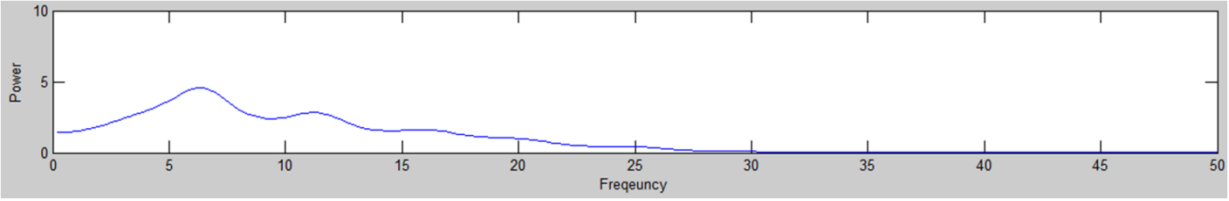

(a) A reference ECG signal without MA component which is detected from the E-Bra system

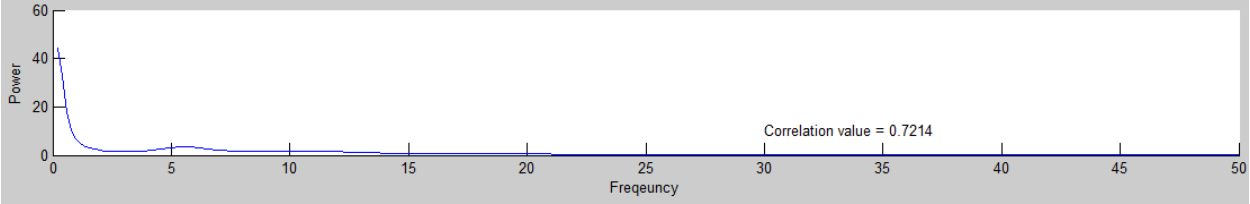

(b) An ECG signal with MA component which is detected from the E-Bra system

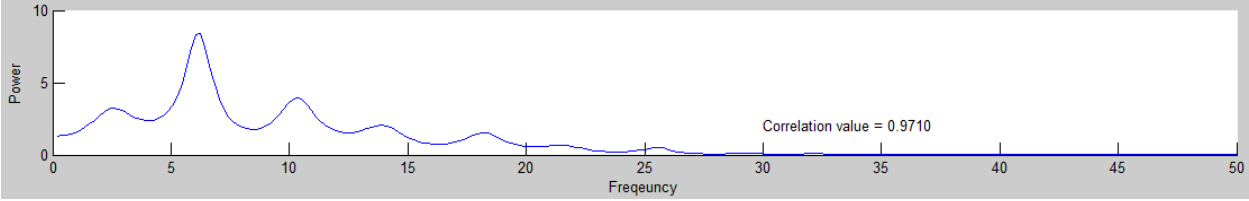

(c) An ECG signal estimated by MARA with AF structure

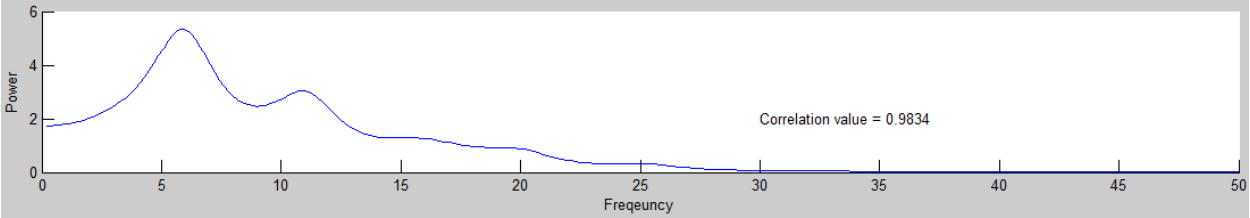

(d) An ECG signal estimated by MARA with ICA structure

Figure 52. The correlation values extracted in the stationary test case

Figure 52 (c) shows the ECG signal estimated by MARA with AF structure, and Figure 52 (d) shows the ECG signal estimated by MARA with ICA structure. The frequency shapes shown in the two graphs are quite similar to the graph shape of Figure 52 (a). This means that the ECG

frequency components estimated by two MARAs are quite closed to the reference ECG signal not affected by MA component. Moreover, the correlation values marked on the right side in the graphs, which are 0.9710 and 0.9834, are acquired by comparing the reference signal with the two ECG signals estimated from the collected ECG signal by using two MARAs. The values reveal not only that the two estimated ECG components are quite similar to the reference ECG signal, but also that the MA component due to deep respiration action is appropriately removed.

5.3 Simulation results in the walking test case

Figure 53 shows three ECG waveforms. The first ECG waveform as shown in Figure 53 (a) represents an ECG waveform collected by the E-Bra system in the walking test case. In comparison to the ECG waveform of Figure 51 (a), the ECG waveform of Figure 53 (a) includes steep baseline wandering noise, and we can recognize that MA components created by walking action have an effect on the ECG waveform. The ECG waveform is distorted by the MA components as shown in the extended red color box.

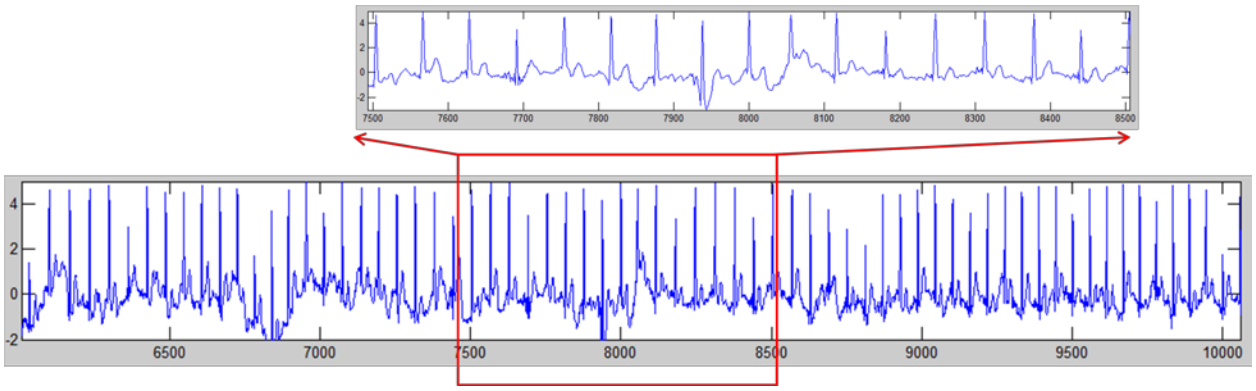

(a) An ECG data set collected from the E-Bra system in the walking test case

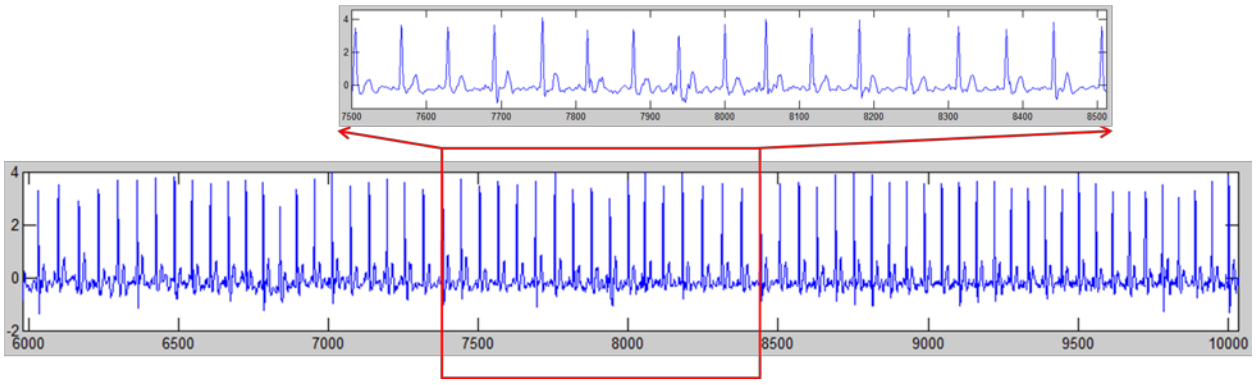

(b) An ECG data set estimated by the MARA with AF structure in the walking test case

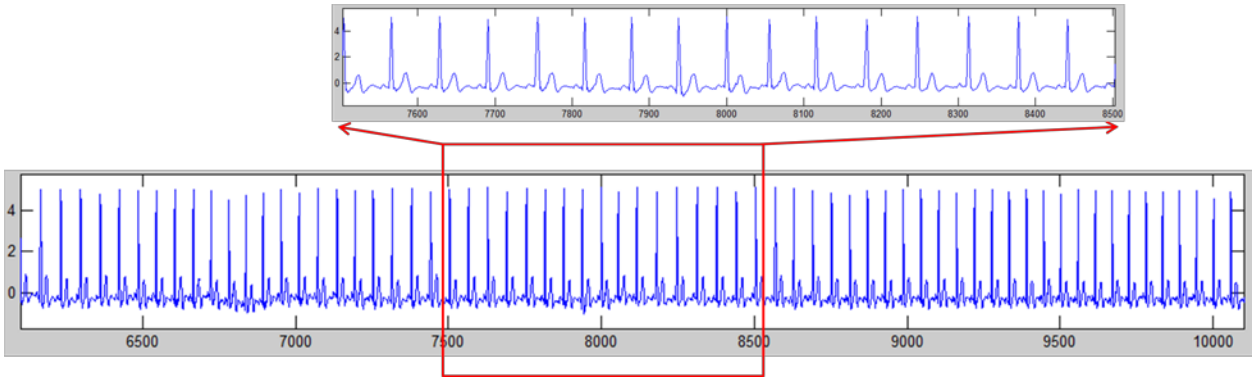

(c) An ECG data set estimated by the MARA with ICA structure in the walking test case

Figure 53. ECG waveforms estimated by the two MARAs in the walking test case

Figures 53 (b) and (c) show the ECG waveforms estimated by the two MARAs. The ECG waveform as shown in Figure 53 (b) is estimated by the MARA with AF structure, and the ECG waveform as shown in Figure 53 (c) is estimated by the MARA with ICA structure. The two ECG waveforms appear visually free from the influence of the MA component that is represented in Figure 53 (a), because the fluctuation of the ECG waveform due to baseline wandering noise is removed and the ECG components, P-QRS-T, as shown in the extended red color box appear to follow regular ECG waveform. The visual impression can be confirmed by the numerical figures of the correlation values as shown in Figure 54.

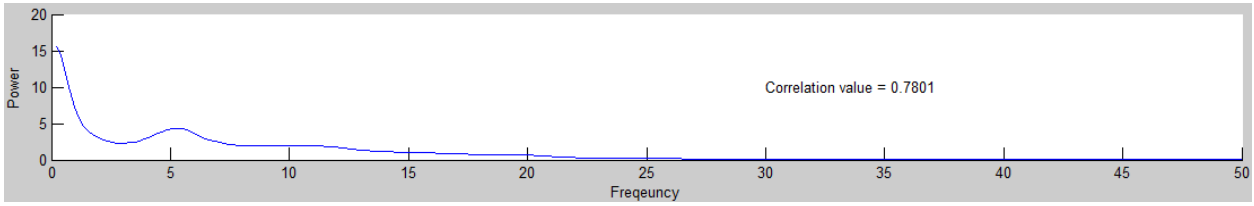

(a) Frequency analysis graph of the ECG data set collected from the E-Bra system in the walking test case

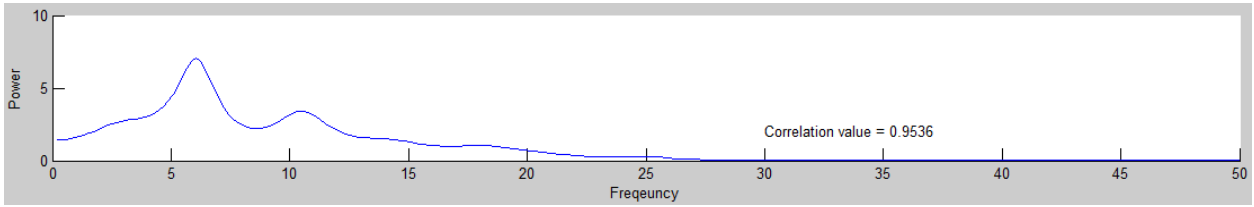

(b) Frequency analysis graph and correlation value of the ECG data set estimated by MARA with AF structure

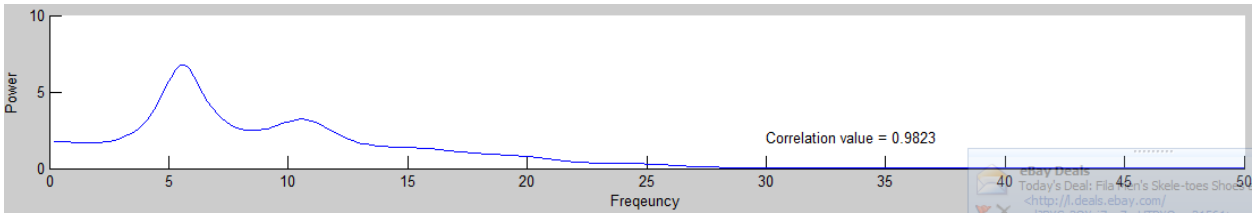

(c) Frequency analysis graph and correlation value of the ECG data set estimated by MARA with ICA structure

Figure 54. Frequency analysis graphs of the ECG data sets estimated by two MARAs in the walking test case.

The correlation value marked in Figure 54 (a) presents the degree of the similarity between the ECG data set collected in the walking test case and the reference ECG signal as shown in Figure 51 (a). The correlation value noted in Figure 52 (a), 0.7801, is higher than the correlation value marked in Figure 51 (b), 0.7214. The reason why the correlation value acquired in the walking test case is larger than the correlation value acquired in the stationary test case with deep breathing is that the noise amplitude due to deep breathing is higher than the noise amplitude due to walking actions. Even though the amplitude level of the noise due to walking test case is lower than the stationary test case, the degree of the signal distortion due to walking test case is quite higher than the degree of the signal distortion due to stationary test case because the impedance between skin and electrode sensors is changed with fast movement with small fluctuation. Therefore, the result shows that the ECG data set detected in the walking test case is affected by the MA component more than the stationary deep breathing test case. Figures 54 (b) and (c) show the results of the frequency analysis implemented with the ECG data sets estimated by two MARAs. The frequency components shown in the two graphs of Figures 54 (b) and (c) reveal that the two frequency analysis graphs are visually very similar compared to the frequency graph as shown in Figure 52 (a), and the correlation values marked in the right sides of the two graphs,

0.9536 and 0.9823, show that the two ECG waveforms estimated by the two MARAs include very similar ECG components, P-QRS-T, compared to the reference ECG signal of Figure 51 (a).

5.4 Simulation results in the running test case

As shown in Figure 55 (a), we can visually recognize that the ECG waveform in the graph is severely influenced by the MA components produced in the running test case. The graph shown in the extended red color box shows not only that the fluctuation level is quite higher than those fluctuations that are shown in Figure 51 (b) and Figure 53 (a), but also that the degree of the distortion is increased. The ECG graph shown in the extended red color box reveals that the ECG data in the test period has been affected by the MA component created by the running test case. The degree of the distortion is the highest compared with other cases. Fortunately, the R waves are still dominant in each ECG beat. Therefore, we can expect that the two MARAs will remove the MA component.

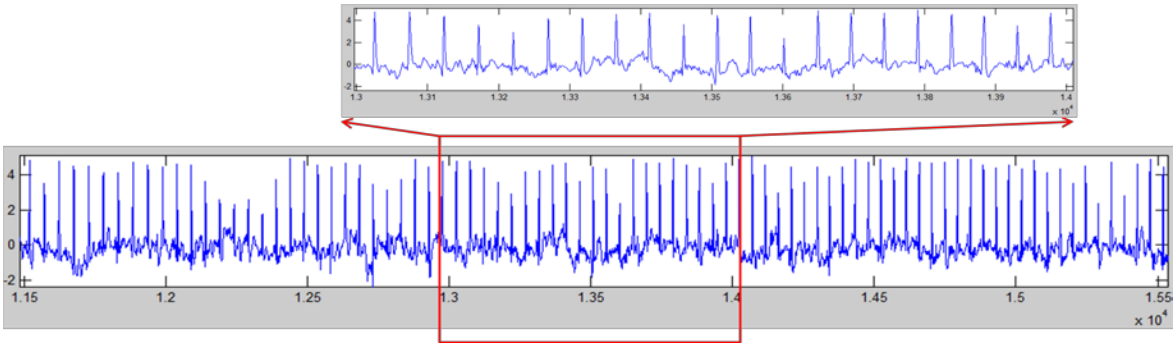

(a) An ECG data set collected from the E-Bra system in the running test case

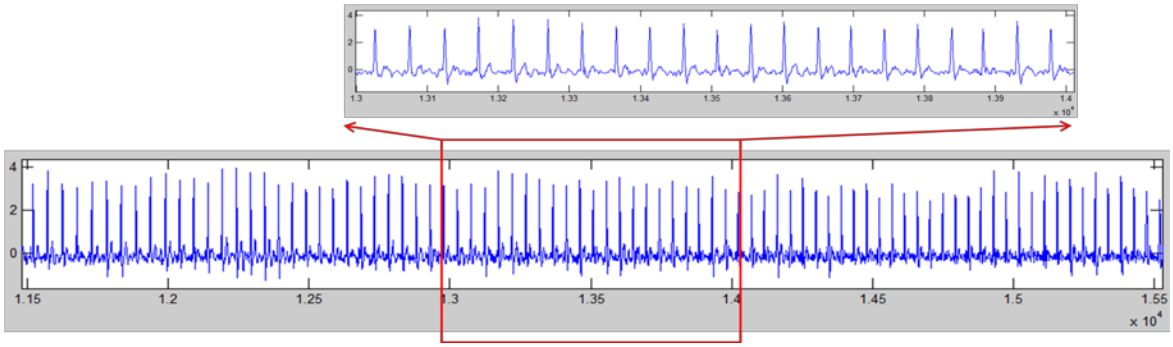

(b) An ECG data set estimated by the MARA with AF structure in the running test case

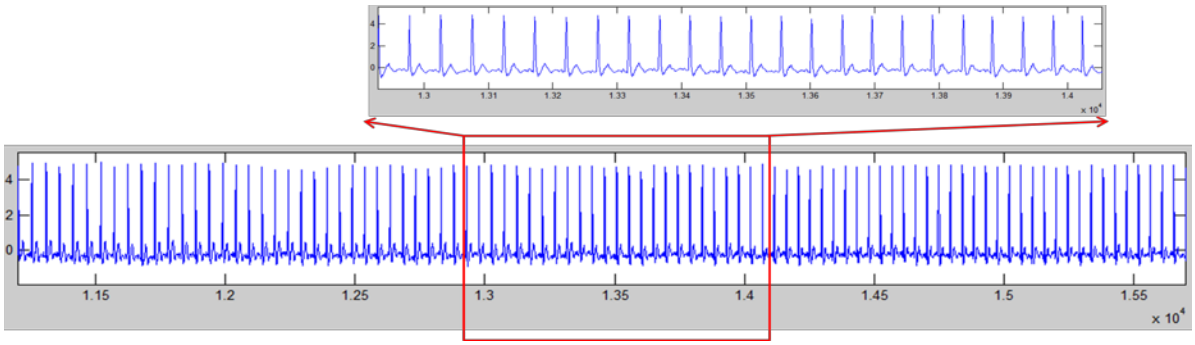

(c) An ECG data set estimated by the MARA with ICA structure in the running test case

Figure 55. . The ECG waveforms estimated by the two MARAs in the running test case

Figure 55 (b) and (c) show the ECG waveforms estimated by the two MARAs. The effectiveness of the two MARAs is well shown in the two graphs. There are no fluctuations in the two graphs, and the majority of the ECG waveform is appropriately recovered from the distorted parts. The visually abstractive performance of the two MARAs is further confirmed by the numerical values shown in Figure 56. The correlation value marked in Figure 56 (a), 0.8111, shows the degree of the similarity between the reference ECG signal shown in Figure 51 (a) and the ECG signal detected in the running test case. The correlation value is a little higher than correlation values acquired in the walking and stationary test case. However, because the impedance between skin and electrode sensor is changed with fast movement due to running action, as we can see in Figure 55 (a), the degree of the signal distortion is higher than the degree of the signal distortion due to walking and stationary test case. It means that the MA component has a severe impact on distortion of the ECG components; P-QRS-T. However, the correlation values shown in Figures 56 (b) and (c), 0.9415 and 0.9852, show that the two ECG signals are very similar to the reference ECG signal. This means that the two MARAs performance are very high to remove MA even in the case that critical MA components dominants the measured ECG signal.

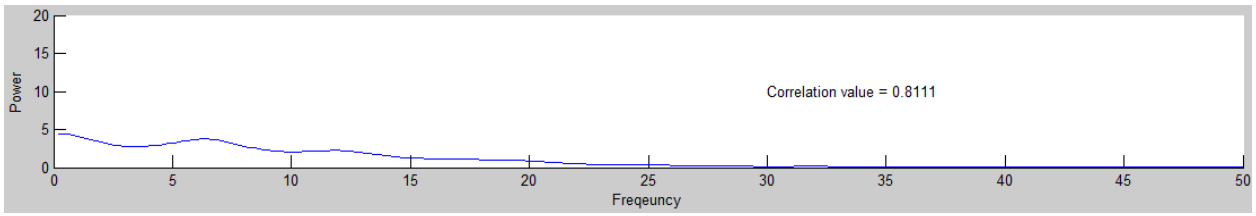

(a) Frequency analysis graph of the ECG data set collected from the E-Bra system in the running test case

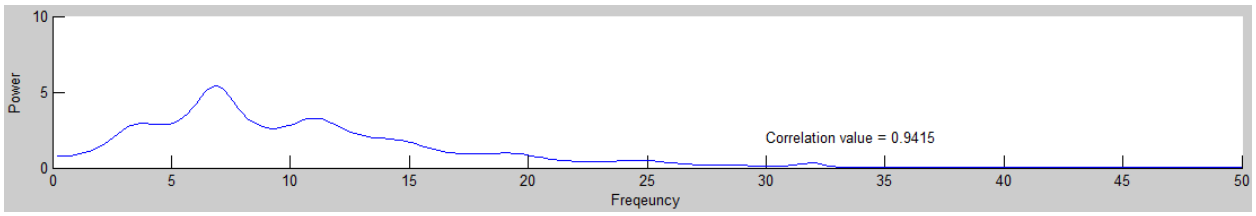

(b) Frequency analysis graph and correlation value of the ECG data set estimated by MARA with AF structure

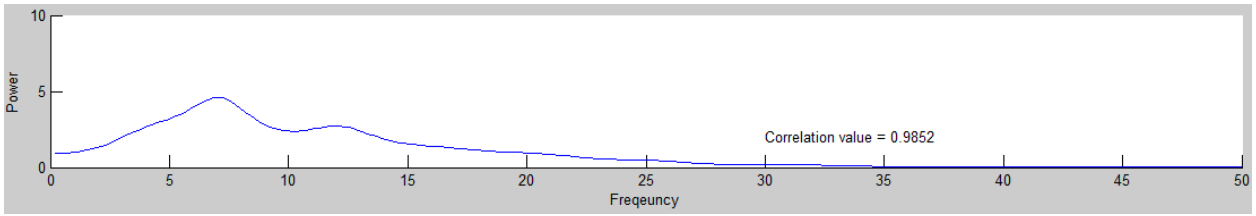

(c) Frequency analysis graph and correlation value of the ECG data set estimated by MARA with ICA structure

Figure 56. Frequency analysis graphs of the ECG data sets estimated by two MARAs implemented in the walking test case.

5.5 Performance evaluation of the MARA with FA Structure and the MARA with ICA sructure for the E-Bra system

The results shown in the previous sections represent the results acquired from one of the 30 ECG data sets collected from three women volunteers, and the explained results were then separated into three different test cases; a test case with a resting position with exaggerated deep breathing, a test case with walking, and a test case with running. In previous section, each ECG data set estimated by two MARAs on each test case was evaluated by comparing it with correlation values in order to reveal the similarity between the reference ECG data set and the ECG data set estimated by two MARAs. In this section, correlation values and SNR values acquired by simulations with other ECG data sets will be explained.

Figure 57 shows the variation of the correlation values acquired by the other 29 ECG data sets, and the values were calculated not in the specific test period, such as walking or running, but in the whole test period on each ECG data set.

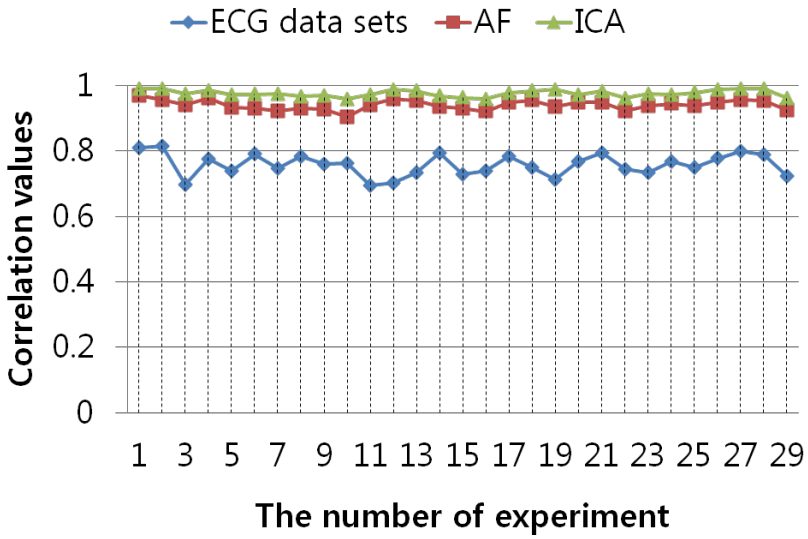

Figure 57. Correlation values comparison in all data sets estimated by two MARAs

The correlation values with blue color in the graph were acquired by comparing the correlation between the reference ECG signal without MA component and the ECG data sets acquired by the E-Bra system. The correlation values are variously distributed between 0.6943 and 0.8151. This means that the MA component due to a variety of subject movements in each test case has an effect on the ECG data set collected by the E-Bra. The dark red color graph shows the variation of the correlation values extracted by comparing degree of the similarity between the reference ECG signal and the ECG data set estimated by the MARA with AF structure, and the correlation values are distributed between 0.9034 and 0.9687. The green color graph shows the variation of the correlation values extracted by comparing degree of the similarity between the reference ECG signal and the ECG data set estimated by the MARA with ICA structure, and the correlation values were distributed from 0.9587 to 0.9911. Given the distribution density of the correlation values, we can see that the distribution density of the correlation values estimated by the MARA with ICA structure is more uniform than the correlation values estimated by the MARA with AF structure. This means that not only does the MARA with augmented ICA structure reduce the noise impact more than the MARA with AF structure, but also the ECG components estimated by the MARA with ICA structure have about a 5% higher similarity to the reference ECG signal than the ECG components estimated by the MARA with AF structure. This pattern repeats in the SNR value examination. As shown in Figure 58, the SNR values acquired by the MARA with ICA structure are higher than the SNR values acquired by the MARA with AF structure. However, we need to keep in mind that the suggested MARA with AF structure is also suitable for ambulatory ECG measurement system and the E-Bra system but into slightly lower prediction efficiency. As shown in the previous simulations, the results extracted

by the MARA with AF structure illustrate performance removing the MA component with about 94% recovering ability.

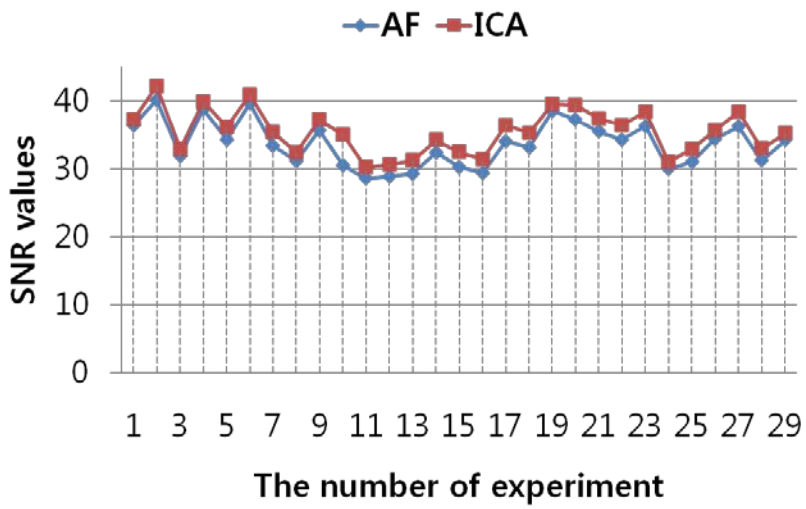

Figure 58. SNR values comparison to ECG data sets estimated by two MARAs with AF and ICA

Chapter 6: Conclusion

6.1 Conclusion

The demand and requirement of the ambulatory ECG measurement system for women was explained in the chapter 1, and demand naturally led to the development of the E-Bra system. The E-Bra system is one of the portable and ambulatory ECG measurement systems for women, and is able to provide continuous ECG data sets for clinicians who are trained to treat abnormal heart function or for people who need to check their own heart functions. The E-Bra system can be used in any place with mobile phone access is available, and the unlimited transmission distance is accomplished by GPRS communication. However, because the E-Bra system is one of the ambulatory ECG measurement systems with a single channel, it is not free from the MA components due to subject movements such as respiration, walking, and running which are common actions in peoples' lives. Given that the main purpose of the E-Bra system is to provide reliable ECG data sets identical to the quality of the ECG data sets collected in the hospital, the MA components should be removed to attain high quality in ECG data set through the E-Bra system. In chapter 2, the two concepts of the ICA and AF were introduced as the representative algorithms for removing MA.

The architecture of the E-Bra system was explained in chapter 3. The E-Bra system consists of a transmission module and a computer. The transmission module includes two sensors, 3 stage amplifier for data acquisition, and GPRS module. The computer located in a remote area includes a program called "E-Bra pro". A data protocol was suggested to distinguish between ECG data set and system information, and to protect from data loss due to signal disconnection.

The two MARA architectures; MARA with AF structure and MARA with ICA structure, were discussed in chapter 4. The NCEA was included in the two MARAs in order to isolate noise components from the ECG data sets collected from the E-Bra system. To check the suitability of the two MARAs and to evaluate the performance, three ECG data sets were collected from the website www.physionet.org . Among three ECG data sets, one ECG data set was for healthy persons, and two ECG data sets were myocardial infarction cases. The healthy case and one of the myocardial infarctions were used for the simulation of the MARA with AF structure, and the ECG data set with another case of the myocardial infarction was used for the simulation of the MARA with ICA structure. An artificial MA with three different frequencies such as 0.2Hz, 3Hz, and 7Hz was created as the MA components, and the artificial MA was mixed with the three ECG data sets. The mixed ECG data sets were simulated with the two MARAs to extract a pure ECG data set without the artificial MA component. The correlation values calculated by comparing the ECG data set collected from physionet.org with the ECG data sets estimated by the two MARAs were higher than 0.92. Showing the estimated ECG data sets were very similar to the collected ECG data sets.

In chapter 5, the two suggested MARAs were implemented on the 30 ECG data sets collected from three women volunteers of different ages for the E-Bra system evaluation. The three different test cases were selected to simulate normal human life activities such as a stationary test case with exaggerated deep breathing to produce a baseline wandering MA component due to respiration, a walking test case, and a running test case. Each test case was performed for about 1 minute, so total test time for collecting 1 ECG data set from a subject was about 3 minutes. The ECG waveforms estimated by the two MARAs were visually observed and

compared for evaluating the degree of distortion due to the MA components that were produced during each test stage, and the correlation values extracted by comparing the reference ECG signal which was not influenced by the MA components and the ECG signal estimated by two MARAs were used to compare and evaluate the two algorithms' performances. The correlation values extracted by the MARA with AF structure were distributed between 0.9034 and 0.9687, and the correlation values extracted by the MARA with ICA structure were distributed between 0.9587 and 0.9911. This reveals that the performance of the MARA with ICA structure is better than the performance of the MARA with ICA structure.

6.2 Future work

The E-Bra system developed in our lab is one of the ambulatory ECG measurement systems for women, and the configuration of the augmented V1 and V2 was used as a position to measure ECG signal. The ECG signal collected by the E-Bra system has an impact on the pure ECG components because it is very common to create MA components in ambulatory ECG measurement systems due to the subject's movement. To evaluate the performance of the two suggested MARAs, three test cases; a stationary test case with exaggerated deep breathing, a walking test case, and a running test case were selected as common activities that create MA components in everyday life. However, from the experiments, we found that there are several other activities that create MA components such as arm movements, up and down actions, etc. Therefore, further investigations for the MA components produced by other types of activities are needed, and simulations for the performance evaluation of the suggested two MARAs are needed with the MA components produced by subject's other types of activities.

The ECG signals used in this dissertation were collected from a compact transmission module, which is attachable to the bottom layer of the special sports brassiere including dry electrode sensors attached at the augmented V1 and V2 positions. Therefore, the ECG signals collected by the E-Bra system are acquired at present from the augmented V1 and V2 positions. However, there are several other precordial leads such as V3, V4, V5 and V6 as shown in Figure 7. If the E-Bra system was designed to detect ECG signals from these extra chest positions and the MARA is implemented to remove the MA components produced from the extra chest positions, the E-Bra system then would be able to provide more detailed information. Of course, there are a couple of disadvantages in extending ECG measurement channels such as cost and

size impact due to the multiplication of hardware elements; capacitor, inductor, op amp chipset, etc. However, if the challenges with respect to the hardware development are overcome, the E-Bra system with multi channels could provide additional ECG information for people who have a high risk of heart disease.

In addition, investigation regarding the impact of the MA components due to the subject's sports activities can be studied as an important future work. Actually, athletics are at greater risk for abnormal heart activities such as inversion of the T wave. The suggested two MARAs can be implemented not only in an ambulatory ECG measurement system but also in any kind of ECG measurement system. Thus, the study of reducing estimation time and improving the similarity between the reference ECG signal and the estimated ECG signal will improve the MARA's performance in all kinds of ECG measurement applications.

REFERENCE

[1] Council of Economic Advisers, "THE ECONOMIC CASE FOR HEALTH CARE REFORM," Executive Office of the President of the United States, JUNE 2009.

[2] Jean C McSweeney et al., "Women's Early Warning Symptoms of Acute Myocardial Infarction," in *Circulation Journal of the American Heart Association*, vol. 108, November 3, 2003, pp. 2619-2623.

[3] US. Departmentof Health and Human Services, "Health, United States 2011," Centers for Disease Control and Prevention, DHHS Publication No.2012-1232, MAY 2012.

[4] Melonie Heron, "Death leading causes for 2009," National Center for Health Statistics, October 26, 2012.

[5] Mayo Clinic Staff. (2013, JAN 16) Mayo Clinic Center. [Online]. http://www.mayoclinic.com/health/heart-disease/DS01120

[6] UW Medicine. (2012) UW Medicine Center. [Online]. http://www.uwmedicine.org/Patient-Care/Locations/UW-Neighborhood-Clinics/Patient-Education/Documents/Cardiovascular%20Disease.pdf

[7] Mozaffarian D Go As, VL Roger, and et. al., "Heart disease and stoke statistics-2013 updates," American Heart Association, 2013.

[8] American Heart Association, "Heart Disease and Stroke Statistics-2010 Update Circulation," American Heart Association, 2010.

[9] Anthony S Leicht, David A Hirning, and Graham D Allen, "Heart rate variability and endogenous sex hormones during the menstrual cycle in young women," in *Experimental Physiology*, vol. 88 no.3, 2003, pp. 441-446.

[10] Hulley S et al., "Randomized trial of estrogen plus progestin for secondary prevention of coronary heart disease in postmenopausal women," in *AMA*, vol. 280 No.7, 1998, pp. 605-613.

[11] Lori Mosca, Heidi Mochari-Greenberger, Rowena J Dolor, L.Kristin Newby, and Robb J

Karen, "Twelve-Year Follow-up of American Women's Awareness of Cardiovascular Disease Risk and Barriers to Heart Health," *Journal of American Heart Association*, no. 3, pp. 120-127, FEB 10. 2010.

[12] McSweeney JC, Cody M, and Crane PB, "Do you know them when you see them? Women's prodromal and acute symptoms of myocardial infarction," in *Journal of Cardiovasc Nurs*, vol. 15, 2001, pp. 26-38.

[13] E-service-expert.com. (2013) e-service-expert.com. [Online]. http://www.e-service-expert.com/e-Health-Korea.html

[14] Nitish V Thakor, John G Webster, and Willis J Tompkins, "Estimation of QRS Complex Power Spectra for Design of a QRS filter," in *IEEE TRANSACTIONS ON BIOMEDICAL ENGINEERING*, vol. 11, 1984, pp. 702-705.

[15] J. A. Van alste and T. S. Schilder, "Removal of baseline wander and power-line interference from the ECG by an efficient FIR filter with a reduced number of taps," in *IEEE TRANSACTION AND BIO*, vol. 12, 1985, pp. 1052-1060.

[16] Bernard Widow et al., "Adaptive Noise Cancelling:Principles and Applications," in *Proceedings of the IEEE*, vol. 63 No.12, 1975, pp. 1692-1716.

[17] James Stone, "Overview of Independent Component Analysis," in *Independent Component Analysis:A Tutorial Introduction*. London, England: The MIT Press, 2004, pp. 5-11.

[18] Roberts Stephen and Everson Richard, *Independent Component Analysis:Principles and Practice*. London, The United Kingdom: Cambridge, 2001.

[19] Aapo Hyvarinen, Juha Karhunen, and Erkki Oja, *Independent Component Analysis*. The United States: John Wiley & Sons, 2001.

[20] Nicholas Demytko and Kevin S English, "Echo Cancellation on Time-Variant Circuits," in *Proceedings of the IEEE*, vol. 65 No.3, 1977, pp. 444-453.

[21] R.B. Wallace and R.A Goubran, "Noise Cancellation Using Parallel Adaptive Filters," in *IEEE Transactions*, vol. 39 No.4, 1992, pp. 239-243.

[22] Sung-Pil Cho, Mi-Hye Song, Young-Cheol Park, Ho-Seon Choi, and Kyoung-Joung Lee, "Adaptive Noise Canceling of Electrocardiogram Artifacts in Single Channel Electroencephalogram," in *Engineering in Medicine and Biology Society. 29th Annual International Conference of the IEEE*, 2007, pp. 3278-3281.

[23] Wijayamuni N.M. Soysa, Roshan I. Godaliyadda, Janaka V Wijayakulasooriya, Mervyn P.B. Ekanayake, and Iresh C. Kandauda, "An Eigenfilter Based Approach for Extraction of Fetal Heart Signals Under Noisy Conditions Using Adaptive Filters," in *Computational Intelligence, Modelling and Simulation, IEEE conference*, 2012, pp. 254-259.

[24] Delgado E Rafael, Ozdamar Ozcan, Rahman Syed, and Lopez N. Carlos, "Adaptive Noise Cancellation in a Multimicrophone System for Distortion Product Otoacoustic Emission Acquisition," in *IEEE TRANSACTIONS ON BIOMEDICAL ENGINEERING*, vol. 47 No.9, SETEMBER 2000, pp. 1154-1164.

[25] Nitish V Thakor and Yi-Sheng Zhu, "Application of adaptive filtering to ECG analysis: Noise Cancellation and Arrhythmia Detection," in *IEEE TRANSACTIONS ON BIOMEDICAL ENGINEERING*, vol. 38 No.8, AUGUST 1991, pp. 785-794.

[26] John G Webster, "Reducing Motion Artifacts and Interference in Biopotention Recording," in *IEEE TRANSACTIONS ON BIOMEDICAL ENGINEERING*, vol. BME-31 No.12, 1984, pp. 823-826.

[27] Hyejung Kim et al., "Motion rrtifact removal using cascade adaptive filtering for ambulatory ECG monitoring system," in *Biomedical Circuits and Systems Conference*, 2012, pp. 160-163.

[28] Do-Un Jeong and Se-Jin Kim, "Development of a Technique for Cancelling Motion Artifact in Ambulatory ECG monitoring System," in *Covergence and Hybrid Information Technology*, vol. 1, 2008, pp. 954-961.

[29] Christopher Brouse, Guy Dumont, Felix Herrmann, and J. Mark Ansermino, "A wavelet Approach to Detecting Electrocautery Noise in the ECG," in *Engineering in Medicine and Biology 27th Annual Conference*, 2005, pp. 3876-3880.

[30] V.S. Nimbergi, V.M Gader, and S. Mukherji, "Characterization of ECG motion artifacts using wavelet transform and neural network," in *Indian Conference on MEdical Informatics*

and Telemedicine, 2005.

[31] S.W Yoon, S.D Min, Y.H Yun, S Lee, and M Lee, "Adaptive motion artifacts reduction using 3-axis accelerometer in E-textile ECG measurement system," in *Journal of Medical System*, vol. 32, 2008, pp. 101-106.

[32] D.T Pham, "Mutual infomation approach to blind separation of stationary sources," in *IEEE TRANSACTIONS ON INFORMATION THEORY*, vol. 48 No.7, JULY 2002, pp. 1935-1946.

[33] K Todros and J Tabrikian, "Blind Separation of Independent Sources Using Gaussian Mixture Model," in *IEEE TRANSACTIONS ON SIGNAL PROCESSING*, vol. 55 No.7, 2007, pp. 3645-3658.

[34] Zhishun Wang, Zhenya He, and J.Z. Chen, "Blind ECG Separation Using ICA Neural Networks," in *Engineering in Medicine and Biology Society, Proceedings of the 19th Annual International Conference of the IEEE*, vol. 3, 1997, pp. 1351-1354.

[35] Torfinn Berset, Di Geng, and Inaki Romero, "An Optimized DSP Implementation of Adaptive Filtering and ICA for Motion Artifact Reduction in Ambulatory ECG Monitoring," in *34th Annual International Conference of the IEEE EMBS*, 2012, pp. 6496-6499.

[36] I Romero, "PCA and ICA applied to Noise Reduction in Multi-lead ECG," in *Computing in Cardiology*, 2011, pp. 613-616.

[37] B Widrow and M.E Hoff,.: Proc. Of WESCON Conv.Rec., 1960, ch. Part 4, pp. 96-140.

[38] B Widow and S.D Stearns, *Adaptive Signal Processing*.: Prentice-Hall, 1985.

[39] S Haykin, *Adptive Filter Theory*. NJ: Prentice Hall, 1991.

[40] A Hyvarinen and E Oja, "A fast fixed-point algorithm for independent component analysis," in *Neural Comput.*, vol. 9, 1997, pp. 1482-1492.

[41] B Pearlmutter and L Parra, "Maximum likelihood blind source separation: A context sensitive generalization of ica," in *Advances in Neural Information Processing Systems*, vol.

9, 1997, pp. 613-619.

[42] A.J Bell and T.J Sejnowski, "An information-maximization approach to blind separation and blind deconvolution," in *Neural Computation*, vol. 7, 1995, pp. 1129-1159.

[43] A Jessop, *Informed assessment:An introduction to information, entropy, and statistics*. London, England: Prentice Hall, 1994.

[44] T.M Cover and J.A Thomas, *Elements of Information Theory*.: Wiley, 1991.

[45] A Hyvarinen, "New approximation of differential entropy for independent component analysis and projection pursuit," in *Advances in Neural Information Processing Systems*, vol. 10, 1998, pp. 273-279.

[46] A Hyvarinen, "Fast and robust fixed-point algorithm for independent component analysis," in *Neural Networks*, vol. 10, 1999, pp. 626-634.

[47] Kleber and G Andre, "ST segment elevation in the electrocardiogram: a sign of myocardial Ischemia," in *Cardiovasc Res*, vol. 45 No. 1, 2000, pp. 111-118.

[48] Sanjiv M Narayan, "T wave alternans and human ventricular arrhythmias," in *J.Am.Coll.Cardiol*, vol. 49, 2007, pp. 347-349.

[49] Vijay Varadan, Sechang Oh, Hyeokjun Kwon, and Phillip Hankins, "Wireless Point-of-Care Diagnosis for Sleep Disorder With Dry Nanowire Electrode," in *J.Nanotechnol. Eng. Med*, 2010, pp. 1-11.

APPENDIX

210 Administration • Fayetteville, Arkansas 72701 • (479) 575-2208 • (479) 575-3846 (FAX)
Email: irb@uark.edu

Research Compliance
Institutional Review Board
September 25, 2012

MEMORANDUM

TO:	Vijay Varadan Pratyush Rai Prashanth Shyamkumar
FROM:	Ro Windwalker IRB Coordinator
RE:	PROJECT CONTINUATION
IRB Protocol #:	11-09-093
Protocol Title:	*Smart Textile Sensor System for Health Monitoring*
Review Type:	☐ EXEMPT ☒ EXPEDITED ☐ FULL IRB
Previous Approval Period:	Start Date: 09/28/2011 Expiration Date: 09/27/2012
New Expiration Date:	09/27/2013

Your request to extend the referenced protocol has been approved by the IRB. If at the end of this period you wish to continue the project, you must submit a request using the form *Continuing Review for IRB Approved Projects*, prior to the expiration date. Failure to obtain approval for a continuation on or prior to this new expiration date will result in termination of the protocol and you will be required to submit a new protocol to the IRB before continuing the project. Data collected past the protocol expiration date may need to be eliminated from the dataset should you wish to publish. Only data collected under a currently approved protocol can be certified by the IRB for any purpose.

This protocol has been approved for 100 total participants. If you wish to make *any* modifications in the approved protocol, including enrolling more than this number, you must seek approval *prior to* implementing those changes. All modifications should be requested in writing (email is acceptable) and must provide sufficient detail to assess the impact of the change.

If you have questions or need any assistance from the IRB, please contact me at 210 Administration Building, 5-2208, or irb@uark.edu.